



Universiteit
Leiden
The Netherlands

Controlling growth and morphogenesis of the industrial enzyme producer *Streptomyces lividans*

Mangiameli, G.

Citation

Mangiameli, G. (2014, June 12). *Controlling growth and morphogenesis of the industrial enzyme producer *Streptomyces lividans**. Retrieved from <https://hdl.handle.net/1887/25980>

Version: Not Applicable (or Unknown)

License: [Leiden University Non-exclusive license](#)

Downloaded from: <https://hdl.handle.net/1887/25980>

Note: To cite this publication please use the final published version (if applicable).

Cover Page



Universiteit Leiden



The handle <http://hdl.handle.net/1887/25980> holds various files of this Leiden University dissertation.

Author: Mangiameli, Giulia

Title: Controlling growth and morphogenesis of the industrial enzyme producer *Streptomyces lividans*

Issue Date: 2014-06-12

**Controlling growth and morphogenesis
of the industrial enzyme producer
*Streptomyces lividans***

PROEFSCHRIFT

ter verkrijging van de graad van doctor
aan de Universiteit Leiden,
op gezag van de Rector Magnificus prof. mr. C.J.J.M. Stolker
voorzitter van het College voor Promoties
in het openbaar te verdedigen
op donderdag 12 juni 2014
klokke 10:00

door
Giulia Mangiameli
geboren te Torino, Italië
2 mei, 1984

PROMOTIECOMMISSIE

Promotor: Prof. dr. G.P. van Wezel
Co-promotor: Dr. E. Vijgenboom

Overige leden: Prof. dr. J. Brouwer
Prof. dr. H. de Winde
Prof. dr J. Anné
Dr. P. Punt

This research was supported by the European Research Area for Industrial Biotechnology (ERA-IB) under the acronym EPOS (Enzyme Production in Optimized *Streptomyces*).

Printed by Smart Printing Solutions, Gouda, the Netherlands

Table of contents

Chapter 1	5
Introduction	
Chapter 2	9
Host-vector optimization in <i>Streptomyces lividans</i> for heterologous protein production	
Chapter 3	39
Apical synthesis of an extracellular polysaccharide involved in aerial growth and hyphal attachment of <i>Streptomyces lividans</i> depends on CslA and GlxA	
Chapter 4	67
Analysis of the transcriptome of <i>Streptomyces lividans</i> <i>cslA</i> and <i>glxA</i> null mutants reveals disturbance in the transcription of genes relating to morphogenesis and osmoprotection	
Chapter 5	85
Identification of strong constitutive promoters for protein expression in <i>Streptomyces lividans</i> 1326.	
Chapter 6	105
Functional analysis of the SsgA-like proteins in <i>Streptomyces lividans</i> 1326	
Chapter 7	123
General Discussion	
NEDERLANDSE SAMEVATTING	131
REFERENCES	137
APPENDIX	149
CURRICULUM VITAE	164

Chapter 1

Introduction

Streptomyces are Gram-positive, soil dwelling bacteria that raised interest in the last 50 years for their high potential in antibiotic (Hopwood 2007) and protein production (Vrancken and Anné 2009; Anné et al. 2012). The work presented in this thesis is part of a project funded by the European Research Area for Industrial Biotechnology (ERA-IB) under the acronym EPOS (Enzyme Production in Optimized *Streptomyces*). According to the ERA-IB, the definition of Industrial Biotechnology is “the application of biotechnology for the environmentally-friendly production and processing of chemicals, pharmaceuticals, materials and bio-energy”, thus using biological catalysts (enzymes) instead of the classical chemical processes. It therefore aims at sustainable production of goods, with less dependency on non-renewable fossil resources.

The number and amount of enzymes needed for industrial applications has been increasing steadily in the last years. The preferred production platforms are fungi and bacteria, with a predominant role of *Escherichia coli* and *Bacillus* spp. in the second category. The aim of this project is to extend the currently available range of enzyme production platforms by optimizing *Streptomyces* and, in particular, the best protein producer *Streptomyces lividans*.

Thanks to their saprophytic nature, streptomycetes secrete a massive amount of industrial enzymes. They have a relatively low level of endogenous extracellular proteolytic activity when compared to other expression hosts (e.g. *Bacillus*), they are generally more suited to produce proteins encoded by high G+C actinomycete genes in their native form, coupled to efficient secretion so as to avoid that the proteins end up in inclusion bodies (often a problem when using e.g. *E. coli*) and making downstream processes easier. Despite their attractive potential, *Streptomyces* present several constraints which so far limit their application in industry. The first constraint is morphology: by growing as a network of hyphae, they produce dense pellets in liquid cultures that hold *Streptomyces* back from being one of the first choice cell factories in large scale fermentations. In addition, the limited availability of efficient expression systems for high-level transcription/translation and subsequent secretion is a further bottleneck. A review on recent developments in strain improvement from

the perspective of a host-vector optimization is presented in **Chapter 2**.

A rational morphological engineering by addressing proteins involved in growth and morphology had proven successful in the past. The overexpression of SsgA, an activator of cell division, led to a fragmenting phenotype with higher growth rate and protein secretion when compared to the wild type (van Wezel et al. 2006). Following this idea, genes involved in growth and development were identified and the related mutant strains analyzed. In particular, a cellulose-like protein CslA and a copper oxidase GlxA were shown to be functional partners in the process of synthesis and accumulation of an extracellular, chitin-like glycan at hyphal tips, whose absence leads to disruption of pellet aggregation in liquid cultures. These findings, presented in **Chapter 3**, allowed identifying new potentially interesting strains for protein production and expanding further our understanding of the processes and contributors in bacterial morphogenesis.

To further analyze the morphology and physiology of these strains, we took advantage of the next generation sequencing technologies applied to the transcriptome, such as RNA-Seq. **Chapter 4** presents an overview of the expression state at mRNA level of the *glxA* and *cslA* mutants compared to wild type, providing potential novel hints for future engineering.

In addition to strain improvement, the design of an efficient expression vector remains to be solved. We addressed this issue by identifying new strong promoters to drive high levels of transcription in our system. In **Chapter 5** a new pipeline is described, starting from the identification of strong constitutive promoters from RNA-Seq and microarray data, screening via a newly optimized Lux system and validation with the production of a small laccase (SLAC) from *S. coelicolor*. This allowed us to expand the list of available strong promoters and optimizing/developing new reporter systems.

The success of SsgA for morphological engineering and strain design also prompted analysis of the SsgA-like proteins (SALPs) in *S. lividans*, as a primer towards future rational strain engineering approaches. Genes for SALPs other than SsgA were deleted and the effect on *S. lividans* tested in terms of phenotype and

enzyme production. The results are presented in **Chapter 6**.

A general discussion is presented in **Chapter 7**, with reflections on how the experiments presented in this thesis – combined with the current state of the art – can provide insight on how to obtain better *Streptomyces* production hosts.

Chapter 2

Host-vector optimization in *Streptomyces lividans* for heterologous protein production

Giulia Mangiameli and Erik Vijgenboom

Manuscript in preparation

ABSTRACT

The growing demand for sustainable production of goods has led to an increased need for enzymes and production hosts in the last decades. Bacteria are usually the preferred hosts because of their easy genetic manipulation and fast growth. Among them, *Streptomyces* is recognized as a highly attractive enzyme production host with several advantages over other bacterial hosts but also with some constraints that require improvement. In this review, the efforts made in the last years to remove the disadvantages related to its mycelial growth and to widen the selection of expression vectors and consequently improve *Streptomyces* for heterologous protein production, will be presented.

INTRODUCTION

Streptomyces spp. belong to the family of *Actinomycetaceae* and are Gram positive, soil dwelling bacteria with a filamentous structure and a complex morphological development which has a strong resemblance with that of filamentous fungi. They are primarily known as important producers of secondary metabolites including antibacterial, anticancer, immunosuppressive, antihelmintic and antifungal agents (Hopwood 2007). In fact, 60% of the currently used antibiotics are produced by this organism. In addition, *Streptomyces* is a producer of commercially valuable proteins naturally secreted to adapt to a changing environment and to different nutritional sources (Chater et al. 2010). In particular, it produces enzymes for the degradation of many organic polymers such as cellulose, chitin and lignin, which are very much needed for the production of second generation biofuels (Jing 2010; Amore et al. 2012; Noda et al. 2013).

The application of recombinant proteins in industrial and pharmaceutical processes has grown steadily in the last decades and has become an indispensable part of the manufacturing of many products. While in the past these proteins were isolated from classical sources like plants and animals, at present they are mainly expressed in heterologous hosts, which allows a faster and safer production with improved quality and stability. More than 200 peptides and recombinant proteins have been approved so far by the FDA and they have a large variety of applications, such as in the production or modification of biofuels, textiles, leather, paper, detergents, polymers and plastics, human and animal health, medicine, diagnostics, food and nutrition. The total market of industrial enzymes, such as laccases, amylases, cellulases and proteases, was estimated in 2012 at € 2,8 billion p.a. (Novozyme report 2012).

For the production of industrial relevant proteins, yeasts and filamentous fungi are used for more than 50% of the proteins while bacteria for 30% and animals and plants are preferred in the remaining cases. Bacterial hosts include *Escherichia coli*, the most used because of its fast growth and high level of protein expression, *Bacillus* species such as *Bacillus subtilis* and *Bacillus licheniformis* and the less

frequently used *Ralstonia eutropha* and *Pseudomonas fluorescens* (Demain and Vaishnav 2009). Nevertheless, none of these systems proved to be an optimal and universal production platform. Within academic and industrial research, the design of alternative and efficient hosts continues to be a theme of interest.

Streptomyces and in particular *Streptomyces lividans* have been successfully tested for the production of proteins including human therapeutics and industrially relevant enzymes (Vrancken and Anné 2009; Anné et al. 2012). The highest production yields are assessed to be over 500 mg/L, including proteins with low or zero expression in other traditional bacterial systems (Sianidis et al. 2006). The latter makes *Streptomyces* a valuable if not the only alternative. Despite the encouraging perspectives, there are several constraints against the utilization of this organism on a larger industrial scale. From a host point of view, the main bottleneck is its mycelial growth, which results in rather dense clumps of mycelium in liquid cultures. This morphology strongly influences the overall efficiency of the fermentation, and the secretion and integrity of the desired final product. Furthermore, the very limited choice of stable vectors with strong promoters for expression of heterologous proteins is often a drawback for the selection of *Streptomyces* as host.

The classical method for strain improvement was represented in the past by random mutagenesis. For example, cycles of UV mutagenesis and screening led to remarkable yield improvements in the case of the industrial penicillin producer *Penicillium chrysogenum*, with an improvement of 100,000 fold compared to the original Fleming strain (Rokem et al. 2007). However, the labor intensity and the accumulation of unknown or unwanted mutations called for a different approach. The improved genetic tools for targeted mutation and the overall increase in understanding the morphology and physiology of bacterial and fungal production platforms contributed to the development of a rational genetic approach.

Although directed mutagenesis can be applied to improve morphology to increase the protein secretion capacity and/or modify metabolic pathways, at least one more issue needs to be resolved. To obtain high yields of heterologous proteins, optimized expression vectors are required that combine strong transcriptional and

translational elements with good secretion signals. This review will focus on the recent developments in the application of *Streptomyces* as a platform for heterologous protein production from the perspective of host-vector optimization.

HOST OPTIMIZATION

From the host perspective, optimization can take place at different levels. At the morphology level, the best phenotype for the production of the desired product can be selected through directed genetics. Improving secretion together with controlling proteolysis are also efficient tools to increase the total yield of protein produced. Finally, the control of fermentation parameters and medium composition can further boost protein production.

Morphology

Mycelial growth

The mycelial behavior of *Streptomyces* presents a serious challenge for the wider use in fermentation and protein production.

In the soil, *Streptomyces* develops from a spore to a dense branched network of vegetative mycelium, a syncytial network in which cell division is not essential and cross walls are occasionally observed. In contrast to other bacteria which grow through binary fission, *Streptomyces* shows an apical polarized growth, with extension and cell wall synthesis at the hyphal tips. The hyphal tip is a hub for the recruitment of proteins involved in growth and has been recently renamed as TIP Organizing Center (TIPOC) (Holmes et al. 2013). The molecular assembler Scy acts as a protein scaffold by recruiting, among others, DivIVA, which directs apical growth (Flärdh et al. 2012). DivIVA has a preference for negatively curved membranes (Lenarcic et al. 2009) and accumulates in multiprotein foci called polarisomes at the tips (Hempel et al. 2012). It is active through a splitting mechanisms (Richards et al. 2012), in which an existing polarisome breaks off, leaving behind a smaller aggregate that marks the site for branching along the hyphae. The disassembly of the foci seems to

be dependent on a phosphorylation mechanism via the protein kinase AfsK (Hempel et al. 2012). These studies show that TIPOC is not only required for apical growth but also establishes the branching points including new tips in the hyphae.

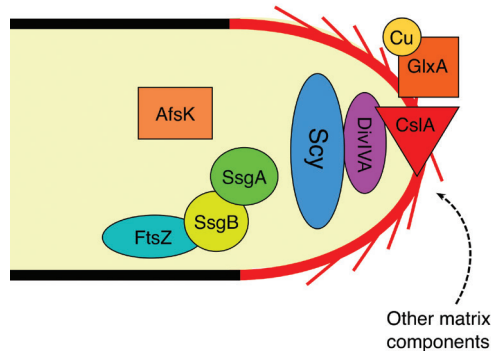


Figure 1. A schematic summary of proteins present in the tip that are required for tip growth, septum formation, aerial growth and attachment/penetration of solids such as agar.

The Tip Organizing Center TIPOC is made by the protein scaffold Scy and the polar growth determinant DivIVA, whose regulation is modulated by AfsK. CslA interacts with DivIVA at the very front of the tip and is responsible for the synthesis of a chitin-like glycan, together with its functional partner GlxA. The glycan is responsible for aerial development and attachment to solid substrates. Other matrix components such as chaplins, rodlin and SapB take part in the formation of the matrix during development and erection of the aerial mycelium. The proteins belonging to the cell division machinery, SsgA, SsgB and FtsZ, are also shown in the picture, although their interaction with the TIPOC remains to be elucidated.

Following an external signal such as nutrient depletion, the vegetative mycelium is broken down in concert with the erection of new hyphae, the so-called aerial mycelium. During this process, an important role is played by proteins which lower the surface tension at the air-water interface: the lantibiotic-like peptide SapB (de Jong et al. 2012), the rodlin proteins RdlA and RdlB (Claessen et al. 2002), together with the eight chaplins ChpA-H (Claessen et al. 2003; Elliot et al. 2003). They coat the hyphae providing a hydrophobic sheath known as the rodlin layer that is essential for aerial growth (Claessen et al. 2004). Recently, the extracellular matrix was also shown to be essential for attachment to solid substrates. A chitin-like extracellular polysaccharide synthesized by the concerted action of the glycosyl transferase CslA and the radical copper oxidase GlxA, both present at the hyphal tips, is required for attachment to and growth into substances as agar (Chapter 3).

After the erection of the aerial mycelium, multiple processes such as septation and chromosome segregation occur, giving rise to spore formation. The family of SsgA-like proteins (SALPs) plays an important role in the process of cell division prior to sporulation (Noens et al. 2005; Traag and van Wezel 2008), including the recruitment of FtsZ and the formation of the cell divisome (Willemse et al. 2011). SsgA in particular seems to have a central role in septum formation (van Wezel et al. 2000a; van Wezel et al. 2006).

In submerged cultures, many *Streptomyces* grow vegetatively and only a small number had been recognised as forming submerged spores, with *Streptomyces griseus* and *Streptomyces venezuelae* as well known examples (Kendrick and Ensign 1983; Glazebrook et al. 1990). However, a recent investigation showed that morphological development in submerged culture is much more common than originally anticipated, with half of a collection of randomly selected streptomycetes producing submerged spores (Girard et al. 2013). A specific signature consisting of six amino acids in the SsgA protein allowed prediction of the ability to produce submerged spores, thus dividing the phylogenetic tree of streptomycetes into an LSp (liquid sporulation) branch and an NSLp (no liquid sporulation) branch. The signature also correlates to a single amino acid residue in SsgB, with Thr128 corresponding to the LSp phenotype, and Gln128 to NSLp phenotype.

The mycelia of streptomycetes form aggregates of various sizes that can be categorized according to their diameter into pellets (950 μm), clumps (600 μm), branching and not branching hyphae (Pamboukian et al. 2002) (Fig 2A). No differentiation in liquid cultures was reported until two different growth phases were detected in *S. coelicolor* submerged cultures (Manteca et al. 2008). A first phase starts with the germination of the spores, followed by radial growth of the pellet and growth arrest due to cell death in the inner part, after which a second phase starts with new growth from the inside and ends when the maximum diameter of the pellet is reached. A link between development and metabolite production was also demonstrated, with exclusive production of the antibiotics undecylprodigiosin and actinorhodin during the second growth phase. The exact process behind pellet aggregation is still

largely obscure. Two mechanisms have been proposed: a coagulating one, with the agglomeration of multiple germinating spores, and a non-coagulating one, with the independent germination of separate single spores (Metz and Kossen 1977). Pellets can also arise from hyphal aggregates and fragments of broken down mycelium (Whitaker 1992).

Recently, two populations of pellets differing in size have been described in *Streptomyces* liquid cultures (van Veluw et al. 2012), in line with the heterogeneity observed in other microbial strains. The large size population is dependent on the strain and parameters such as medium composition and age of the culture, while the small size population is strain and medium independent and remains constant through time. Moreover, the deletion of the chaplins and CslA affects the size of the larger pellets, demonstrating the involvement of the cell surface proteins and matrix components in the aggregation process. The smaller pellets are not affected by these deletions and therefore seem to be an intrinsic property of *Streptomyces* growth, independent of the extracellular matrix components.

In other microorganisms, different substances have been described to be involved in cell aggregation. Surface polysaccharides are involved in spores aggregation of *Phanerochaete chrysosporium* in liquid cultures (Gerin et al. 1993). They are also implicated in biofilm formation, cell aggregation and pathogenicity in various bacteria (Zogaj et al. 2003; White et al. 2003; Latgé 2007; Saldaña et al. 2009; Lenardon et al. 2010). Hyaluronic acid is an example of a polysaccharide responsible for biofilm formation and virulence as shown in *Streptococcus pyogenes* (Cho and Caparon 2005), while extracellular DNA is a main component of the extracellular matrix in *Pseudomonas aeruginosa* (Whitchurch et al. 2002). Other cell aggregation processes require specific molecular recognition mediated through outer membrane proteins like shown for the TraA protein of Myxobacteria (reviewed in Wall 2013).

In *Streptomyces*, pellet aggregation seems to be affected by different factors. An amine oxidase (HyaS) associated to the vegetative mycelium has been identified as an enzyme required for aggregation in liquid cultures (Koebisch et al. 2009). Deletion of *hyaS* led to fluffy clumps with protruding hyphae (Fig 2B). Moreover,

overexpressing SsgA led to a highly fragmenting phenotype in liquid cultures (Fig 2C). The independent deletion of the synthase and the oxidase responsible for the synthesis of a chitin-like polysaccharide associated to the cell wall resulted in the formation of nonpelleting mycelium in various liquid media (Chapter 3 and Fig 2D). Other studies related *Streptomyces* pelleting behavior to biofilm formation, with a crucial role for substances such as DNA, hyaluronic acid and calcium (Kim and Kim 2004).

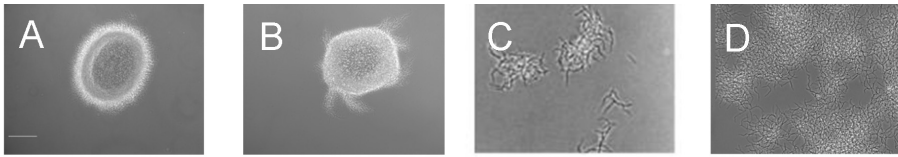


Figure 2. Different morphologies of *S. lividans* 1326 in liquid cultures: pellets (A), pellets with branching hyphae (B), fragmenting mycelium (C), open mycelium (D). Scale bar: 100 μm .

The mycelial nature of these organisms strongly affects fermentation. On the one hand, large pellets suffer from transfer limitation of oxygen and nutrients as they are made of distinct layers, with actively growing hyphae in the outer part and progressively less active cells towards the center (Celler et al. 2012). On the other hand, a dispersed mycelium causes high viscosity of the medium, presenting problems in maintaining a homogeneous and well mixed culture, with the formation of stagnant zones and nutrient gradients, requiring high stirring speeds and expensive downstream processes. Different approaches to overcome filamentous growth, including physical or genetic methods, will be presented in the next section.

Controlled growth and morphology during fermentation

Different strategies have been established to enhance protein production through the control of growth and morphology during industrial fermentation. However, with the production of enzymes and antibiotics by *Streptomyces* as an example (discussed in more detail below), the preferred morphological behavior depends very much on the combination between production host and product of interest.

The first studies focused mainly on antibiotic production. In *Penicillium*

chrysogenum, only pellets with diameters less than 400 μm were considered as actively metabolizing (Schügerl et al. 1983). In *Saccharopolyspora erythraea*, there is a critical pellet diameter (80–90 μm) below which production of erythromycin was abolished (Martin & Bushell, 1996). The correlation between morphology and antibiotic productivity in this organism was further investigated, with the best production obtained in variants with enhanced strength and reduced branching rates (Wardell et al. 2002). In *Streptomyces*, an alteration from long to short hyphae corresponded to a block in antibiotic production (Kuznetsov et al. 1992). It is generally believed that pellet and clump formation is fundamental to obtain good production of secondary metabolites (Vecht-Lifshitz et al. 1992; Sarrà et al. 1997), supporting the hypothesis that antibiotics are produced at a fixed distance from the hyphal end. Nevertheless, shake-flask cultures of *Streptomyces hygroscopicus* with glass beads reduced pellet size with simultaneous increase of the geldanamycin production (Dobson et al. 2008).

It is unclear how these observations can be applied for the production of proteins. In the case of filamentous fungi, production of enzymes is generally favored by a small/loose pellet morphology, which allows better oxygen and nutrient transfer. This is the case, for example, for the production of glucoamylase by *Aspergillus niger* (Papagianni and Moo-Young 2002) or to obtain acid phosphatase from *Neurospora crassa* (Wen Su and Jun He 1997).

In order to control the morphology of filamentous microorganisms in liquid cultures, different approaches can be applied, for example by altering the inoculum, the pH or the stirring speed (reviewed in Papagianni 2004). A low inoculum typically leads to pellet formation, while a dense inoculum results in dispersed growth. The initial pH of the medium (or in precultures) plays a role influencing the aggregation properties of the surface of the hyphae, with a more open mycelium at lower pH values. A strong agitation in stirred tank bioreactors forms free filaments rather than pellets but the maximum rate is limited as it causes physical damage to the mycelium. The use of microparticles affects the growth of filamentous organisms in liquid, changing the morphology from pellets to single hyphae (Walisko et al. 2012). The shear stress and consequent oxygenation of cultures grown in different types of flasks

affects morphology as well as production to a great extent (Gamboa-Suasnavart et al. 2011). The smaller pellet morphology obtained in baffled and coiled flask resulted in three-time higher production and higher glycosylation of the APA antigen from *Mycobacterium tuberculosis* in *S. lividans* when compared to standard flasks. This was successfully scaled up by changing the power input in a small scale bioreactor (Gamboa-Suasnavart et al. 2013).

Nevertheless, physical methods show some limitations as they create a mix of different morphologies and do not allow a precise control. Therefore, a rational genetic approach can be used to favor a specific phenotype in submerged cultures.

In *Streptomyces*, a specific case is represented by the overexpression of SsgA, a protein belonging to the SALP family and involved in septation during cell division and peptidoglycan maintenance (van Wezel et al. 2006). Enhanced expression of this protein led to a fragmenting phenotype in three species (*S. coelicolor*, *S. lividans* and *S. roseosporus*), clearly underlying a correlation between septation and the degree of fragmentation (see Fig. 2C for *S. lividans*). A fragmented phenotype presents a potential improvement for large scale liquid cultivations in terms of mass and nutrients transfer. In fact, the *S. lividans* SsgA overexpressing strain showed higher growth rates and a halved fermentation time, coupled to an increase in enzyme production when tyrosinase, a phenoloxidase, was used as a reporter. The effect on antibiotic production is less predictable. While enhanced expression of SsgA strongly enhanced the production of prodiginines, it completely blocked production of actinorhodin. This may be explained by the fact that undecylprodigiosin is produced during an earlier growth phase than actinorhodin, and that SsgA locks streptomycetes in an earlier phase of the life cycle (van Wezel et al. 2009).

Extending a rational genetic approach for a wider use is strongly depending on the current knowledge about genetic control and regulatory pathways. The *S. lividans* SsgA overexpressing strain is a clear example of scientific and industrial success towards the building of *Streptomyces* as a valuable alternative for commercial protein production (van Wezel and Vijgenboom 2003). Therefore, it is worthwhile to invest more research time to extend the knowhow on morphology related processes.

Secretion

Secretion pathways in Streptomyces

From a downstream processing point of view, heterologously expressed proteins can be best secreted into the fermentation broth. Therefore, increasing the secretion capacity is an important parameter towards optimization of the yield. The Sec pathway is the major secretion pathway in bacteria, and translocates unfolded proteins over the membrane (recently reviewed in (du Plessis et al. 2011). The Sec translocase is a highly flexible transmembrane channel constituted by a SecYEG heterotrimeric complex, associated to the motor protein SecA (Zimmer et al. 2008; du Plessis et al. 2009). Two different energy sources are used to create the mechanical motion: ATP and the proton motive force (PMF) (Driessen 1992). In *Streptomyces*, Sec-substrate proteins bind co-translationally to the signal recognition protein (SRP) prior translocation (Palacín et al. 2003). The substrate is gradually bound and released from the complex until the complete expulsion, followed by cleavage of the signal sequence.

The twin arginine translocation (Tat) presents a second secretion pathway. Firstly discovered in the thylakoid membrane of chloroplasts, it has been subsequently identified in the membrane of many bacteria and studied extensively in *E. coli*. For a detailed overview see Palmer and Berks (2012). The route takes its name from the two arginines present in the recognition sequence, which play a crucial role during recognition. The ability of the Tat pathway to translocate folded substrates makes it the preferred route for a number of proteins: (1) those who require the insertion of complex cofactors, (2) proteins that need to avoid competition of metal ions for binding to their cofactor site, (3) the transport of hetero-oligomeric complexes and (4) substrates that need accessory proteins in the cytoplasm for folding or maturation or cannot be kept unfolded after translation.

Homologues of *E. coli* Tat proteins, TatA, TatB and TatC, have been identified and characterized in *S. lividans* (Hicks et al. 2006). TatB and TatC have a key role in triggering the assembly of the complex and binding the substrate, while TatA is abundantly present in the membrane, oligomerizing into a ring shaped channel

suggested to act as a translocon (De Keersmaecker et al. 2005; De Keersmaecker et al. 2007). TatA is recruited by PMF, which is used as the only energy source. After transport, the protein is cleaved by a signal peptidase and the complex dissociates.

Recently, it was shown that during normal growth the Tat complex localises near the tips of growing hyphae (Willemse et al. 2012). The Tat complex shows a highly dynamic localization pattern, with more foci present along the hyphae including the tips. The assembly of the TatA complex was followed in time and space via a single particle tracking technique (Celler et al. 2013). Three different stages were identified in the assembly: an inert state followed by movement along the hyphae and wobbling prior final localization at about 2 μm from the tip. All these results confirm that Tat secretion occurs at the hyphal tips, in agreement to what is observed in fungi. The tip localization of TatABC suggests that increasing the number of apical sites and reducing branching and hyphal length would be a good strategy for enhancing the secretion of Tat-secreted enzymes. Indeed, increased fragmentation of the hyphae (which effectively increases the number of apical sites) resulted in enhanced secretion of the Tat substrate tyrosinase (van Wezel et al. 2006), which points at an intimate relation between morphology and secretion in *Streptomyces*. This example shows that better understanding of the behaviour, dynamics and localization of the proteins involved in secretion may lead to rational design of production hosts.

In contrast with most bacteria, substrate prediction programs revealed an exceptionally high number of Tat substrates in *S. coelicolor* genome: 129 proteins predicted by TATscan (Li et al. 2005) against 22 in *E. coli* (Dilks et al. 2003). The major role of this pathway in this organism is confirmed by proteomic studies on *tat* mutants in *S. coelicolor* (Widdick et al., 2006), with 25 out of 43 proteins verified as Tat-targeted. Moreover, 63 proteins were identified as Tat substrates in *S. lividans* (Guimond and Morosoli 2008), among which only 7 were expected from *in silico* prediction, and 47 out of the 73 proteins predicted from proteomic experiments in *S. scabies* were confirmed to be secreted through this pathway (Joshi et al. 2010). In addition, *S. lividans* mutants ΔtatB and ΔtatC showed a retarded development on solid media and a dispersed growth in liquid (Schaerlaekens 2004), underscoring that

proteins essential for morphological development are secreted via the Tat pathway. The evidence suggests a different and more important role of the Tat pathway in *Streptomyces* than in other bacteria. This assumes a particular relevance in case of production of recombinant proteins that might need to be exported in an active form or that fail to be secreted through the Sec system.

Enhancing heterologous protein production through secretion improvement

Reaching elevated yields of heterologous proteins is often impeded by the saturation of the secretion system. This paragraph will give a brief overview of the various strategies tested to enhance production levels through modification of the secretion capacity.

Enhancing secretion by simultaneous overexpression of the three components of the Tat pathway (TatA, TatB, TatC) proved to be an efficient tool in the case of xylanase C (XlnC) production in *S. lividans*, enhancing secretion of five fold (De Keersmaecker et al. 2006). The same strategy has been successfully tested in other bacteria such as *Corynebacterium glutamicum* (Kikuchi et al. 2009) and might therefore present a general way to improve protein secretion in various systems. The overexpression of Sec components could also present an alternative to increase protein secretion. However, the relative high number of proteins required for a functional Sec system seems to be a drawback. Only the overexpression of the core components SecYEG has been reported in *E. coli* (Douville et al. 1995), resulting in a 30 fold increase in translocation of the preprotein proOmpA.

Several experiments have shown that cross talk seems to exist between the Sec and Tat pathways, leading to an increase in secretion from one route when the other one is inactivated. This has been exploited in the case of the *S. lividans* TatB mutant, in which the Sec secretion of the human interleukin 10 (hIL10) showed a 15-fold increase compared to the wild type (Schaerlaekens et al. 2004). The opposite effect on Sec secretion has been observed in the TatABC overexpressing strain, with a strong reduction of XlnB secretion (De Keersmaecker et al. 2006). How the two secretion pathways communicate and how this is regulated is not understood.

Another interesting example of improvement of the secretion efficiency is presented by the overexpression of the phage shock protein A (PspA). Phage-shock protein response is a cell response activated in situation of stress such as phage infection, which causes dissipation of the proton motive force and alteration of redox state (reviewed in Joly et al. 2010). PspA, the main effector protein, reduces membrane depolarization and damage by blocking the proton leakage by a still unknown mechanism. A block in protein secretion is known to activate the response, although the exact nature of this interaction is still unclear. Recently, a PspA-TatA complex has been purified and analyzed in *E. coli*, suggesting an involvement of PspA in the control of membrane stress at active translocons (Mehner et al. 2012). The overexpression of PspA increased Tat dependent secretion in the case of XlnC and heterologous eGFP in *S. lividans*, while a limited effect (20%) was observed for the Sec pathway (Vrancken et al. 2007). This result is expected as the Tat translocation is solely dependent on the PMF, while the Sec translocation requires also hydrolysis of ATP. An increase in protein production through the Tat pathway in a *pspA* overexpressing strain is in accordance with experiments in *E. coli*, where the secretion of the exoglucanase (Exg) of *Cellulomonas fimi* was achieved, avoiding the previously reported saturation of the Sec system (Wang et al. 2011).

Proteolysis and product integrity

Proteolysis is a general mechanism to regulate levels of native proteins, removing the defective ones or inactivating them and recycling amino acids. In case of protein overexpression, proteolysis can be triggered due to folding problems and hamper final expression levels and protein integrity. The involvement of proteases in stress response after induction of heterologous protein expression has been well described in *E. coli* (Gill et al. 2000) and the use of protease-deficient mutants reduces protein degradation (Jiang et al. 2002).

Among streptomycetes, *S. lividans* has a lower level of endogenous secreted protease activity when compared to other strains. However, extracellular (Lichenstein

et al. 1992; Butler et al. 1995), intracellular (Butler et al. 1994) and mycelium-associated proteases (Binnie et al. 1995) are present. In *S. lividans*, a proteasome-deficient mutant proved to enhance protein production (Hong et al. 2005). The proteasome is an intracellular, self-compartmentalizing protease with confined proteolytic activity. It was first discovered in eukaryotes, followed by archaea and bacteria belonging to order of *Actinomycetales* such as *Streptomyces* (De Mot et al. 1999). A comprehensive review covering the different domains of life has been recently published (Maupin-Furlow 2012). The physiological role in bacteria is unclear, as no cellular targets have been identified and no physiological changes have been observed in the deficient mutants, neither in *Mycobacterium* (Knipfer and Shrader 1997) nor in *S. coelicolor* (Nagy et al. 2003) or *S. lividans* (Hong et al. 2005). However, the level of protein expression increased in *S. lividans* proteasome mutant compared to wild type strain in case of the human tumor necrosis factor receptor II (shuTNFR_{II}) and salmon calcitonin (sCT), while no effect was demonstrated on shuTNFR_I (Hong et al. 2005). These results suggest that protein expression may benefit from deleting the proteasome genes in the host.

In bacteria, proteins are tagged and directed to the proteasome by prokaryotic ubiquitin-like protein (Pup), similar to the ubiquitin system in eukaryotes (Burns and Darwin 2010). The pupylation mechanism is active in *S. coelicolor*, with 20 potential targets identified (P. Mazodier, J.L. Pernodet, personal communication). Therefore the pupylation system may be an interesting target for increasing heterologous protein production.

Despite the increase in protein expression obtained in a proteasome-deficient mutant, few studies describing the influence of the deletion of other proteolytic enzymes have been published so far. Several protease mutants of *S. lividans* were studied for their protein secretion but none of them showed a better protein secretion level than the wild type (Arias et al. 2007).

Fermentation

Optimizing fermentation of *Streptomyces* for its use at industrial level requires insights in more aspects than the already discussed growth and morphology related issues (vide supra). *Streptomyces* is generally cultivated in batch fermentation in stirred tank reactors with a blade turbine impeller. Usually, a dispersed mycelium is the predominant form in these cultures while pellets are formed in shake flasks. In addition to genetic engineering (van Wezel et al. 2006), bioreactor operating conditions such as agitation and aeration influence to a great extent growth, morphology, oxygen and nutrient transfer. The impact of hydrodynamics on *Streptomyces* cultures in shaking flasks and stirred bioreactors has been recently reviewed (Olmos et al. 2012).

A major limiting aspect for fermentation of filamentous organisms is the transfer of oxygen and nutrients. Especially for a strictly aerobic microorganism as *Streptomyces*, oxygen availability is a limiting step because of its diffusion at the gas-liquid interface and transfer to the center of the pellet. Due to the great interest in *Streptomyces* as an antibiotic producer, most of the fermentation studies are focused on the effects of oxygen on secondary metabolism rather than on production of primary metabolites or heterologous proteins. Antibiotic production is coupled with an increase in oxygen consumption and a higher dissolved oxygen tension enhances production (Olmos et al. 2012). Concerning primary metabolism, it has been demonstrated that in *S. lividans* strain producing mTNF α , the dissolved oxygen percentage dropped to approximately 10% compared to the 30% for the WT strain (D’Huys et al. 2011), demonstrating also in this case a higher oxygen consumption as seen for antibiotic production. This is in agreement with studies in *E. coli*, where more oxygen is needed for protein production (Özkan et al. 2005), while a positive effect of hypoxic conditions has been described for *Pichia pastoris* (Baumann et al. 2010).

One way to facilitate oxygen transfer is to increase the agitation rate, but this affects the rheology of the cultures, with fragmentation of the clumps, increase in viscosity, cell damage and even lysis. The dependence of morphology on the agitation

rate has been reported for *S. fradiae*, where a decrease in shear stress caused a shift in morphology from free filaments to pellets (Tamura et al. 1997). Cell lysis was also studied in correlation to the power input, a parameter that depends on agitation rate, airflow and reactor geometry. The effect of power input and consequent shear stress has been quantified for *S. clavuligerus* in batch cultivations with defined media, supplemented with different carbon and nitrogen sources (Roubos et al. 2001). The study led to the conclusion that this strain is extremely shear-sensitive and that cell lyses occurs even at low agitation rates. The identification of threshold values below which no major lysis was observed was strictly dependent on the medium composition, with mycelium grown on glutamate and maltose or succinate as the most sensitive to lysis. Moreover, the power input can also influence the morphology of the cultured strain and the production of post-translationally modified proteins. This is the case for the production of *Mycobacterium tuberculosis* APA protein in *S. lividans*, where a controlled agitation rate led to a higher degree of mannosylation compared to cultures in shake flasks (Gamboa-Suasnavart et al. 2013).

As an alternative to increasing the agitation rate, pure oxygen can be supplied during fermentation to increase the productivity without affecting the morphology of the culture. This is the case, for example, in the production of the immunosuppressant rapamycin in *S. hygroscopicus* (Yen and Hsiao 2013) where, despite a high requirement of oxygen, a high agitation rate resulted in pellet damage and lower production. Nevertheless, supplying pure oxygen is expensive and costs need to be carefully evaluated for commercial applications. It remains to be seen if this approach also works for protein production.

Beside the control of the bioreactor parameters, medium composition and nutrient dosing influence the efficiency of fermentation and protein production. This was demonstrated in early studies (Payne et al. 1990) where a continuous feeding of both glucose and tryptone led to a 25-fold increase in production for a *Flavobacterium* hydrolase in *S. lividans*, with an enhanced specific activity. Complex media increase protein production (Pozidis et al. 2001) and are usually preferred by industry for their low cost.

Various studies have dealt with the importance of the amino acid composition of the medium for different protein production platforms as *Saccharomyces cerevisiae* (Görgens et al. 2005b) and *Pichia stipitis* (Görgens et al. 2005a). The same approach has been applied to *Streptomyces*, unraveling the importance of amino acid supplementation in heterologous protein production. A systematic study based on a statistical set up identified aspartate, phenylalanine and methionine as the essential amino acids for the production of the recombinant human interleukin-3 (rHuIL-3) in a glucose-based medium (Nowruzi et al. 2008). Moreover, a metabolite analysis in *S. lividans* producing mTNF α (Kassama et al. 2010) identified seventeen metabolites at a higher level in the protein producing strain. Their role as energy source and in maintaining the membrane potential necessary for secretion was postulated.

Nevertheless, no clear connections with metabolism were demonstrated until recently, when the amino acid uptake in fed batch cultures for *S. lividans* producing mTNF α was described, representing the first link between biomass and protein production (D’Huys et al. 2011). The analysis of the wild type strain in minimal medium supplemented with a complex mixture of amino acids allowed the identification of two distinct growth phases: the first based on glutamate and aspartate consumption, and the second with glucose as the limiting substrate. Due to the unusual excess of nitrogen and glucose during fermentation, a lot of by-products as pyruvate, α -ketoglutarate, succinate and alanine were detected. In addition, lactic acid was produced during the entire growth, probably as a result of the limitation in oxygen in the central part of the pellets, resulting in a microaerobic environment. On the other hand, the analysis of the mTNF α producing strain showed a lower growth rate, formation of bigger clumps and a shift in metabolism. This was represented by an increase in lactate and a decrease in by-product formation as a consequence of the increase in pellet size, with a less active metabolizing biomass.

The metabolic network of *S. coelicolor* had been investigated at genome scale, allowing the identification of 121 genes essential for metabolism and the simulation of growth and antibiotic production in media with different carbon and nitrogen sources (Borodina et al. 2005). To expand the knowledge obtained in this study, a

genome scale metabolic model based on flux analysis in different limiting conditions (glucose-ammonium, amino acids, organic acids and alanine) was investigated (D’Huys et al. 2012). Depletion of glutamate and aspartate diminished growth rate and biomass formation with consequent increase in protein production. It is clear from these observations that a complex equilibrium exists in the metabolism of expression strains and that the type and availability of carbon and nitrogen sources need to be optimized to promote heterologous protein production at the expense of biomass formation or undesired metabolites.

To conclude, a general protocol for optimal fermentation parameters has not been written yet. Improvement of the process needs to be done experimentally on a case by case basis and strongly depends on multiple factors such as host, morphology, hydrodynamics parameters, medium composition and metabolism.

EXPRESSION VECTOR OPTIMIZATION

An efficient expression vector is an indispensable element to be combined with an engineered host for a maximum level of heterologous protein production. As for strain optimization, the design of an expression vector has to take into consideration all the possible processes that can be improved to get to a better protein production, with transcription, translation, posttranslational modification and secretion as the main ones. However, issues such as the selection used to maintain the plasmid, which is nowadays mainly done by antibiotic resistance, should be taken into account as well. The progresses in design of recombinant expression systems in actinomycetes have been reviewed (Nakashima et al. 2005). An overview of all the important elements is given in the following section.

Copy number

The vectors used for genetic manipulation in *Streptomyces* can be classified into two categories: integrative and multicopy (Kieser et al. 2000). The integrative vectors provide higher stability through integration into the genome using specific phage attachment sites. Based on the pioneering work of Maggie Smith, Keith Chater and

colleagues, in particular the attachment site for Φ C31 was exploited. This integration system found its way, among others, into the Eli Lilly vector pSET152 (Bierman et al. 1992) which is one of the most used vectors worldwide and revolutionized the field. Another frequently used vector system for genomic integration is based on pSAM2 (Pernodet et al. 1984; Smokvina et al. 1990). Although the integration should result in a single copy in the genome, expression from such vectors is often higher than expected, which may be explained by the fact that tandem integrations occur, with up to 10 integrations events at the same time (Combes et al. 2002). For industrial applications, integrative vectors may have the disadvantage of requiring antibiotic resistance markers. Therefore, strategies for genomic integration based on homologous recombination are a valuable alternative. Recently, major advances have been made in markerless integration of DNA into the genome of streptomycetes (Siegl and Luzhetskyy 2012).

The autonomously replicating vectors occur at high, medium or low copy, depending on the *ori*. Industry typically uses high copy number vectors, which in streptomycetes are based on the vector pIJ101, such as pIJ702 (Katz et al. 1983) and pIJ486 (Ward et al. 1986), with up to 300 copies per chromosome. *E. coli-Streptomyces* shuttle vectors are also available, and usually preferred to simplify cloning and amplification, although there are major stability issues. The multi-copy shuttle vector pWHM3 is so unstable that it is used for gene disruption strategies as it is lost at an extremely high frequency when antibiotic pressure is relieved (van Wezel et al. 2005). Recently, novel high copy shuttle vectors derived from pIJ101 have been constructed for protein overexpression: pL97 and pL98 were tested in protein production using *eGFP* and *redD* as reporters (Sun et al. 2012), while pZRJ362 produced a four fold increase in the enzyme activity of the endoglucanase Cel6A from *Thermobifida fusca* when *S. lividans* is compared to *Pichia pastoris* (Li et al. 2013).

Selection markers

The choice of a selection marker is usually restricted to antibiotics. However, *Streptomyces* is naturally resistant to several of them (chloramphenicol, tetracycline

and β -lactams) limiting considerably the choice. Moreover, the necessity of keeping a constant antibiotic selection pressure is undesirable for large-scale industrial processes due to the risk of contaminating the final product. Recently, a promising alternative represented by a toxin-antitoxin system has been functionally tested in *Streptomyces* (Sevillano et al. 2012). The system consists of two small proteins, which act as a toxin-antitoxin complex in which the first one is inactivated by the latter one. This mechanism is wide spread among bacteria and archaea, with up to 33 TA systems identified in *E. coli*, although their specific function in nature remains unclear. In *Streptomyces*, three different systems have been identified *in silico*. Among them, the proteins encoded by SCO2235/2236 in *S. coelicolor* have been studied and re-named YefM and YoeB by analogy to the YefM/YoeB system in *E. coli* (Sevillano et al. 2012). An *S. lividans* $\Delta yefM/yoeB$ null mutant strain carrying a copy of the toxin integrated in the genome and a copy of the antitoxin on a multicopy plasmid was tested for stable protein expression (Sevillano et al. 2013). High level of both xylanase and amylase were obtained. The expression system proved to be stable and to keep its expression level even after storage of the mycelium/spores, demonstrating the potential of this system as an alternative to antibiotic selection.

Promoters

A strong promoter resulting in a high level of transcript is an essential element in the design of an expression vector for optimal protein production. Very few promoters are known to be strong in *Streptomyces* and those that have been studied can be divided into constitutive and inducible (Table 1).

The inducible promoters have the advantage that production can be started when sufficient biomass is available, although the addition of an inducer is undesirable for industrial applications. Constitutive promoters such as the frequently used P_{ermE} and P_{vsi} do not show the same strength under all conditions and in all hosts and therefore are far from optimal. The addition of thiostrepton when using the inducible promoter P_{tipA} gives collateral expression of undesired proteins in *Streptomyces* genome that can saturate the expression machinery and thus have a negative effect on the production

Table 1 List of promoters in *Streptomyces* expression vectors

Gene	Product	Host	Reference
<i>vsI</i>	subtilisin inhibitor	<i>Streptomyces venezuelae</i>	(Lammertyn et al. 1997)
<i>ermE</i>	resistance gene to erythromycin	<i>Saccharopolyspora erythraea</i>	(Bibb et al. 1985)
<i>ssmp</i>	metalloendopeptidase promoter	<i>Streptomyces cinnamoneus</i>	(Hatanaka et al. 2008)
<i>pld</i>	phospholipase D	<i>Streptoverticillium cinnamoneum</i>	(Noda et al. 2010)
<i>actI</i>	actinorhodin biosynthetic gene cluster	<i>Streptomyces coelicolor</i>	(Rowe et al. 1998)
<i>dagA</i>	agarase gene	<i>Streptomyces coelicolor</i>	(Parro and Mellado 1993)
<i>nitA</i>	nitrilase inducible by ϵ -caprolactam	<i>Rhodococcus rhodochrous</i>	(Herai et al. 2004)
<i>amdS</i>	inducible acetamidase promoter	<i>Mycobacterium smegmatis</i>	(Triccas et al. 1998)
<i>tipA</i>	thiostrepton induced promoter	<i>Streptomyces lividans</i>	(Murakami et al. 1989)
<i>xysA</i>	xylanase A, xylose inducible	<i>Streptomyces halstedii</i> JM8	(Adham et al. 2001)
<i>tc</i>	tetracycline inducible promoter	<i>Streptomyces coelicolor</i>	(Rodríguez-García et al. 2005)

of the desired protein/enzyme. Further investigation and characterization of new promoters is therefore a must for the design of optimal expression vectors.

To characterize strong promoters, extensive studies were carried out in the past in bacteria as *E. coli*, leading to the identification of essential elements for binding of the RNA polymerase, namely the -35 box, the -10 box for recognition by σ factors, the region upstream (between roughly -60/-35) for binding of the α subunit of the RNAP and other regions that determine the local structure of the DNA (reviewed in (Hook-Barnard & Hinton, 2007)). However, the specific elements involved in promoter strength in *Streptomyces* are still largely unknown. More than a hundred sequences directly upstream from mapped transcriptional start sites have been compared (Strohl 1992; Bourn and Babb 1995), showing a wide variety of features with only a small group of *E. coli*-like promoters, while the majority did not resemble any known prokaryotic promoters. In *Streptomyces*, the work is complicated

by the existence of a large number of σ factors, such as the 66 σ factors encoded by the *S. coelicolor* genome, most of which are so-called ECF σ factors for extracellular functions (Bentley et al. 2002). This large number sharply contrasts with the seven σ factors found in *E. coli* (Pérez-Rueda and Collado-Vides 2000). Some of the σ factors are developmentally controlled, like *bldN* and *sigF* (Kelemen et al. 1996; Bibb et al. 2000) or activated in response to different stimuli (reviewed in Gruber & Gross 2003).

Despite the interest in *Streptomyces* as an industrial host, few studies have been published in the last years on the identification of new strong promoters. An interesting study was provided by the Virolle group (Seghezzi et al. 2011), who created a synthetic library of randomized promoters based on the promoter for the household σ factor RpoD (σ^{70} or σ^{HrdB}). The results showed an over-representation of the guanine nucleotide in strong promoters in the -10 region and the -35 region, in addition to a motif related to an “extended -10 region”, an imperfect repetition particularly important in *E. coli* for recognition and positioning of the RNA polymerase. The abundance of guanine residues can be explained by the high GC-content in *Streptomyces* strains, which might have led to an evolution driven towards highly G-rich strong promoters. The synthetically derived consensus sequence shows remarkable sequence similarity to P_{ermE} although none of the identified clones showed higher strength.

Recently, a combination of rational and random mutagenesis of the promoter of *kasO*, which encodes the pathway-specific transcriptional activator gene for the cryptic type-I polyketide Cpk, led to the design of a stronger version of the promoter when compared to the original P_{kasO} or P_{ermE} (Wang et al. 2013). The promoter is recognized by the σ^{HrdB} and repressed by the concerted action of two regulatory proteins, ScbR and ScbR2. The ScbR/ScbR2 binding site was deleted by rationally truncating the sequence up to an optimal length, while the second repressor binding site for ScbR2 was situated in an essential part of the sequence and was therefore inactivated by random mutagenesis. The recombinant promoter showed a higher strength both in *E. coli* and *Streptomyces* with luciferase and the antibiotic actinorhodin used as reporters, respectively. Such promoter optimization strategies

could be followed up for other vector-promoter systems. Moreover, this study also underlined the importance of the 20 nucleotides upstream of the -35 region (where the α subunit of the RNAP binds) and of the 18 nucleotide spacer between the -35 and -10 region, as substantial modifications in nucleotide composition or length strongly affected promoter activity.

Strong transcriptional elements from species other than streptomycetes can be tested as well for their efficiency. The mostly used expression system in *E. coli* is the T7 system based on the T7 bacteriophage polymerase and promoter. An *S. lividans* expression strain based on the same system has been created, combining the ability of transcribing large fragments of DNA with a high copy number pIJ101-derivative vector (Lussier et al. 2010). Nevertheless, no applications are reported in literature for protein expression at present.

In addition to a high level of transcription, the control of gene expression is sometimes also desirable for protein expression, for instance when the product has a negative effect on growth or is even lethal. An example of such control elements are riboswitches. Riboswitches are sequences present at the 5' end of a transcript and made of a ligand-binding/sensor domain and an expression platform. Upon binding of specific ligands, they adopt an altered conformation resulting in activation or repression of transcription or translation (Serganov and Nudler 2013). In *Streptomyces*, recent work has shown the applicability of the synthetic design of such sequences. The efficiency of at least two of the six tested theophylline-dependent riboswitches derived from *B. subtilis* was demonstrated in combination with three different promoters (P_{gal2} , P_{ermE} and SF14). Gene expression could be activated in a dose-dependent manner up to 260 fold, confirming the technique as a promising tool to regulate protein expression in *Streptomyces* (Rudolph et al. 2013).

In this thesis, a rational approach towards the identification of strong, constitutive promoters was tested based on RNA-Seq and microarray data (Chapter 5). With this approach, three sequences were identified with strength higher or comparable to P_{ermE} when tested for the production of a small laccase in *S. lividans*. These sequences were the promoters of SCO1947 for glyceraldehyde-3-phosphate

dehydrogenase (GADPH), SCO3484 encoding a sugar binding protein and for SCO4253 for an uncharacterized protein.

Ribosome binding sites and codon usage

The next step in the design of an expression vector is to optimize the translation of the transcript. Two of the main factors to be taken into account are: an efficient Ribosome Binding Site (RBS) and the codon usage. The RBS sequence is involved in binding and correct positioning of the ribosome. Typically, the RBS is located between 5-12 nucleotides upstream of the start codon, and has the consensus sequence AGGAGG, complementary to the sequence 5'-CCUCCU-3' at the 3' end of the 16S rRNA. In *Streptomyces*, analysis of the interaction with the ribosome showed that a high complementarity is not required (Strohl 1992). In addition to this, some genes do not show any obvious RBS in the 20 nucleotides sequence upstream of their translational start, implying that the binding to this region is not a prerequisite for ribosome translation. A well studied example is the *ermE* gene, encoding the 23S rRNA methylase of *Saccharopolyspora erythrae*, where the transcript initiates at the translational start codon without any sequence upstream for ribosome recognition (Bibb et al. 1994). In other cases, two putative translational starts are preceded by a RBS-like sequence (as for mannase, cellulase A, chitosanase, subtilisin inhibitor and esterase genes) (Morosoli et al. 2006). Evidence suggests that both RBS's might be used as a way to increase the efficiency of protein translation, with two ribosomes binding the same mRNA molecule.

In *Streptomyces* the most often used RBS is obtained from the *tuf1* gene from *S. ramocissimus*, which encodes the highly expressed elongation factor EF-Tu1. This ribosome binding site and linker have been cloned downstream of the *ermE* promoter (Motamedi et al. 1995) and use of his ribosome binding site allows very efficient recruitment of the ribosome (van Wezel et al. 2000a).

Codon usage has a strong influence on the efficiency of translation. Heterologous mRNA species have a high probability of containing rare codons when moved to another host (Gustafsson et al. 2004). This is particularly relevant in

Streptomyces, which has a high G+C content, and is reflected by a strong bias towards G or C in the second and third (wobble) codon positions. As a result expression of genes from lower G+C organisms such as *E. coli* and *B. subtilis* can be less efficient. Moreover, the translation of some rare codons such as the leucine codon TTA are strictly regulated by development (Takano et al. 2003). Codon modification has been reported to increase expression of heterologous proteins in *E. coli* between 5- and 15-fold (Gustafsson et al. 2004). Several reports on codon optimization for reporter enzyme systems such as *lux* (Craney et al. 2007), eGFP (Sun et al. 1999), *creA* (Fedoryshyn et al. 2008) or signal sequences (Zhu et al. 2011) have been published but none of them was aimed at high level protein production.

Signal peptides

The transport across the membrane is another target for modification to obtain maximal yield of heterologous proteins. In addition to the strategies discussed before in this chapter, the choice of an appropriate signal peptide has as well a strong influence on directing protein secretion. Sec signal peptides such as the one derived from the subtilisin inhibitor of *S. venezuelae* (*vsi*) and the cellulase A (*celA*) from *S. lividans* are most frequently used. The *vsi* signal peptide was successfully used for the production of high levels of TNF- α (Lammertyn et al. 1997) while *celA* signal peptide increased the production of xylanase A (XlnA) (Pagé et al. 1996). Including a Tat pathway signal sequence in the expression construct is a prerequisite when expressing proteins that require folding and/or cofactor incorporation prior to secretion, as in the case of GFP (Thomas et al. 2001; Santini et al. 2001; Vrancken et al. 2007). As mentioned above, *Streptomyces* have the highest number of predicted Tat substrates. However, results of protein secretion through this route have not always been promising. The mouse tumor factor α (TNF α) and the human interleukin-10 (hIL10) were fused to the Tat signal peptide of *xlnC* of *S. lividans* and of the tyrosinase chaperone *melC1* from *S. antibioticus*, but the levels of production were not competitive with the secretion via Sec by the *vsi* signal peptide (Schaerlaekens et al., 2004). Recently, a novel expression

vector has been tested for the production of human interleukin-6 (IL-6) in *S. lividans* (Zhu et al. 2011). The signal peptides of MelC1 and of CagA were tested and only the latter turned out to support secretion of IL-6. Attempts to obtain better Tat secretion of XlnC by using a number of other Tat signal sequences identified by various prediction programmes were not successful. Moreover, a mutation analysis of the signal peptide of XlnC did not result in more efficient secretion, suggesting that at least this signal sequence is already optimal (Li et al. 2006). Positive results using the Tat pathway were obtained recently, when 25 degrading enzymes of *Thermobifida fusca* and *S. lividans* were analyzed for secretion in *S. lividans* (Miyazaki et al. 2013). Using a cytoplasmic enzyme, β -glucosidase from *T. fusca*, as reporter, 17 promising signal peptides for both the Sec and Tat pathway, were tested if they could drive secretion of the reporter. The Sec signal of phospholipase D was used as reference (Noda et al. 2010). Three Tat-dependent signals, including the XlnC signal peptide, showed higher enzyme secretion.

Gauthier et al. (2005) showed that secretion of xylanase B1, through the Tat and Sec pathway in one transformant resulted in the sum of the enzyme levels obtained from transformants using only one of the secretion systems. In this way, the maximum secretion capacity of the host is utilized and therefore a promising approach if applicable to other enzymes.

CONCLUSION

Generating a general *Streptomyces* host capable of efficient high level enzyme production has come a long way but is far from complete, in particular when compared to the extremely efficient vector-host combinations for production platforms such as *E. coli* and *B. subtilis*.

From a morphological point of view, a balance needs to be reached between reducing pellet size and preventing high viscosity due to fragmentation or mycelial mat production. The first steps in this process have been established and the focus can now be set on creating strains that have the ultimate submerged culture morphology. Testing and selecting different fermentation parameters will be strictly dependent on the chosen strain and desired product. Moreover, the tool box for the design of strong expression vectors has been expanded in the last decade and now contains sufficient parts to assemble expression vectors to meet the needs of a given production system.

Since the publication of the complete genome of *S. coelicolor* in 2002 (Bentley et al. 2002), a fast improvement in last generation sequencing has occurred, allowing a large number of streptomycetes genome sequences being available (<http://www.genomesonline.org>). This increasing volume of data has rapidly led to post-genomic and system biology studies in this organism. Integrating the results coming from these different techniques is a potent tool, on the one hand to identify novel actors in morphogenesis and, on the other hand, to study metabolism and growth during fermentation and protein production. Overall, this combinative approach might lead in the future to a substantial strain improvement for industrial purposes.

A comment on the best *Streptomyces* production host that can be assembled at this moment can be found in the General Discussion section of this Thesis.

Chapter 3

Apical synthesis of an extracellular polysaccharide involved in aerial growth and hyphal attachment of *Streptomyces lividans* depends on CslA and GlxA

Giulia Mangiameli, Gilles P. van Wezel, Marloes L.C. Petrus, Joost Willemse, Clotilde Pilot, Giulia Colombo, Erik Vijgenboom and Dennis Claessen

Revised manuscript in preparation

ABSTRACT

Extracellular polysaccharides are produced by many microorganisms and play pivotal roles in various aspects of their biology. The cellulose synthase-like protein (CslA) synthesizes a β -(1,4)-glycan at hyphal tips in the filamentous bacterium *Streptomyces coelicolor*. Here we show that the downstream located *glxA*, which encodes a radical copper oxidase, acts in conjunction with *cslA* in the production of a β -(1,4) glycan in *Streptomyces lividans*, and is required for its apical localization. The extracellular glycan becomes microscopically visible as fibrillar structures upon binding to a chimeric eGFP-chitin-binding domain fusion protein, suggesting that it consists at least in part of chitin. Perhaps as a consequence of the failure to produce the glycan polysaccharide, colonies of *S. lividans cslA* and *glxA* mutants could not grow invasively into the agar and were developmentally arrested. In liquid-grown cultures, *cslA* and *glxA* mutants did not form pellets but rather produced open mycelial networks. Taken together, our data demonstrate the involvement of *cslA* and *glxA* in the control of mycelial architecture in liquid- and solid-grown cultures.

INTRODUCTION

Streptomycetes are filamentous soil-dwelling bacteria, which establish branched networks of vegetative hyphae. When nutrients become limiting, a developmental program is initiated, producing on solid media erect aerial hyphae that eventually differentiate to generate chains of spores, which are then dispersed. Unlike unicellular bacteria, which grow by lateral wall extension, growth of *Streptomyces* hyphae occurs at the hyphal tips, and exponential growth is achieved by combination of tip growth and branching. A pivotal role in the control of apical growth is exerted by the polar-localized protein DivIVA, which orchestrates cell wall synthesis (Flårdh et al. 2012). DivIVA is part of a larger so-called tip-organizing center (TIPOC) and in recent years, several proteins and complexes have been identified that are (transiently) localized at the hyphal tip. These include the cytoskeletal protein Scy (Holmes et al. 2013), the Tat secretion system (Willemse et al. 2012) and the cell wall remodeling protein SsgA (Noens et al. 2007). Furthermore, new chromosomes are also replicated near the tip in so-called replisomes (Wolanski et al. 2011). This complex TIPOC likely ensures that all apical processes, such as DNA replication and cell wall synthesis, are carried out in coordinated fashion, while cell damage is prevented (Ditkowski et al. 2013; Fuchino et al. 2013).

The TIPOC protein CslA, which stands for cellulose synthase-like protein (Bentley et al. 2002), plays multiple roles in growth and development; mutants lacking the *cslA* gene fail to form aerial hyphae and are affected in attachment to solid surfaces (Xu et al. 2008; de Jong et al. 2009). Furthermore, CslA plays an important role in the morphology of mycelial clumps in liquid cultures (Xu et al. 2008; van Veluw et al. 2012). CslA is classified as a family 2 glycosyltransferase (GT2, <http://www.cazy.org/>). This family does include cellulose synthases but also chitin synthases and other polysaccharide synthases. The polymers produced by these synthases have many different functions, often directed at providing structural integrity.

Cellulose is the most abundant natural polymer on earth and present in plants, where it provides strength to the cell wall (Bringmann et al. 2012), and

in bacteria (Römling 2002), where it contributes to the formation of biofilms and plays a role during infection (Beloin et al. 2008). For instance, *Rhizobiaceae* produce cellulose to adhere to plants (Smit et al. 1992), while *Salmonella* spp. and *Escherichia coli* require cellulose for virulence (Zogaj et al. 2003; White et al. 2003; Saldaña et al. 2009). Like cellulose, chitin typically also has a structural role (Martinez et al. 2009). In fungi chitin is a major component of the cell wall, where it plays crucial roles in tip growth, cytokinesis, spore formation and also pathogenicity (Latgé 2007; Lenardon et al. 2010). It is also produced in pathogenic amoebae, in parasitic nematodes and is abundantly present in the exoskeletons of invertebrates (Merzendorfer 2011). In *Streptomyces*, chitin is found among others in the spore coat (Smucker and Pfister 1978; Gomes et al. 2008).

The polysaccharide synthesized by CslA has not yet been characterized. Typically, genes involved in bacterial cellulose synthesis are organized in an operon, containing the *bcsABCD* genes (Römling 2002). However, *Streptomyces* lacks a c-di-GMP binding protein (BcsB), which is essential for the synthesis of cellulose according to the currently accepted model (Ross et al. 1991). Interestingly, *cslA* is translationally coupled to *glxA*, which encodes a radical copper oxidase that requires for its activity the Cu cofactor and the formation of a characteristic Tyr-Cys covalent bond. GlxA has weak homology to galactose oxidases and does not utilize galactose efficiently as substrate (Whittaker and Whittaker 2006). Besides in streptomycetes, this particular gene organization is only found in the myxobacterium *Stigmatella aurantiaca*, where deletion of either *fbfA* or *fbfB* hampers fruiting body formation following starvation (Silakowski et al. 1996). While *cslA* and *glxA* mutants of the model streptomycete *Streptomyces coelicolor* are blocked in development on rich media (Liman et al. 2013), the functional correlation of these two genes has not yet been clarified.

In this work, we show that GlxA cooperates with the synthase CslA in forming a β -(1,4)-glycan, presumably chitin-like, that is deposited at the hyphal surface fulfilling multiple roles in growth and development.

RESULTS

Conserved gene synteny around *cslA*-*glxA* in streptomycetes

The overlapping *cslA* and *glxA* genes of *S. coelicolor* encode the cellulose synthase-like protein CslA (SCO2836) and the radical copper oxidase GlxA (SCO2837), respectively. In *S. lividans*, the equivalent gene cluster consists of SLI_3187-3189 (Cruz-Morales et al. 2013) (Fig. 1).

Transcriptome analysis performed in our laboratory (Chapter 4) shows that *cslA* and *glxA* have similar expression levels in both *S. coelicolor* and in *S. lividans*, supporting the idea that *cslA*-*glxA* form an operon. *cslA*, *glxA* and SCO2838-SLI3190, encoding a polysaccharide hydrolase, are likely functionally linked and present in nearly all streptomycetes. Interestingly, some of them, including *S. griseus* and *S. albus*, have a second copy of the *cslA*-*glxA* operon elsewhere on the genome, with 54 and 66% end-to-end amino acid identity between the paralogous of CslA and GlxA proteins in *S. griseus*, respectively (not shown).

In terms of broader gene synteny, it is interesting to point at the following genes that are found in close proximity to *glxA*-*cslA* in nearly all streptomycetes: *chb* (SCO2833/SLI_3182), for a chitin binding protein that is part of the chitinolytic system of *S. coelicolor* (Schrempf 2001; Colson et al. 2007), SCO2834/SLI_3183 for a flotillin domain protein implicated in localizing multiprotein complexes to the membrane, SCO2835/SLI_3184 for a peptidoglycan binding protein, SCO2841/SLI_3192 for sortase E and SCO2843/SLI_3194 for a sugar hydrolase related to N-acetylglucosamine deacetylase (Table 1). Thus, at least two genes near *cslA*-*glxA* correlate to chitin or its subunit N-acetylglucosamine.

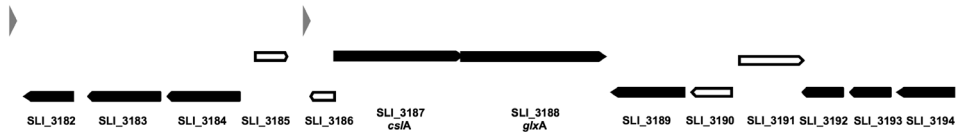


Figure 1. Gene organization around the *csIA-glxA* operon.

The gene context of the chromosomal locus around *csIA* and *glxA* i. The filled arrows represent genes that are conserved in nearly all streptomycetes. The open arrows represent genes that are not conserved, while the grey arrowheads represent tRNA loci.

Table 1. Annotation and gene numbers in *S. lividans* and *S. coelicolor*.

<i>S. lividans</i> gene #	<i>S. coelicolor</i> or gene #	Annotation
SLI_3182	SCO2833	Chb, Copper-dependent lytic polysaccharide monooxygenase (LPMO); chitin binding domain; AA10 family1
SLI_3183	SCO2834	Penicillin acylase/amidohydrolase, flotillin
SLI_3184	SCO2835	Protein with C-terminal putative peptidoglycan binding domain
SLI_3185		doubtful ORF
SLI_3186		doubtful ORF
SLI_3187	SCO2836	CsIA, Glycosyl Transferase Family 21
SLI_3188	SCO2837	GlxA, Radical copper oxidase
SLI_3189	SCO2838	Glycosyl Hydrolase Family 6
SLI_3190	SCO2839	Lipoprotein
SLI_3191	SCO2840	LysR-family transcriptional regulator
SLI_3192	SCO2841	Peptidase C60 Family, Sortase E
SLI_3193	SCO2842	Putative substrate of SCO28412
SLI_3194	SCO2843	Sugar (GlcNAc-6P) phosphatases of the HAD superfamily

The csIA and glxA mutants are stalled in development and are hampered in agar invasion

To study the role of *csIA* and *glxA* in growth and morphogenesis of *S. lividans*, deletion mutants were constructed (see Material and Methods) and grown on different media (Fig. 2). Unlike *S. coelicolor* A3(2), *S. lividans* 1326 is delayed in development when grown on R5 agar plates, but the development can be stimulated by adding 2-10 μM Cu(II) to the medium (Fig. 2A and (Keijser et al. 2000). Null mutants of *csIA* or *glxA* in *S. lividans* failed to form aerial hyphae on R5 agar plates with 10 μM copper. In

contrast, development of the mutants was comparable to that of the parental strain when grown on MS agar plates. Development of the mutant was restored when a copy of the respective genes, expressed from the *csIA* promoter, was re-introduced (Fig 2A). This shows that the mutant phenotypes were specifically caused by absence of *csIA* or *glxA*.

Notably, the mycelia of *csIA* and *glxA* mutants had lost the ability to adhere to and grow into the agar (Fig. 2B). As a result, colonies of the mutant strains could easily be removed from the agar surface. Introduction of a copy of the respective wild-type genes restored the ability of colonies of the *csIA* mutant and (although to a somewhat lesser extent) of the *glxA* mutant to grow into the agar (Fig. 2B).

CslA and GlxA control pellet architecture in liquid-grown cultures

The *S. coelicolor csIA* mutant was previously shown to form significantly smaller pellets than the wild-type strain (Xu et al. 2008; van Veluw et al. 2012). To see if the same was true for a mutant lacking the *glxA* gene, the morphology of the *csIA* and *glxA* null mutants was compared to that of the parental strain *S. lividans* 1326 in YEME and TSBS liquid-grown cultures (Fig. 2C). This revealed that like *csIA* mutants, *glxA* mutants also formed less dense pellets in YEME. The most striking effect was observed in TSBS medium, wherein the mutants formed open mycelial networks (mycelial mats) rather than the clumps typical of the parental strain. These results indicate a role for CslA and GlxA in pellet architecture. In addition, the similarity between the phenotypes of the *csIA* and *glxA* mutants in liquid-grown cultures further supports functional linkage between the two genes.

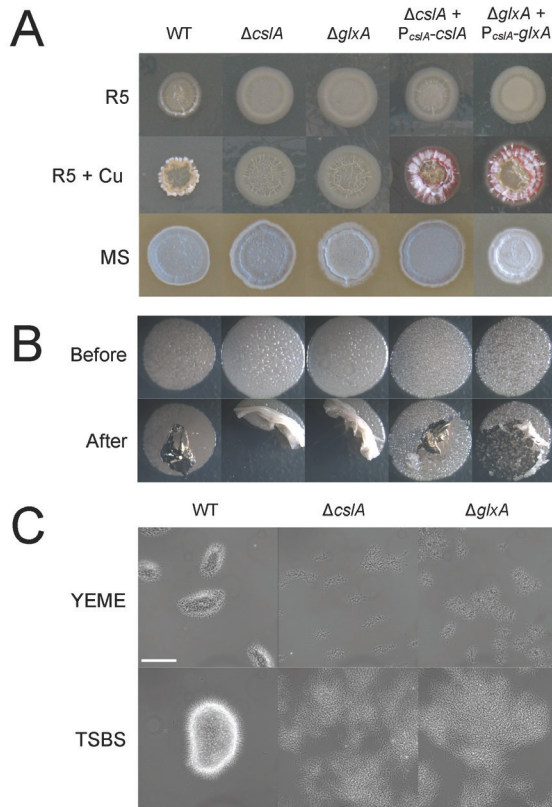


Figure 2. Morphology, copper dependency and hyphal attachment of *csIA* and *glxA* mutants in *S. lividans*.

(A) The wild type, *csIA*, *glxA* mutants and the mutants complemented with a plasmid expressing the corresponding gene (pGMMP3 and 4) were grown for 4 days on R5, R5 supplemented with $10\mu\text{M}$ Cu(II) and MS. Drops of $10\mu\text{L}$ containing 1000 spores were spotted on the plates followed by incubation at 30°C . Both the mutants and the complemented strains are bald on R5, while the wild type strain is entering aerial growth (top row). Supplementing the R5 medium with $10\mu\text{M}$ Cu(II) does stimulate development in the wild type and complemented strains, but not in the mutants (middle row). Note that on both R5 and R5 supplemented with Cu(II) the wild type grows in a more compact manner than the mutants and the complemented mutants. All the strains do produce spores on MS medium (bottom row).

(B) The ability of the mycelium to invade the agar resulting in attachment of the mycelium to the agar is demonstrated on Nutrient Agar. The top row shows the growth of the spotted spores before the attempt to lift the mycelium with a flat toothpick. The bottom row shows the result after the lifting attempt. The wild type is growing into the agar, while the two mutants do not and their mycelium can be lifted/removed as an intact sheet. Growth inside the agar is fully restored in the complemented *csIA* mutant but only partially in the complemented *glxA* mutant. The same effect was observed on R5 media (data not shown).

(C) The wild type and the *csIA* and *glxA* mutants show very different mycelium morphology in liquid cultures after 24 hrs of growth. The two mutants are growing in smaller and more open clumps in YEME (top) and they show a completely open phenotype in TSBS (bottom). The wild type on the other hand shows the familiar dense mycelium structure. Complemented mutants have wild type pellet size and morphology (data not shown). Bar size: $150\mu\text{m}$

GlxA and CslA colocalize in two distinct positions in hyphal tips

To localize CslA and GlxA, CslA-eGFP and GlxA-eGFP fusion proteins were studied by fluorescence microscopy, using a low autofluorescent *S. lividans* derivative, 1326-FM, as a host. This strain was isolated by a similar selection procedure as for the low autofluorescent derivative of *S. coelicolor* (Willemse and van Wezel 2009). To create the chimeric genes, either gene was cloned without its stop codon upstream of the gene for eGFP in low-copy number shuttle vector pGFP-strep, behind the *cslA* promoter for *cslA-egfp* or the *ftsZ* promoter for *glxA-egfp* (see Materials and methods).

CslA is a predicted membrane protein, with six membrane-spanning domains and a cytoplasmic catalytic domain (<http://www.cbs.dtu.dk/services/TMHMM/>). Consistent with previous results, CslA-eGFP localized in bright foci at the hyphal tips of *S. lividans* 1326-FM (Fig. 3A). In addition to the bright foci at the tips, many additional but less intense foci were always observed throughout the hyphae. Furthermore, its localization was not dependent on GlxA, as a similar localization pattern was observed in a *glxA* mutant derivative of 1326-FM. However, around six times more foci of the CslA-eGFP fusion were observed in the *glxA* null mutant (Fig. 3B). In agreement, semi-quantitative RT-PCR analysis confirmed that the number of *cslA* transcripts was some 7.5-fold enhanced when *glxA* was deleted (Fig. 3C).

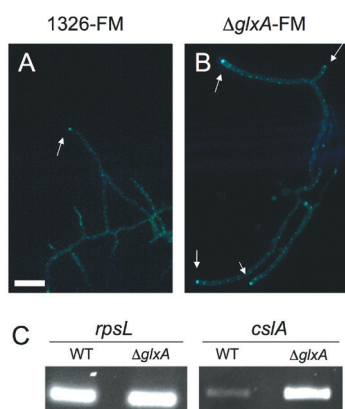


Figure 3. Hyphal tip localization of CslA-eGFP.

Localization of CslA-eGFP in *S. lividans* 1326-FM (A) and in *glxA*-FM (B) was studied with fluorescence microscopy after the strains were grown for 24 hrs on MS. CslA localizes at the tips of the hyphae (arrows) and does not require GlxA. (C) RT-PCR analysis of the amount of *cslA* transcripts in the wild type and $\Delta glxA$ strain grown for 24 hrs on MS. The *rpsL* gene encoding ribosomal protein S9 is used as an internal control. In the *glxA* mutant, 7.5 times more mRNA of *cslA* is detected. This is consistent with the amount of fluorescence observed with the CslA-eGFP construct in the *glxA* mutant which is approximately six-fold up. Bar, 5 μ m.

GlxA contains a predicted N-terminal transmembrane helix that likely acts as a membrane anchor. Mycelium fractionation followed by Western blot analysis with anti-GlxA antibodies showed that about half of GlxA resides in the insoluble fraction, whereas the other half is soluble (Fig. 4A). It was previously suggested that a putative C-terminal sortase sequence could anchor GlxA to the peptidoglycan layer (Whittaker and Whittaker 2006), and a gene for sortase E is in close proximity in all streptomycetes. To establish the role for the putative sortase signal in anchoring of GlxA, a recombinant GlxA protein lacking the C-terminal 35 residues, including the putative sortase sequence, was expressed, but the proportion of the truncated protein found in the insoluble fraction was similar as for wild-type GlxA (Fig. 4A).

Like CslA-eGFP, GlxA-eGFP localized as bright foci at apical sites, and also for GlxA-eGFP many less intense foci were observed further away from the tips. Apical sites also stained intensely with fluorescent wheat germ agglutinin (f-WGA), which binds to N-acetylglucosamine subunits from among others precursors of peptidoglycan or chitin (Wright et al. 1991; see arrow in Fig. 4B). Further away from hyphal tips, at subapical sites that are by definition the older parts of the hyphae, GlxA-eGFP foci and f-WGA staining frequently did not overlap (arrowhead in Fig. 4B). To analyze the relative spatial localization of CslA and GlxA foci, their distances from the hyphal tip were assessed, relative to the f-WGA staining (Fig. 4C). Analyzing at least 40 tip located foci revealed that both CslA-eGFP and GlxA-eGFP localize in two distinct positions, one precisely in the hyphal tip, and a second at some distance (around 0.5 μm) behind the tip.

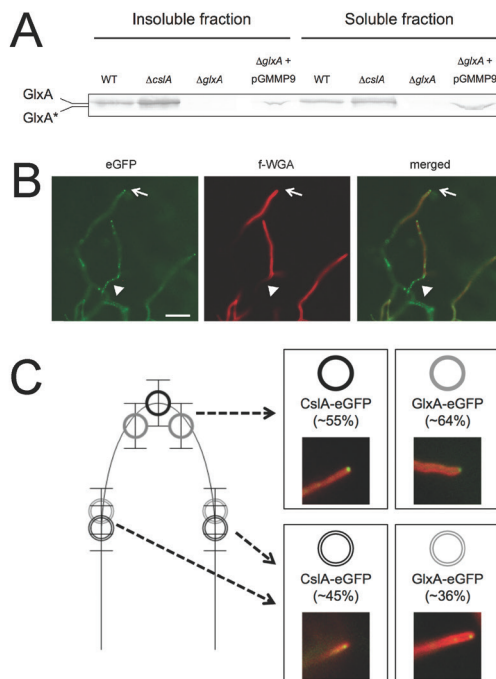


Figure 4. Localization of GlxA in *S. lividans*.

(A) Western blot analysis with anti-GlxA antibodies on the insoluble and soluble fraction of mycelial extracts. Strains were *S. lividans* 1326, its *cslA* and *glxA* mutants and the *glxA* mutant harboring pGMMP9. The latter plasmid contains the gene for a truncated GlxA (designated GlxA*) lacking the C-terminal 35 residues. The strains were grown for 24 hrs on solid MS. GlxA (around 71 kDa) is present in the insoluble and soluble fractions of the wild type strain and in the *glxA* mutant harboring pGMMP9, enhanced in the *cslA* mutant, but absent in the *glxA* mutant. Sample loading was adjusted to the wet weight of the mycelium and the cytosolic fraction is two-fold diluted as compared to the membrane fraction.

(B) Localization of GlxA-eGFP in *S. lividans* 1326-FM was studied with fluorescence microscopy, and in conjunction with staining with the lectin fluo-WGA (f-WGA, middle column). Right column shows the merged images. GlxA localizes at the tips of the hyphae (arrows). f-WGA staining is also observed at the tips, as well as further away from apical sites. Hyphal sections with GlxA-eGFP foci further away from the apical site (arrowheads) are not always stained with f-WGA. Bar size: 5 μ m

(C) Fluorescence micrographs and derived cartoon of the localization of CslA-eGFP (black circles) and GlxA-eGFP (grey circles) in *S. lividans*. Both proteins show localization at the tip ($60 \pm 5\%$ of the foci) or localization away from the tip ($40 \pm 5\%$ of the foci). For each of the fusion proteins 40 foci were analyzed.

CslA and GlxA ensure the production of a polysaccharide at hyphal tips

It was shown previously that CslA is required for the accumulation of a β -(1,4) polysaccharide at apical sites during vegetative growth, identified by the fluorescent dye calcofluor white (CFW) (Xu et al. 2008; de Jong et al. 2009). This dye binds to a range of β -(1,4)-linked polysaccharides including cellulose and chitin (Herth and Schnepf 1980). Staining of wild-type mycelium of *S. lividans* revealed fluorescence of CFW in approximately 60% of the hyphal tips. Notably, stained hyphal tips were invariably swollen (see arrows in Fig. 5). Accumulation of CFW, as well as tip swelling, was completely absent in the *S. lividans cslA* and *glxA* null mutants grown on solid medium (Fig 5). However, while accumulation of CFW at hyphal tips was absent in the *glxA* mutant, bright fluorescence was frequently detected at subapical sites (arrowheads). Similar results were obtained in liquid-grown cultures (not shown). These results show that GlxA is involved in the biosynthesis and/or modification of the same β -(1,4) polysaccharide produced by CslA at apical sites.

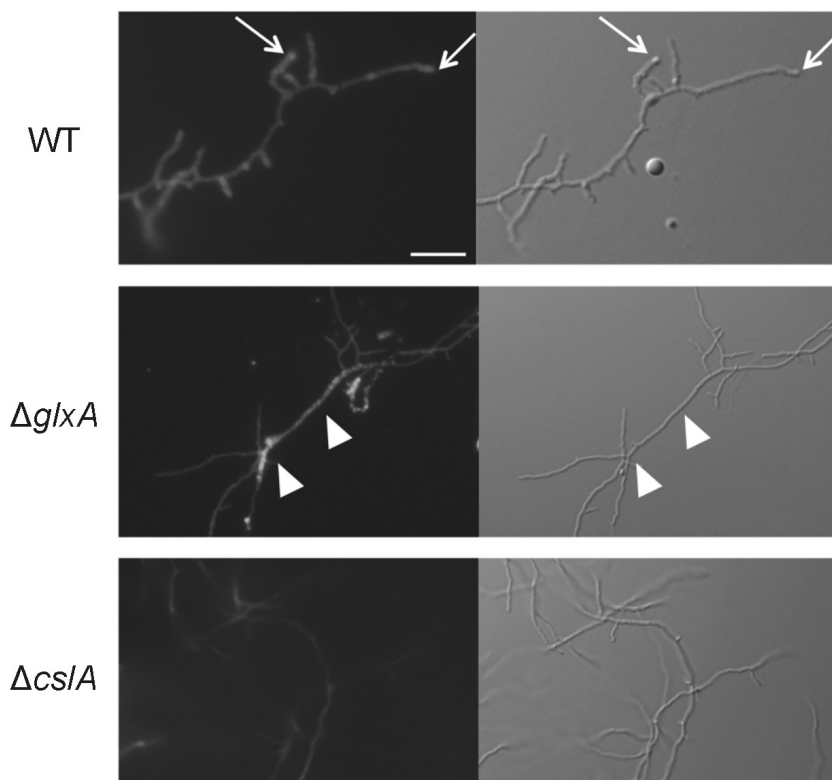


Figure 5. Visualization of β -(1,4) glycan production by calcofluor white (CFW) staining.

The wild type strain (top), and its *glxA* (middle) and *csIA* (bottom) mutants were grown for 24 hrs on MS agar plates and subsequently stained with CFW. Left panel, fluorescence micrograph; right panel, bright field image. CWF revealed accumulation of polysaccharides at the apical sites of the wild-type strain. In *glxA* null mutants, CFW failed to stain the tips, and instead accumulated in older sections of the hyphae (arrowheads). No CFW staining (other than occasional background fluorescence) was observed in the *csIA* mutant. Note the widening of apical sites of wild-type hyphae (arrows) due to the binding of CFW, indicative of CFW-induced lysis, which was not seen in either mutant incubated in precisely the same manner. The same results were observed on R5 media (data not shown). Bar size: 5 μ m.

The CslA-dependent polymer becomes visible upon binding to a chitin-binding protein

The presence of genes related to chitin binding and N-acetylglucosamine metabolism around the *cslA-glxA* operon were reason to analyze whether CslA together with GlxA in fact synthesizes a polymer consisting perhaps in part of N-acetylglucosamine. Therefore, the sequence for a His₆-tagged version of a chitin-binding domain (CBD) derived from chitinase A1 from *Bacillus circulans* WL-12 (Watanabe et al. 1994) was fused to the C-terminal end of the gene for eGFP, expressed in *E. coli* and purified. To assess its affinity for chitin, we incubated the eGFP-CBD fusion protein with chitin beads (Fig. 6A). The strong fluorescence of the chitin beads after binding of the fusion protein confirms its affinity for chitin polymers. Strikingly, fibril-like structures were identified when the purified eGFP-CBD fusion protein was added to mycelium of the wild-type strain (Fig 6B). After binding by eGFP-CBD, the long fibrils were also observed by light microscopy, and were often detected in close proximity to the hyphae (Fig. 6F). This strongly suggests that the chitin binding protein resulted in bundling of the fibrils. Notably, these bundled fibrils could also be stained with CFW, whose fluorescence co-localized with that of the eGFP-CBD fusion (Fig 6E-F). Similar fibrils were also occasionally observed in *glxA* mutants, but were invariably absent in the *cslA* mutant (data not shown). Taken together, these experiments identify an extracellular glycan whose production is dependent on CslA and to a lesser extent on GlxA, and which under these conditions is loosely associated to the mycelium.

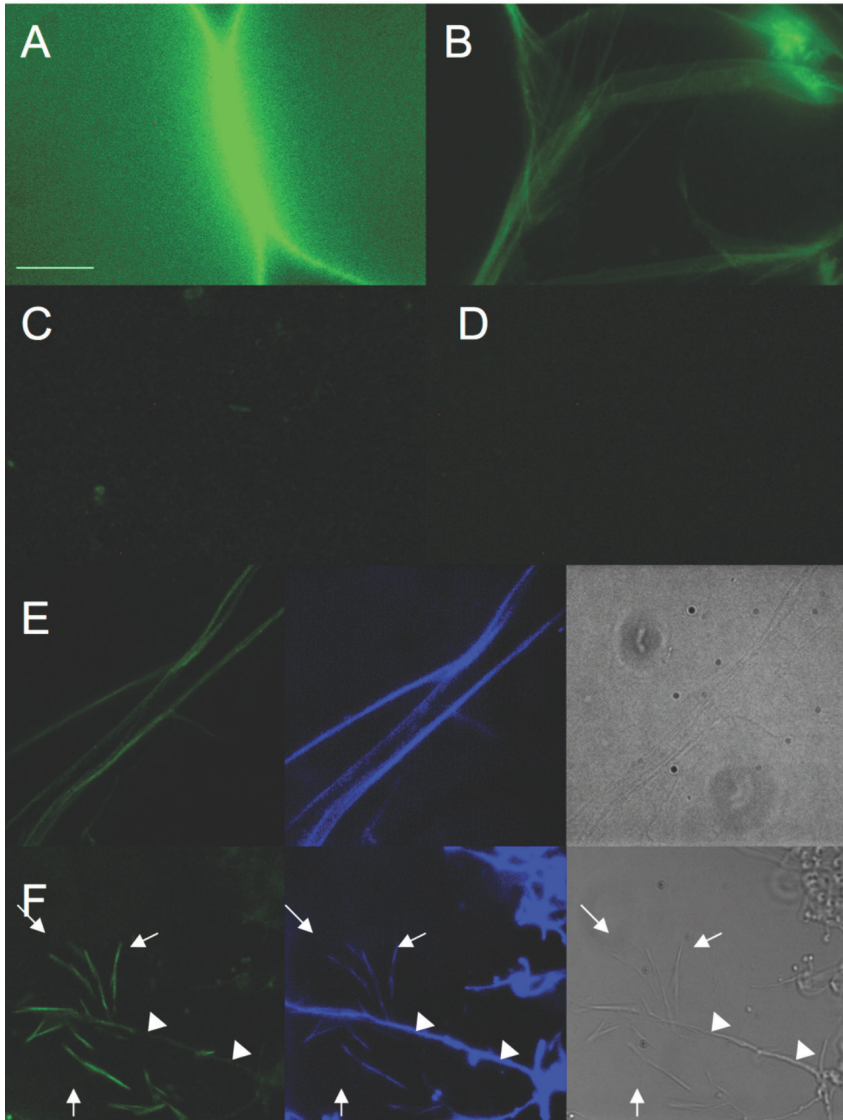


Figure 6. Visualization of extracellular fibrils using a chitin-binding domain fused to eGFP.

Chitin beads become fluorescent upon binding to the eGFP-CBD fusion protein (A). Long, extracellular structures were visualized in *S. lividans* 1326 following incubation of mycelia grown for 16 hrs on MS agar with eGFP-CBD (B). Control experiments showed that no background fluorescence was visible for the protein alone (C) or for the MS agar plates alone (D). The long fibrils bound by eGFP-CBD are stained by CFW and are also visible with light microscopy (E). These fluorescent fibrils were observed in close proximity to the mycelium of the wild type strain (F). Arrows: fibrils. Arrowheads: hyphae, as assessed by fluorescence microscopy. Bar size: 5 μ m.

DISCUSSION

Streptomycetes are mycelial microorganisms that resemble filamentous fungi, with apical growth of the hyphae and similar challenges associated with growth in the soil. In particular, the apical sites are constantly being remodeled during elongation of the hyphae and this likely requires an additional surface layer to protect the hyphal tips from damage. We here show that in streptomycetes, the synthase CslA and the modifying oxidase GlxA together produce an extracellular β -(1,4) glycan that plays a critical role in growth and morphological development. Considering the presence of a CESA domain in CslA and the fact that CslA-dependent fibrils can be stained with calcofluor white (CFW), it was suggested previously that this glycan might consist of cellulose (Xu et al. 2008). However, CFW is not specific for cellulose and also efficiently binds to chitin. Additionally, *Streptomyces* lacks the c-di-GMP binding protein that is conserved in cellulose-producing organisms and that is required for cellulose synthesis (Ross et al. 1991; Römling 2002). We provide evidence that CslA and GlxA cooperate to produce an extracellular polysaccharide that may consist at least in part of chitin. This is suggested by experiments that showed that the CslA-dependent fibrils are efficiently bound by a chitin-binding protein, which presumably causes aggregation of smaller submicroscopic fibrils into larger structures that are easily discerned by light microscopy. Additionally, gene synteny analysis indicates that the *cslA-glxA* region (SCO2836-2837/SLI_3187-3188) is conserved in streptomycetes and contains *chb* (SCO2833/SLI_3182) for chitin binding protein Chb, which is part of the chitinolytic system (Schrempf 2001; Colson et al. 2007) and an N-acetylglucosamine metabolism-related enzyme (SCO2843/SLI_3194). Finally, the lectin f-WGA, which stains apical sites, binds to N-acetylglucosamine, allowing detection of peptidoglycan precursors as well as chitin oligosaccharides.

In filamentous fungi, polar growth requires chitin synthesis at apical sites (Bowman and Free 2006). The cell wall of filamentous fungi contains chitin (Lenardon et al. 2010) and other carbohydrate polymers (mostly β -(1,3) glucans and mannans), interspersed with glycoproteins (Levitz 2010), whereby a highly cross-linked, yet dynamic structure is formed. Chitin synthases transfer N-acetylglucosamine subunits

to the growing chitin chain, which is simultaneously exported to the extracellular environment. The chitin polymers are then bundled to form protective crystalline structures, or further processed to chitosan, the deacetylated form of chitin, or cross-linked to other cell-wall polysaccharides (Davis and Bartnicki-Garcia 1984).

We previously showed that CslA might play a role in attachment by forming fibrillar glycan structures that are associating with chaplins to form so-called fimbriae (de Jong et al. 2009). These fibrillar structures could be removed by incubation with fungal extracts containing cellulases, which suggested the presence of cellulose in the fibrils. However, analysis of the crude enzyme preparation by MALDI-ToF mass spectrometry revealed that, in addition to cellulase, the extract contained a number of other polysaccharide hydrolases that act on β -(1,4) glucans (not shown). Chemical characterization of the polysaccharide structure produced by CslA and GlxA in *Streptomyces* should provide the precise nature of the β -(1,4) glycan. The composition of the polymer produced by CslA and GlxA may in fact be different depending on the growth condition. Indeed, the bacterium *Gluconacetobacter xylinus*, which has served as a model organism for bacterial cellulose biosynthesis, can also incorporate glucosamine and/or N-acetylglucosamine in addition to glucose (the preferred substrate) into the growing polysaccharide chains. The net result is heteropolymers consisting of mixed sugar moieties, revealing the apparent promiscuous nature of the synthase (Lee et al. 2001).

Multiple roles in growth and development for the CslA- and GlxA-dependent glycan

Calcofluor white staining revealed that CslA and GlxA are both required for the synthesis of the β -(1,4) glycan at apical sites. Interestingly, CFW induced widening of apical sites in *S. lividans*. This is most likely indicative of the initial stages of lysis, consistent with the complete absence of such widening in either mutant. Such tip swelling was also observed in filamentous fungi grown in the presence of CFW (Damveld et al. 2005). In *csIA* null mutants, no CFW staining was found, explained by absence of the synthase CslA, while in *glxA* null mutants CFW staining was

observed, but in older sections of the hyphae, rather than at apical sites. This suggests that the immature glycan is produced by CslA, but does not remain associated with apical sites. We propose that the oxidase GlxA - which is predicted to be mycelium associated through a N-terminal transmembrane segment - is involved in the subsequent maturation and apical attachment of the glycan.

Previous and current work indicates that this extracellular polysaccharide plays an important role during growth and development; the polysaccharide polymers facilitate the emergence of aerial hyphae during osmotic stress (Xu et al. 2008; Liman et al. 2013; this work) and contribute to invasion of and attachment to solid substrates, such as soil particles or (in the laboratory) the surface of agar plates. Interestingly, the putative chitin-like glycan dependent on CslA and GlxA is also involved in the architecture of mycelial pellets in liquid-grown cultures. Pellet formation is observed in many streptomycetes, although their specific sizes can be quite different, dependent on pH and other media-related factors as well as temperature, but also cell-wall related genes (van Veluw et al. 2012). Indeed, polymers such as hyaluronic acid but perhaps also extracellular DNA (eDNA) contribute to pellet integrity in *S. coelicolor* (Kim and Kim 2004). The chitin-related glycan produced by CslA and GlxA may play a role in formation of these structures. The open mycelial networks formed in the absence of the glycan fibrils suggest a role for these fibrils in surface adhesion so as to connect the hyphae, thus leading to the compact pellet structure. In this respect, mycelial pellets may be reminiscent of biofilm-like structures, which are embedded in an extracellular matrix (Flemming and Wingender 2010). Notably, such matrices also often contain amyloid proteins (Gebbinck et al. 2005). It is interesting to note that the conserved *Streptomyces* chaplin proteins, which can assemble into amyloid fibrils (Claessen et al. 2003) are also required for maintaining pellet integrity (M.L.C. Petrus and D. Claessen, unpublished).

Besides the fundamental implications for understanding hyphal growth and development in *Streptomyces*, the open mycelial structures formed by *csIA* and *glxA* null mutants in liquid-grown cultures could also have implications in industrial processes. Pellet morphology directly relates to viscosity and mass-transfer issues

(efficiency of nutrient and oxygen uptake), and thus to the efficiency in protein or secondary metabolite production and secretion (van Wezel et al. 2006).

GlxA and the Cu-dependence of S. lividans development

Copper-dependent morphological development is common in *Streptomyces* and is most pronounced in *S. lividans*. At low Cu levels, *S. lividans* displays a delayed development, while the removal of all the available metal results in vegetative growth arrest (Ueda et al. 1997; Keijser et al. 2000). This dependency is related to the *ram* (rapid aerial mycelium) genes, which produce the secreted RamS protein, eventually processed to the lantibiotic-type molecule SapB (Willey et al. 1991; Kodani et al. 2004). Indeed, the copper dependence of *S. lividans* development can be complemented by the introduction of an extra copy of *ramSAB* (Keijser et al. 2000). The reason for this is unknown, as none of these genes has a direct correlation with copper. Strains harboring an extra copy of the *ram* cluster have strongly enhanced transcription of *ramS*. An interesting hypothesis to test is whether more SapB is sufficient to provide compensation for the too low amounts of the CslA/GlxA synthesized glycan in the matrix under limited copper conditions.

Development of *S. lividans* requires the copper chaperone Sco1 and the deletion of the gene leads to vegetative arrest, which can be restored by the addition of 10 μ M Cu (Fujimoto et al. 2012; Blundell et al. 2013). What then is the acceptor of the copper atom offered by Sco1, which could explain the copper dependence of *S. lividans* development? The cytochrome c oxidase (CcO), which requires Sco1 for its maturation, is not the effector, as a *cco* deletion mutant still showed full development, suggesting that Sco1 has yet another target (Blundell et al. 2013). In this work, we show that *glxA* null mutants cannot develop on R5 agar plates, and do not attach nor invade the agar surface, which in fact is the same phenotype as observed for *sco1* mutants (Worrall & Vijgenboom, unpublished). Since the phenotype of the *glxA* null mutant cannot be rescued by copper, GlxA could be the Sco1-dependent enzyme that is responsible for the Cu-dependence of the development of *S. lividans*. However, this awaits further evidence.

Localization of GlxA

In agreement with previous observations, GlxA and CslA localise to apical sites. We observed very bright foci for both proteins at apical sites, and in addition many less intense foci distributed throughout the hyphae. It is known from previous studies that CslA is most likely membrane-associated and localizes at apical sites independent from the radical copper oxidase GlxA (Liman et al. 2013) and interacts with the apically situated DivIVA (Xu et al. 2008). GlxA has a predicted secretion signal, but was found at least partially in the membrane fraction (Whittaker and Whittaker 2006). A putative C-terminal sortase signal might anchor the protein to the peptidoglycan layer (Whittaker and Whittaker 2006), but we show here that deletion of the C-terminal 35 residues of the protein has no effect on the localization of GlxA, consistent with a recent study that argues against a covalent attachment to the cell surface (Liman et al. 2013). How secreted GlxA remains associated with the hyphae remains to be established.

CslA and GlxA were fused to mCherry C-terminally, so as to allow colocalization of CslA-eGFP with GlxA-mCherry and *vice versa*, but the fluorescence of the mCherry fusions was not bright enough to allow their visualization. Therefore, the localization of the foci at the hyphal tips was assessed as the relative distance from the cell wall stained by f-WGA. In 60% of the cases, CslA-eGFP and GlxA-eGFP localized immediately at the tip, while 40% was found close to but not immediately in the apex. Whether the two proteins fully colocalize awaits further analysis.

Model

Our data are consistent with a model of polysaccharide synthesis and attachment at the hyphal tips of *Streptomyces* requiring the action of GlxA and CslA (Fig. 7). The mature form of GlxA migrates at the hyphal tips, where it is secreted and associated with the membrane by a yet unknown mechanism. GlxA colocalizes with its functional partner CslA and they cooperate to produce a glycan-type polysaccharide - such as cellulose as previously suggested or perhaps chitin, or even a combination thereof - at the hyphal apices. CslA is the synthase, while GlxA presumably modifies the glycan

through oxidation, allowing its extracellular association with the mycelium. The glycan then becomes part of an extracellular matrix and likely acts in concert with other matrix components and proteins, such as the chaplins, rodmins and/or SapB. The drastic changes in morphology and absence of hyphae capable of invading agar media in both the *cslA* and *glxA* mutant highlight the important and intriguing role of matrix components in the control of (liquid) morphology, growth and development of streptomycetes.

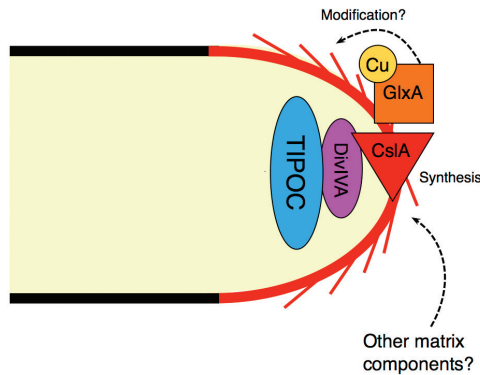


Figure 7. Summarizing model for the production of extracellular polysaccharides by CslA and GlxA.

GlxA localizes at the hyphal tips, where it is involved in the modification and accumulation of the polysaccharide produced by CslA. The polysaccharide may function together with other matrix components, such as the chaplins or SapB, in mediating its function in growth and development. Note that CslA interacts with DivIVA, which is an important member of the tip-organizing center (TIPOC) that controls polarized growth.

MATERIAL AND METHODS

Strains and media

All mutant strains were constructed in *S. lividans* 1326 (*S. lividans* 66, stock number 1326 from the John Innes Centre; (Hopwood et al. 1985). The low fluorescent *S. lividans* strain 1326-FM was isolated as described (Willemse and van Wezel 2009). *Escherichia coli* JM109 was used for routine cloning and plasmid amplification (Messing et al. 1981). All strains used and constructed are presented in Table S1. Soy flour mannitol (MS) agar plates were used for the isolation of spores from *Streptomyces* strains. For growth and phenotypical characterizations, R5 agar plates with or without 10 μ M Cu(II), tryptic soy broth with 10% sucrose (TSBS) and yeast extract-malt extract medium (YEME) were used (Kieser et al. 2000). *E. coli* strains were routinely grown on Luria-Bertani medium (LB). Nutrient agar was obtained from Difco.

Constructs for gene replacement and deletion mutants

All the plasmids used in this work are listed in Table S2. The strategy for creating knock-out mutants is based on the unstable multi-copy vector pWHM3 (Vara et al. 1989) as described previously (van Wezel et al. 2005). For the deletion of *csIA*, the -1260/+78 and +1828/+3263 regions relative to the start of *csIA* were amplified by PCR, using primer pairs *csIA*-1260F/ *csIA*+78RV and *csIA*+1828F/*csIA*+3263RV, respectively (Table S3). Fragments were cloned into pWHM3, and the engineered XbaI site was used for insertion of the apramycin resistance cassette *aac(3)IV* flanked by *loxP* sites between the flanking regions. The constructed plasmid was called pGMMP1. Using essentially the same strategy as for pGMMP1, we constructed plasmid pGMMP2 for the single gene replacement of *glxA*. pGMMP2 contains the -1498/+59 and +1917/+3428 regions relative to the start of *glxA*. The antibiotic cassettes were subsequently removed from the mutants by the Cre-*lox* recombinase using plasmid pUWLcre (Fedoryshyn et al. 2008). This resulted in the *csIA* and *glxA* null mutants, which had the corresponding genes replaced by a scar *loxP* site flanked

by *Xba*I restriction sites. The mutants were complemented by plasmids pGMMP3 and pGMMP4, respectively carrying *cslA* and *glxA* under the control of P_{*cslA*} in plasmid pHJL401 (Larson and Hershberger 1986). This plasmid is ideally suited for complementation experiments for its very high stability and low copy number (van Wezel et al. 2000b). All plasmids were introduced through protoplast transformation (Hopwood et al. 1985). The primers used for PCR amplification are listed in Table S3.

Construction of eGFP fusion proteins

To create eGFP fusions, we used a low-copy number shuttle vector pGFP-strep, which is based on pHJL401, and carried a version of the gene for eGFP codon-optimized for expression in *Streptomyces*, which is transcribed from the *ftsZ* promoter region. This construct showed good results in other experiments and was therefore selected (J. Willemse, personal communication). For localization of CslA, the *cslA* gene with 500 bp of the upstream promoter region was cloned in pGFP-strep, whereby the *ftsZ* promoter was removed (pGMMP5). To localize GlxA, the *glxA* gene was cloned into pGFP-strep (pGMMP6). In this construct, expression of the fusion is under control of P_{*ftsZ*} (pGMMP6). The fusion constructs were introduced in 1326-FM and/or Δ *glxA*-FM.

Microscopy

Light microscopy was used to check the phenotypes of the strains in liquid culture, using a Carl Zeiss Standard 25 microscope and a 20x lens. The agar invasion capacity of strains was tested on various agar media and recorded with a Leica DFC295 stereomicroscope. The GFP fusion proteins were observed with a fluorescence microscope (Axioscope A1) and analyzed with the Axio Vision software to assess localization using filter set 38HE (470/40 nm excitation, 495 nm dichroic, 525/50 nm emission). The spores were inoculated at the edge of glass slides inserted at an angle of 45° in MS plates and grown for 24 hrs, generating a sample of vegetative mycelium. For CFW staining, mycelium was grown for 24 hrs on glass slides and MS plates as described above. The mycelium was stained with 5µl of a 10x diluted solution of a 1:1

mixture of CFW:10% KOH and analyzed at the fluorescent microscope (Axioscope A1). Alternatively, spores were inoculated in 10 ml liquid TSBS and grown for 24 hrs. A sample of 5 μ l of the culture was mixed with 5 μ l of a 10x diluted solution of a 1:1 mixture of CFW:10% KOH and analyzed. For CFW staining filter set 49 was used (excitation 365 nm, dichroic 395 nm, emission 445/50 nm).

For fluorescently conjugated wheat germ agglutinin staining (f-WGA), spores were inoculated on glass slides and MS plates as discussed above and grown for 24 hrs, incubated with 5 μ l of a 10x diluted solution of f-WGA in glycerol and analyzed with filter set 63HE (572/25 nm excitation, 590 nm dichroic, 629/62 nm emission).

To calculate distances between the fluorescent proteins and the WGA-stained cell wall, ImageJ was used (Schneider et al. 2012). All images were background-corrected using Adobe Photoshop CS4.

Protein methods

For the preparation of protein samples MS plates were overlaid with cellophane disks and inoculated confluent with 10^5 spores. After 24 hrs, the mycelium was harvested and the wet weight determined. Mycelium was resuspended in 10 mM Tris-HCl (pH7; volume adjusted according to wet weight, 20 μ l per mg of protein) and sonicated. After centrifugation, the supernatant was removed and mixed with an equal volume of SDS-PAGE loading buffer containing 1% β -mercaptoethanol. The pellet was directly resuspended in loading buffer, resulting in a 2x concentrated sample compared to the soluble fraction. Following electrophoresis in a 10% SDS PAGE gel, the proteins were blotted on nitrocellulose filters. Standard Western blot protocols and polyclonal antibodies against GlxA (1 μ L per 10 mL) were used for detection with GARAP as the secondary antibody.

Analysis of GlxA anchoring by sortases

To assess the role of sortases in anchoring of GlxA, a truncated version of the *glxA* gene was cloned in pHJL401 under the control of the *csIA* promoter, generating plasmid

pGMMP9. The resulting recombinant protein lacks the C-terminal 35 amino acids, which would include the putative sortase signal (Whittaker and Whittaker 2006).

RT-PCR Analysis

Total RNA for transcript analysis was isolated from cultures grown on MS plates for 24 hrs, purified using the Kirby-mix protocol (Kieser et al. 2000) and additionally treated with DNase I to remove any traces of DNA. RT-PCR was carried on as described previously (Noens et al. 2007) using 200 ng of RNA as a template. Quantification of the amplified RNA on gel was carried out with a Bio-Rad Gel Doc EZ Imager and Image Lab software. The primers used for PCR amplification are listed in Table S3 of the Supporting Information.

Visualization of fibrils using a chitin-binding domain

The *eGFP* gene was amplified using pGFP as template DNA and cloned in pTYB3 (New England Biolabs), upstream of the intein domain and the chitin binding domain (CBD) of chitinase A1 from *Bacillus circulans* WL-12, generating plasmid pGMMP7. The chitin binding domain of chitinase A1 is known to have a strong preference for chitin binding (Watanabe et al. 1994; Chong et al. 1997).

The sequence encoding the eGFP-CBD fusion was amplified by PCR and cloned in pET28a (Novagen), thereby introducing an N-terminal His tag (plasmid pGMMP8). Standard procedures were followed to isolate the eGFP-CBD fusion protein on HisPur™ Cobalt resin (Thermo Scientific). Ultrafiltration (Amicon Ultra, 30 kDa cut off) was used to concentrate the protein. Several wash steps with 50 mM NaPi (pH 8) were performed to reduce the concentration imidazole and NaCl below 0.1 mM. About 3 ng of protein was used to detect the polysaccharide associated with the mycelium of the wild-type, *csIA* and *glxA* mutant strains that had been grown for 16 hrs on cover slips inserted in MS plates.

ACKNOWLEDGMENTS

The authors would like to thank Jacob Gubbens for help with mass spectrometry, Kasia Celler for help with microscopy and James Whittaker for providing GlxA antibodies.

SUPPLEMENTAL MATERIAL

Table S1. Strains used in this study.

Strains	Description	Reference
<i>S. lividans</i>		
1326	<i>S. lividans</i> 1326 wild type strain	Hopwood et al., 1985
1326-FM	derivative of <i>S. lividans</i> 1326 with reduced autofluorescence	This work
<i>cslA</i>	<i>cslA</i> deletion mutant in 1326-FM	This work
<i>glxA</i>	<i>glxA</i> deletion mutant in <i>S. lividans</i> 1326	This work
<i>glxA</i> -FM	<i>S. lividans glxA</i> mutant derivative with reduced autofluorescence	This work
<i>E. coli</i>		
JM109	<i>E. coli</i> K12 strain used for routine subcloning	Messing et al, 1981

Table S2. Plasmids used and constructed in this study

Name	Description	Reference
pWHM3	pIJ486 derived <i>E. coli-Streptomyces</i> shuttle vector, Tsr ^R , Amp ^R	(Vara et al., 1989)
pET28a	<i>E. coli</i> expression vector, Kan ^R	Novagen
pGMMP1	pWHM3 containing the flanking regions of the <i>S. lividans cslA</i> gene, interspersed by the apraloxP_XbaI insert	This work
pGMMP2	pWHM3 containing the flanking regions of the <i>S. lividans glxA</i> gene, interspersed by the apraloxP_XbaI insert	This work
pUWLcre	pUWLoriT derivative containing the gene for the Cre-lox recombinase under the control of P _{ermE}	(Fedoryshyn et al., 2008)
pHJL401	<i>E. coli-Streptomyces</i> shuttle vector, Tsr ^R , Amp ^R	(Larson and Hershberger, 1986)
pGMMP3	pHJL401 containing the <i>cslA</i> gene under the control of the <i>cslA</i> promoter	This work
pGMMP4	pHJL401 containing the <i>glxA</i> gene under the control of the <i>cslA</i> promoter	This work
pGFP	pHJL401 containing a codon-optimized version of the <i>eGFP</i> gene under the control of P _{ftsZ}	This work
pGMMP5	pGFP derivative containing a chimeric <i>cslA-eGFP</i> gene under the control of P _{cslA} cloned as an EcoRI-XbaI fragment	This work

pGMMP6	pGFP derivative containing a chimeric <i>glxA-eGFP</i> gene under the control of P _{<i>fsz</i>} cloned as an NcoI-XbaI fragment	This work
pGMMP7	pTYB3 containing the <i>eGFP</i> gene from pGFP, cloned as an NcoI-XhoI fragment thereby creating an eGFP-intein-CBD fusion.	This work
pGMMP8	eGFP-intein-CBD domain from pGMMP7 cloned into pET28a as an NdeI-EcoRI fragment	This work
pGMMP9	pHJL401 containing the <i>csIA</i> promoter upstream of a truncated version of the <i>glxA</i> gene, which encodes GlxA lacking its 35 amino acids at its C-terminus.	This work

Table S3. Oligonucleotides used in this study.

Name	5'-3' sequence	Restriction site(s) (underlined in sequence)
<i>csIA</i> -1260F	GCGGAATTCGGCGTAGGGCGTGTGCGAGCTTC	EcoRI
<i>csIA</i> +78RV	CGCTCTAGACCGGTGCCCGGCACCC	XbaI
<i>csIA</i> +1828F	GCGTCTAGAGGGTCCCGCCGACAGCAGG	XbaI
<i>csIA</i> +3263RV	CGCAAGCTTCTTCGGGTCTGTCGGCCTTGAGGT	HindIII
<i>csIA</i> F	GCGGAATTCCTCACACTCCCGGTGCGCAGG	EcoRI
<i>csIA</i> RV	CGCGGATCCATATGTCATCCCCCACACGGGGT	NdeI
<i>csIA</i> RV 2	CGCTCTAGATTCTTACGTCCCCCAAGTCCAC	XbaI
<i>csIA</i> RV 3	CGCTCTAGAGCATCATTCTTACGTCCCCAAGTCC	XbaI
<i>glxA</i> -1498F	GCGGAATTCGAGACCGGCACCAAGGTGCG	EcoRI
<i>glxA</i> +59RV	GCGTCTAGACGTGCCTATCGCGAAGCGACG	XbaI
<i>glxA</i> +1917F	GCGTCTAGAGAGTGGGTGCGAGTTCGCTAGCG	XbaI
<i>glxA</i> +3428	GCGAAGCTTGAGTCGGCCGGCAAGCTGTGG	HindIII
<i>glxA</i> F	GCGCCATGGAAGACCGTGCCGGCCG	NcoI
<i>glxA</i> RV	CGCTCTAGACGGCACCCGCACCCACTC	XbaI
<i>glxA</i> F 2	GCGGAATTCATATGAAAGACCGTGCCGGCCG	EcoRI-NdeI
<i>glxA</i> RV 2	CGCAAGCTTGGCGCTACGGAACCTCGCACC	HindIII
GFP F	CGCGAATTCATGCGCAAGGGCGAGGAGCTGTTC	EcoRI-NcoI
GFP RV	GCGAAGCTTCTCGAGCTTGTACAGCTCGTCCATGCC	HindIII-XhoI
pET28 F	CGCAAGCTTTCATATGAGCAAGGGCGAGGAGCTGTTCAC	HindIII-NdeI
CBD RV	GCGGAATTCCTCTGCAGTCATTGAAGCTGCCACAAG	EcoRI
<i>glxA</i> -105nt RV	CGCTCTAGACACCGTCAGCTTGTCCCCGTC	XbaI
<i>rpsL</i> _for	GAGACCACTCCCGAGCAGCCG	none
<i>rpsL</i> _rev	GTAGCGGTTGTCCAGCTCGAGCA	none
<i>csIA</i> _for	TGGGCGTGCACCACTTCTCC	none
<i>csIA</i> _rev	CGCGGTACCGGAAGGTGCCGAACA	none

Chapter 4

Analysis of the transcriptome of *Streptomyces lividans* *csIA* and *glxA* null mutants reveals disturbance in the transcription of genes relating to morphogenesis and osmoprotection

Giulia Mangiameli, Erik Vijgenboom, Dennis Claessen and Gilles P. van Wezel

ABSTRACT

Streptomyces mutants lacking genes *csIA* and *glxA* grow as an open mycelium in liquid cultures. Such a non-pelleting phenotype may be of interest from the perspective of industrial applications. *csIA* and *glxA* form an operon, whereby *csIA* encodes a cellulose synthase-like protein, while *glxA* encodes a copper oxidase. Both proteins are involved in the synthesis and deposition of a glycan at hyphal tips. The absence of this polysaccharide is linked to an alteration in the formation of the matrix and in the aggregation of pellets. To better understand which changes are induced in the mutants and to identify potential targets for the control of morphology, global transcriptome profiling was performed taking advantage of the last generation RNA sequencing (RNA-Seq) with Illumina technology. This led to the identification of genes that are potentially involved in morphogenesis and matrix formation, including a cluster that encodes phage tail-related proteins. The increased expression of genes related to osmoprotection indicates that, in addition, the mutants suffer from osmotic stress. Taken together, the data provide interesting new insights into the role of CslA and GlxA in the control of morphogenesis and stress management.

INTRODUCTION

Streptomycetes are mycelial soil bacteria that grow as an intricate network of branched hyphae. After vegetative growth, the colonies develop and produce aerial hyphae, which grow in the air and eventually differentiate to generate chains of spores. The formation of aerial hyphae is facilitated by various macromolecules. The lantibiotic-like peptide SapB is involved in lowering the water surface tension at the medium-air interface (Willey et al. 1991; Willey et al. 1993), which enables hyphae to leave the aqueous environment. Aerial hyphae then become decorated with a mosaic of pair-wise aligned fibrils, which is known as the rodlet layer. Formation of this surface layer requires the activity of two types of proteins, called chaplins and rodlins. Chaplins are the main constituents of the rodlet layer and were shown to assemble into small fibrils. *In vivo*, these fibrils are deposited in an often pair-wise aligned arrangement on the cell surface by the activity of the rodlins.

Recent evidences unambiguously demonstrated that the chaplins assemble into so-called amyloid structures (Sawyer et al. 2011; Bokhove et al. 2013). Amyloids are proteinaceous aggregates that are rich in β -sheet structure. Amyloid fibrils are associated with the surfaces of many bacteria and fungi, often having roles in biofilm formation, but also in providing surface hydrophobicity or protection. Examples are curli fibers in *E. coli* (Zogaj et al. 2003) and thin aggregative fimbriae (tafi) in *Salmonella* species (White et al. 2003), which are involved in biofilm formation, and hydrophobins of filamentous fungi, which render the aerial hyphae hydrophobic in a similar manner as chaplins do for streptomycetes (Wösten et al. 1999; Linder et al. 2005).

In addition to their role in aerial growth, the *Streptomyces* chaplin proteins are involved in attachment of hyphae to surfaces. Attachment coincides with the formation of a so-called extracellular matrix (de Jong et al. 2009). This matrix is composed of assembled chaplin amyloid fibrils in association with a polymer produced by a protein annotated as a cellulose synthase-like protein, CslA (Xu et al., 2008). The absence of CslA leads to an arrest of development on rich solid media (Xu et al, 2008)

and strongly decreases attachment (de Jong et al., 2009; Chapter 2). CslA is required for the synthesis of a β -(1,4) polymer, although the exact nature of the polymer is unclear. These results demonstrate the important roles that macromolecules play during growth and development of streptomycetes.

Although development is mostly associated with growth on solid substrates, *Streptomyces* also differentiate in liquid-grown cultures. Some streptomycetes fragment and sporulate in submerged cultures, such as the chloramphenicol producer *S. venezuelae* and the streptomycin producer *S. griseus*, whereby submerged sporulation correlates to the specific amino acid sequence (and expression level) of the SsgA and SsgB proteins (Girard et al. 2013), which control sporulation-specific cell division (Willemse et al. 2011). Many strains, however, form so-called pellets in liquid media (Pamboukian et al. 2002). Interestingly, deletion of genes encoding for cell surface proteins such as the chaplins or CslA strongly reduces the size and changes the morphology of pellets (van Veluw et al. 2012; Chapter 3). Recent data indicates that CslA acts in conjunction with GlxA, a copper oxidase with remote similarity to galactose oxidases (Liman et al. 2013), encoded by a gene adjacent to (and cotranscribed with) *cslA*. In particular, the *cslA* and *glxA* mutants form open mycelial structures when grown in rich liquid media (Fig. 1). This effect is likely explained by the absence of a glycan-like polysaccharide, synthesized at the hyphal tips by CslA and associated to the cell wall via non-covalent interactions after modification by GlxA. While the absence of CslA leads to a complete block in polymer formation, the absence of GlxA caused the CslA-produced polymer to be mislocalized. A role for the glycan in hyphal aggregation has therefore been postulated (Chapter 3).

The phenotypes associated with the changes in morphology in liquid-grown cultures will inevitably lead to changes in gene expression. To obtain more insight into the changes as a result of the deletion of *cslA* and *glxA*, global transcription profiling was performed using RNA-Seq analysis. The results not only demonstrate the impact of CslA and GlxA on *Streptomyces* physiology, but also point at genes that may play a role in the observed morphological changes in liquid-grown cultures.

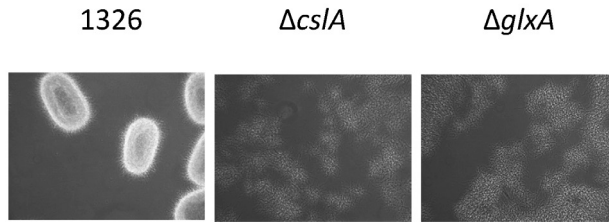


Figure 1. Phenotypic comparison between the wild-type (1326) and the corresponding $\Delta csIA$ and $\Delta glxA$ mutants in liquid-grown cultures

RESULTS AND DISCUSSION

Transcriptome analysis of the csIA and glxA mutants

The global transcription profiles of the *csIA* and *glxA* mutants were compared to those of the parental strain *S. lividans* 1326 and to one another, using RNA seq analysis. For this, RNA was isolated from liquid-grown cultures in the mid-exponential growth phase and sequenced as described in the Materials and Methods section. For the analysis of the transcriptome data, a change of two-fold or more in transcript levels and an RPKM value >10 were chosen as cut-off (RPKM: Reads per Kilobase of exon model per Million mapped reads; Mortazavi et al. 2008).

An overview of the number of genes whose transcription was changed according to the criteria set above is given in Figure 2, while the corresponding RPKM values and fold changes of those genes are provided in the Appendix.

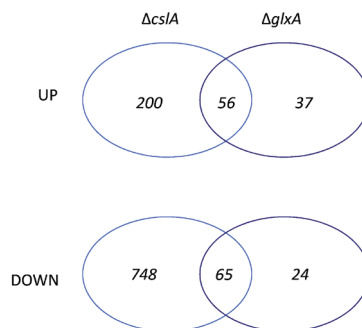


Figure 2. Venn diagram showing the number of genes uniquely up- or down regulated in the *csIA* and *glxA* mutant and those shared by the two mutants.

Following these criteria, deletion of *csIA* resulted in 256 genes whose transcription was upregulated and 813 genes whose transcription was downregulated in comparison to the parental strain. For the *glxA* mutant, 93 genes were upregulated and 89 genes downregulated. Most genes whose transcription levels were changed in the *glxA* mutant showed comparable changes in the *csIA* mutant (Fig. 2 and Appendix).

Despite the remarkable changes in the expression profile, few changes in the transcription of genes encoding transcriptional regulators were observed (Tables S1 and S2). Among the TetR regulators, which control among others efflux pumps and osmotic stress, five genes are upregulated in the *glxA* mutant (SLI_0468, SLI_0641, SLI_2006, SLI_3521 and SLI_4911). Two ArsR regulators (SLI_1107, SLI_7362), involved in modulating metal resistance and stress, are about two-fold upregulated in the *glxA* mutant, while SLI_1891 and SLI_5378, belonging to the GntR family that regulate general metabolism, are two-fold down in both *csIA*/*glxA* mutants.

Changes in transcription of genes related to pellet morphology

In the *csIA* null mutant, transcription of *glxA* was upregulated around 18-fold, perhaps as an attempt to compensate for the absence of the functionally linked *csIA*. Transcripts corresponding to the remainder of *csIA* were also enhanced in the *csIA* mutant (around 17-fold) (Table 1). Interestingly, such a strong increase in transcription of *csIA*-*glxA* was not observed in the *glxA* mutant. This suggests the presence of a CslA-dependent feedback mechanism that is involved in coordination of *glxA* and *csIA* transcription.

Transcription of SLI_3189, located directly next to the *csIA*-*glxA* gene cluster, is two-three fold enhanced in *glxA* and *csIA* mutants respectively (Table 1). It encodes a glycosyl hydrolase previously suggested to be functionally related to CslA and GlxA (Liman et al. 2013). However, our unpublished data suggest that the gene does not play a major role in the control of morphogenesis (D. Claessen, personal communication).

Previous work demonstrated that the overexpression of the *ssgA* gene (SLI_4184) leads to smaller pellets due to increased fragmentation (van Wezel et al. 2006). Furthermore, the deletion of *ssgA* causes a two- to six-fold increase in transcription of *glxA* (Noens et al. 2007). However, in our data no changes in the level of *ssgA* were observed in the *glxA* and *csIA* mutants as compared to the parental strain (Table 1). Pellet morphology is also influenced by the chaplin genes (de Jong et al. 2009; van Veluw et al. 2012; M.L.C. Petrus and D. Claessen, unpublished data). By looking at the transcription of the long chaplins (SLI_3063, SLI_7473, SLI_1979) and short chaplins (SLI_3064, SLI_2108, SLI_3053, SLI_3047, SLI_1980), substantial differences were observed only in the case of SLI_1980 (*chpH*), with a near two-fold increase in the *csIA* mutant, and SLI_7473 (*chpB*), with is around two-fold downregulated in both mutants (Table1).

Table 1. Expression analysis of genes known to be involved in pellet morphology

Gene # <i>S. coelicolor</i>	Gene # <i>S. lividans</i>	1326 (RPKM)	<i>csIA</i> (RPKM)	<i>glxA</i> (RPKM)	<i>csIA</i> /1326	<i>glxA</i> /1326	Annotation
SCO2836	SLI3187	136,3	167,3	129,4	1,2	0,9	CsIA
SCO2837	SLI3188	188,4	3460,9	1,1	18,4	0,0	GlxA
SCO2838	SLI3189	172,9	529,4	312,0	3,1	1,8	glycosyl hydrolase
SCO3926	SLI4184	24,0	20,8	32,4	0,9	1,3	SsgA
SCO2716	SLI3063	1,1	1,6	1,1	1,4	1,0	ChpA
SCO7257	SLI7473	25,0	14,0	12,1	0,6	0,5	ChpB
SCO1674	SLI1979	32,6	32,0	24,7	1,0	0,8	ChpC
SCO2717	SLI3064	6,4	3,4	4,9	0,5	0,8	ChpD
SCO1800	SLI2108	100,6	147,6	69,9	1,5	0,7	ChpE
SCO2705	SLI3053	6,7	11,3	8,5	1,7	1,3	ChpF
SCO2699	SLI3047	2,5	5,3	3,8	2,2	1,5	ChpG
SCO1675	SLI1980	61,8	117,0	62,3	1,9	1,0	ChpH
SCO7657	SLI7885	532,7	985,9	809,2	1,9	1,5	HyaS

Other genes relating to morphology include SLI_7885, which encodes the hyphal aggregation protein HyaS. Transcription of *hyaS* was between 1.5- and 1.9-fold enhanced in the *glxA* and *csIA* mutants (Table 1). HyaS is a putative lysyl/amine oxidase with a suggested role in hyphal aggregation and pellet formation in liquid cultures. Its deletion decreases pellet density and leads to abundant protrusion of hyphae from the pellet surface (Koebsch et al. 2009). Increased transcription of the *hyaS* gene could indicate a compensation effect for the loss of pellet integrity.

Enhanced transcription of a cluster of genes for phage tail-related proteins

Analysis of the differentially transcribed genes indicated that transcription of the gene cluster SLI_4479-SLI_4495 was significantly enhanced in the *csIA* and *glxA* mutants, namely between 1.5-2.5 fold in the *glxA* mutant and between two to five-fold in the *csIA* mutant. These genes are organized in five sets of genes, four of which were suggested to be transcribed from two divergent promoters in *S. coelicolor* (Kim et al. 2005; Table 2 and Figure 3A). The presence of genes SLI_4479-4485 and SLI_4487-4489 is highly conserved among Actinomycetales. They may have been acquired via horizontal transfer, as suggested by the presence immediately upstream of SLI_4478 of a gene for the threonine tRNA that recognises ACA codons. tRNA genes often serve as sites for exogenous gene integration (Williams 2002).

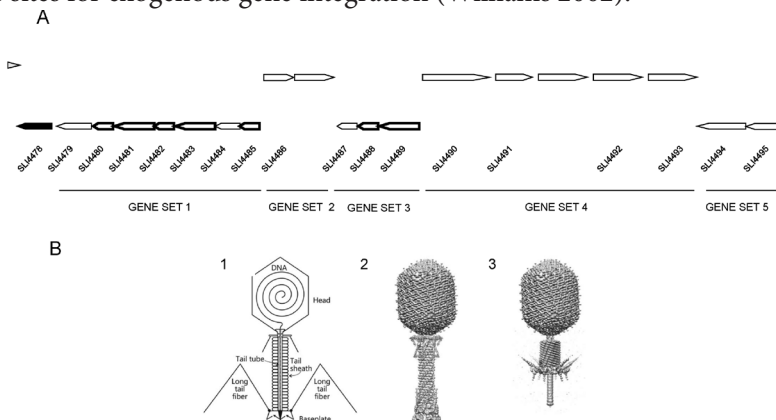


Figure 3. (A) The SLI4479-4495 cluster in *S. lividans*. Thick arrows indicate genes for phage assembly proteins, black arrows genes not involved in the cluster and triangle tRNA genes (B) A representation of phage proteins in the bacteriophage T4 (picture taken from Leiman et al. 2010) (1) Schematic representation of the assembly of the phage and conformation prior to (2) and during (3) bacterial infection.

Table 2. Upregulation of the cluster SLI4479-SLI4495. Two gaps were detected in the *S. lividans* genome sequence, corresponding to the *S. coelicolor* SCO4250 and SCO4256 genes. The data for these genes were obtained with the *S. coelicolor* genome as a reference and normalization of the RPKM values between the two data sets.

Gene # <i>S. coelicolor</i>	Gene # <i>S. lividans</i>	1326 (RPKM)	<i>csIA</i> (RPKM)	<i>glxA</i> (RPKM)	<i>csIA</i> /1326	<i>glxA</i> /1326	Annotation
SCO4243	SLI4480	24,9	98,3	60,7	3,9	2,4	secreted protein
SCO4244	SLI4481	39,3	146,7	85,3	3,7	2,2	hypothetical protein
SCO4245	SLI4482	40,4	146,1	87,9	3,6	2,2	hypothetical protein
SCO4246	SLI4483	38,4	165,0	93,3	4,3	2,4	hypothetical protein
SCO4247	SLI4484	56,0	249,4	138,1	4,5	2,5	hypothetical protein
SCO4248	SLI4485	37,2	174,2	94,9	4,7	2,5	hypothetical protein
SCO4249	SLI4486	18,2	57,5	30,0	3,2	1,7	hypothetical protein
SCO4250		116,7	299,3	128,0	2,6	1,1	ampullate spidroin
SCO4251	SLI4487	575,8	2311,7	1137,6	4,0	2,0	secreted protein
SCO4252	SLI4488	845,1	4425,2	2045,2	5,2	2,4	hypothetical protein
SCO4253	SLI4489	550,1	2388,0	1065,2	4,3	1,9	Phage tail sheath protein FI
SCO4254	SLI4490	12,2	25,2	20,0	2,1	1,6	Hypothetical protein
SCO4255	SLI4491	20,7	73,8	42,5	3,6	2,1	Conserved hypothetical protein
SCO4260		10,5	26,7	29,5	2,6	2,8	hypothetical protein
SCO4257	SLI4492	73,4	236,8	192,1	3,2	2,6	Hydrolytic protein
SCO4258	SLI4493	101,4	325,3	193,6	3,2	1,9	Hydrolytic protein
SCO4259	SLI4494	29,0	94,4	54,5	3,3	1,9	ATPase AAA
SCO4260	SLI4495	80,8	158,2	123,5	2,0	1,5	hypothetical protein

Interestingly, several of the proteins encoded within the gene cluster show striking similarities with those involved in phage assembly. Seven genes encode morphogenetic phage proteins (indicated with thick arrows in Fig. 3A), whose role in the assembly of phages has been recently reviewed (Leiman et al. 2010 and Fig 3B). SLI_4480-SLI_4481 and SLI_4488_SLI_4489 are annotated as genes encoding phage tail proteins. In bacteriophage T4, phage tail proteins organize in a contractile helical structure that is part of the phage tail. Contraction leads to penetration of the cell membrane by the central tail tube and injection of the DNA into the bacterial cell. The protein encoded by SLI_4485 shows similarities with the tail tube. Other phage-related proteins include those encoded by SLI_4483 and SLI_4482, which could form a baseplate component with acidic lysozyme activity, used by viruses to digest the peptidoglycan of the bacterial cell envelope and inject the DNA directly into the cytosol. SLI_4484 encodes a protein with a LysM domain. Proteins containing such domains are typically involved in binding to peptidoglycan and chitin in bacteria and eukaryotes, respectively (Buist et al. 2008). The transcript levels of SLI_4498, described in the past as the transcriptional regulator of at least three of the five gene sets in *S. coelicolor* (Kim et al. 2005), was not significantly changed in *csIA* and *glxA* mutants. This suggests that either the activation of the transcriptional activator is post-translationally regulated, or that its role at least under these conditions is limited.

Phage-related proteins are present in many bacteria, although knowledge about their biological significance is limited. In the pathogenic *E. coli* strain O157:H7, phage tail proteins are described as collagen-like proteins which may play a role in virulence (Ghosh et al. 2012). Similarly, collagen-like proteins have been described in *Streptococcus pyogenes*, with a role in cell adhesion and pathogenicity (Chen et al. 2010). In the food pathogen *Cronobacter sakazakii*, biofilm and extracellular matrix formation are affected in mutants lacking, among others, phage tail proteins (Du et al. 2012). It is interesting to notice that SLI_4488 is one of the most strongly expressed genes in terms of absolute RPKM, with transcription comparable to that of ribosomal protein genes, which suggests a pivotal role for the protein encoded by this gene.

In contrast to genes SLI_4479-4485 and SLI_4487-4489, the presence of

SLI_4486 is less well conserved. In *S. coelicolor*, the homologous SCO4249 is coupled to SCO4250, encoding a protein with weak similarity to the major ampullate spidroin of *Nephila madagascariensis* (Gatesy et al. 2001). In *S. lividans*, there is a gap in the genome sequence, but analysis of the transcription data using the *S. coelicolor* genome as reference suggests that the gene is present but not annotated (data not shown). Spidroin is the major constituent of spider-silk, whose final fiber has striking similarities with amyloid fibrils (Kenney et al. 2002). Amyloid fibrils have an important role in attachment and biofilm formation in various organisms (Zogaj et al. 2003; White et al. 2003; Linder et al. 2005) including *Streptomyces* (Claessen et al. 2003; de Jong et al. 2009; Gras and Claessen, 2014).

The putative role for phage tail proteins in biofilm formation may suggest a role for these proteins in the formation of an extracellular matrix in streptomycetes, perhaps in conjunction with the glycan produced by CslA and GlxA and possibly the chaplins (M.L.C. Petrus and D. Claessen, unpublished data). Their increased transcription might reflect a compensation effect for the loss of pellet architecture. Notably, the involvement of this gene cluster in morphogenesis has been observed previously in a non-pelleting mutant of *S. lividans* (MD Dissel and GP van Wezel, unpublished data). If and how these proteins contribute to extracellular matrix formation and pellet aggregation in *Streptomyces* is under current investigation.

Transcription of genes related to osmoprotection

A second category of genes that stood out in terms of being significantly enhanced in the *csIA* and *glxA* mutants were those encoding ABC transporters for the uptake of amino acids. These include SLI_3177-3180, which lie adjacent to the *csIA-glxA* genes (Table S1). Interestingly, genes SLI_1923-1924 for the putative glycine transporter are also upregulated in the mutants, as well as SLI_5103-5105, which are part of an operon together with SLI_5101-5102, encoding a choline and an aldehyde dehydrogenase (Table 3). Glycine forms bridges in the peptidoglycan in Gram-positive bacteria (Leyh-Bouille et al. 1977). Moreover, glycine betaine is a cellular osmoprotectant that accumulates in the cytoplasm to provide protection against osmotic stress (Landfald

and Strøm 1986; Bursy et al. 2008). Glycine betaine can be imported in the cell via specific ABC transporters or synthesized from glycine (Kimura et al. 2010) or from precursors choline and glycine betaine aldehyde (Lamark et al. 1991). The two best studied systems are genes *betTIBA* in *E. coli* (Lamark et al. 1991) and genes *opuABC* and *gbsAB* in *B. subtilis* (Kappes et al. 1999).

In the *csIA* and *glxA* mutants, transcription of SLI_1923 (an OpuABC-like permease) and SLI_1924 (the likely ATPase of the uptake system) was six- and almost four-fold enhanced, respectively (Table 3). In addition, two- to five-fold upregulation is observed for genes SLI_5101 (similar to *B. subtilis* GbsAB dehydrogenases), SLI_5102, (a putative choline dehydrogenase), SLI_5103 (an ATP-binding protein), SLI_5104 (similar to *B. subtilis* OpuAB transporters) and SLI_5105 (a possible glycine betaine substrate binding protein).

Another molecule that accumulates in the cell in response to salt and temperature stress is ectoine (Bursy et al. 2008). Transcription of the genes involved in ectoine biosynthesis (SLI_2175-2178) was approximately two-fold increased in the *glxA* mutant and between three- and ten-fold in the *csIA* mutant (Table 3). Ectoine is a natural osmoprotectant that is either imported or synthesized through the conversion of the precursor, L-aspartate- β -semialdehyde, via four enzymatic steps involving: acetyl-transferase EctA (SLI_2175), aminotransferase EctB (SLI_2176), ectoine synthase EctC (SLI_2177) and hydroxylase EctD (SLI2178) (Bursy et al. 2008). The increased transcription of genes for choline/glycine betaine transporters and for ectoine synthesis may reflect increased osmotic stress in *glxA* and *csIA* mutants. We hypothesize that the glycan synthesized by CslA and GlxA may play an important role in osmoprotection; in that model, upregulation of genes for osmoprotectants (such as glycine betaine and ectoine) is an attempt to compensate for the absence of the glycan in *csIA* mutants, or of the mature glycan in *glxA* mutants.

Finally, strong downregulation was observed for SLI_3420-3423 and SLI_5205, all of which are involved in histidine catabolism (Table 3). This may reflect an attempt to maintain the histidine pool during osmotic stress. Histidine is a precursor of ergothioneine, a thiourea derivative that is synthesized via methylation of histidine

and incorporation of a cysteine-derived sulfur atom in the imidazole ring (Seebeck 2013). Ergothioneine, naturally produced by Actinobacteria and by filamentous fungi, acts as an efficient antioxidant (Cheah and Halliwell 2012). A possible role of histidine/ergothioneine accumulation in osmotic stress in *Streptomyces* should be investigated.

However, changes in the transcription of known osmotic stress regulatory genes such as *sigB* and *osaC* were not observed, with only a partial effect on *osaB* in the *cslA* mutant (Fernández Martínez et al. 2009 and Table 5). This is consistent with earlier work, where the regulation of *glxA* by these elements has been ruled out (Liman et al. 2013).

CONCLUSION

The analysis of the transcriptome of the mutants reveals a large number of genes whose transcription is significantly up- or downregulated. The most drastic changes are observed in *cslA* mutants. Two classes of genes stood out, namely genes for phage tail-like proteins that possibly relate to matrix formation/morphology and genes related to osmoprotection. Phage tail-like proteins (SLI_4479-4495) are upregulated three to five-fold in the *cslA* mutant and around two-fold in the *glxA* mutant. Their role in bacteria is not clear, but their function in attachment to the bacterial cell wall and their role in biofilm formation suggests a structural role. Moreover, a change in transcription has been observed in other strains with a nonpelleting phenotype, suggesting a direct correlation with pellet morphology. In addition *hyaS*, involved in hyphal aggregation, is also upregulated in both mutants, suggesting that a network of proteins might interact in the determination of morphology. We currently favor a model in which the absence of one of them leads to a compensation effect increasing the transcription of the others. However, this awaits further experimental evidence.

In addition to the observed effect on morphology-related genes, deletion of *cslA* and *glxA* also majorly influence the transcription of genes related to osmoprotection.

Table 3. Transcription data of genes linked to osmotic stress

Gene # <i>S. coelicolor</i>	Gene # <i>S. lividans</i>	1326 (RPKM)	csIA (RPKM)	glxA (RPKM)	csIA/1326	glxA/1326	Annotation
SCO1620	SLI1923	31,5	193,9	117,3	6,2	3,7	Glycine betaine ABC transport system
SCO1621	SLI1924	28,7	153,3	106,7	5,3	3,7	L-proline glycine betaine ABC transport system
SCO4828	SLI5101	20,9	49,8	48,8	2,4	2,3	Betaine aldehyde dehydrogenase GsbAB (EC 1.2.1.8)
SCO4829	SLI5102	17,8	62,4	48,6	3,5	2,7	Choline dehydrogenase (EC 1.1.99.1)
SCO4830	SLI5103	8,2	41,1	26,2	5,0	3,2	Glycine betaine ABC transport system, ATP-binding protein (EC 3.6.3.32)
SCO4831	SLI5104	8,1	33,2	22,0	4,1	2,7	Glycine betaine ABC transport system, permease protein OpuAB
SCO4832	SLI5105	24,4	67,4	50,1	2,8	2,1	Choline/glycine betaine ABC transporter, substrate binding protein
SCO1864	SLI2175	32,4	94,2	52,1	2,9	1,6	L-2,4-diaminobutyric acid acetyltransferase (EC 2.3.1.-)
SCO1865	SLI2176	31,3	167,0	61,8	5,3	2,0	Diaminobutyrate-pyruvate aminotransferase (EC 2.6.1.46)
SCO1866	SLI2177	67,7	666,0	139,3	9,8	2,1	L-ectoine synthase (EC 4.2.1.-)
SCO1867	SLI2178	72,5	614,8	125,1	8,5	1,7	Ectoine hydroxylase (EC 1.17.-.-)
SCO0600	SLI0566	33,1	36,2	35,9	1,1	1,1	sigma factor SigB
SCO5749	SLI6010	447,5	262,7	342,2	0,6	0,8	OsaB
SCO5747	SLI6008	63,7	43,6	56,9	0,7	0,9	OsaC

In the *csIA* and *glxA* mutants, we observed an increase in transcription of genes related to ectoine synthesis and glycine betaine import and synthesis. We postulate that the absence of the polymer synthesized and deposited at the hyphal tips by the concerted action of *csIA* and *glxA* induces possible weakness to the hyphae, which stimulates the increase of intracellular osmoprotectants. The fact that the deletion of *csIA* almost invariably results in stronger changes in gene expression than deletion of *glxA* may be explained by the absence of the glycan in the *csIA* mutant, while this polysaccharide is present but not localized properly in the *glxA* mutant.

Future work is aimed at further analysis and verification of the major changes observed by RNA seq analysis, and to study the role of the phage tail proteins in the control of morphogenesis. In this way we will obtain more insight into the factors that play a role in controlling mycelial architecture.

MATERIAL AND METHODS

Strains and growth conditions

Streptomyces lividans strains 1326 (*S. lividans* 66, stock number 1326 from the John Innes Centre; Hopwood et al. 1985), and the $\Delta cslA$ and $\Delta glxA$ derivatives thereof (Chapter 3) were used in this study. 2.5×10^8 spores were used to inoculate 250 ml flasks containing 50 ml liquid NMMP medium, supplemented with 0.5% glucose and 0.5% mannitol (Kieser et al. 2000).

RNA sequencing

Mycelium was collected after 17 h of growth by centrifugation at 5,000 rpm for 10 min. RNA was immediately isolated using the Kirby protocol (Kieser et al. 2000). The samples were treated with DNase I to remove any traces of DNA. The purity and integrity of the sample was assessed using a Bio-Rad Gel Doc EZ Imager, while the absence of residual DNA was verified by PCR (Fig. 1S). The RNA samples were sent for sequencing to BaseClear, after which the RNA quality was further assessed using a Bioanalyzer. Ribosomal RNA was subsequently removed with a Ribo-Zero kit (Epicenter) and the remaining RNA used as input for the Illumina TruSeq RNA-seq library preparation. Once fragmented and converted into double strand cDNA, the fragments (about 100-200 bp) were ligated with DNA adapters at both ends and amplified via PCR. The resulting library was then sequenced using an Illumina Sequencer. The FASTQ sequence reads were generated using the Illumina Casava pipeline version 1.8.3. Initial quality assessment was based on data passing the Illumina Chastity filtering. Subsequently, reads containing adapters and/or PhiX control signals were removed using an in-house filtering protocol. The second quality assessment was based on the remaining reads using the FASTQC quality control tool version 0.10.0.

RNA-seq analysis

The RNA-Seq analysis was performed by Baseclear BV (Leiden, The Netherlands). Briefly, the quality of the FASTQ sequences was enhanced by trimming off low-quality bases using the “Trim sequences” option present in CLC Genomics Workbench Version 6.0.4. The quality-filtered sequence reads were used for further analysis with CLC Genomics Workbench. First an alignment against the reference(s) and calculation of the transcript levels was performed using the “RNA-Seq” option. Subsequent comparison of transcript levels between strains and statistical analysis was done with the “Expression analysis” option, calculating so-called RPKM values. These are defined as the Reads Per Kilobase per Million mapped reads (Mortazavi et al. 2008) and seeks to normalize for the difference in number of mapped reads between samples as well as the transcript length. It is given by dividing the total number of exon reads by the number of mapped reads (in Millions) times the exon length (in kilobases).

SUPPLEMENTAL MATERIAL

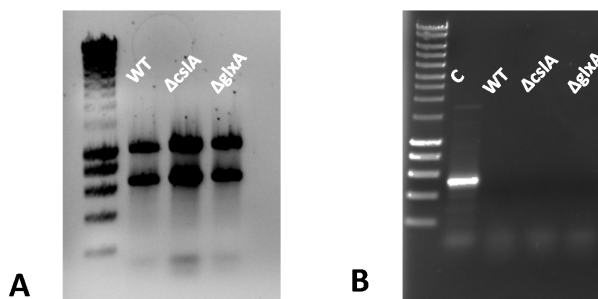


Figure 1S. (A) Quality assessment of the RNA samples on a 1.2% agarose TAE gel. The 23S, 16S and 5S bands are clearly visible in the three samples and no signs of degradation are visible. (B) PCR check for the absence of genomic DNA on 4 μ g of RNA as a template. The first lane include a control sample with *S. lividans* genomic DNA.

Chapter 5

Identification of strong constitutive promoters for protein expression in *Streptomyces lividans* 1326.

Giulia Mangiameli, Kevin Gijselman, Gilles P. Van Wezel and Erik Vijgenboom

Manuscript in preparation

ABSTRACT

A growing number of Gram-positive bacteria are considered as effective hosts for the production of industrial relevant enzymes. In the era of high throughput genome sequencing, many new genes for enzymes are identified. With the expected concomitant increase in the use of heterologously produced enzymes in industry, the optimization of the hosts for all aspects related to production becomes more and more attractive. One of the platforms for the production of enzymes and also secondary metabolites is *Streptomyces lividans*. However, the number of expression vectors with strong promoters is limited. Here we present a short pipeline to identify and apply new naturally occurring promoters in *Streptomyces* that form good alternatives to those currently in use. The strong constitutive promoter P_{ermE} was used as the benchmark. RNA-Seq and DNA-microarray data were analyzed, which resulted in 15 candidate promoters. These promoters were then screened using the *lux* genes as reporters. The most attractive candidate promoters were validated in an expression system based on the secreted laccase SLAC in *Streptomyces lividans* 1326. This resulted in the identification of three promoter sequences ($P_{sco1947}$, $P_{sco4253}$ and $P_{sco3484}$) with higher or comparable strength than the benchmark P_{ermE} .

INTRODUCTION

Streptomyces are Gram positive, soil dwelling bacteria, which are well known for their ability to produce the vast majority of the antibiotics available on today's market and have a great potential in the production of enzymes and therapeutic proteins (Vrancken and Anné 2009; Anné et al. 2012).

Several aspects should be taken into consideration when selecting a bacterial host for heterologous protein production. Among them, the availability of proven expression systems plays a substantial role. The expression system should provide high level transcription and efficient translation and secretion (Nakashima et al. 2005; Vrancken et al. 2010). Plasmids derived from the high copy number pIJ101 are generally preferred, as they are present in the cell in up to 300 copies per chromosome (Kieser et al. 2000). For plasmid maintenance, a selectable marker is required, which is typically a gene conferring antibiotic resistance. To avoid the addition of antibiotics during fermentations, alternatives such as toxin/antitoxin systems have been developed, e.g. for the production of a xylanase and an amylase in *S. lividans* (Sevillano et al. 2013). At a transcriptional level, strong promoters that do not affect the physiology and morphology of the host when present in high copy are required. Furthermore, optimal ribosome binding sites for efficient ribosome recruitment, appropriate signal sequences and optimized codon usage contribute to maximal production.

In this study, we have identified strong and constitutive promoters obtained from *Streptomyces* genomes as valuable alternatives to the current small selection of available sequences. The promoter of the erythromycin resistance gene from *S. erythraeus* (P_{ermE}) is commonly used (Bibb et al. 1985). However, it does not always perform reliably in all strains and conditions (Zhou et al. 2011). An alternative, the constitutive promoter from the subtilisin inhibitor *vsf* from *S. venezuelae*, has also been used for protein expression (Lammertyn et al. 1997). Some inducible promoters such as the thioestrepton-inducible promoter P_{tipA} from *S. lividans* (Murakami et al. 1989) or the xylan-inducible promoter P_{xysA} from *S. halstedii* (Ruiz-Arribas et al. 1997),

which are important for the expression of toxic proteins, have been used in protein production studies but have the drawback of requiring an inducer during industrial production. Moreover, the addition of thiostrepton induces the expression of stress-related proteins in *Streptomyces* (Holmes et al. 1993), while P_{xysA} leads to significant expression only after prolonged fermentation times.

The elements that define a strong promoter have been studied in *Streptomyces* but not completely understood (Strohl 1992; Bourn and Babb 1995). Over 60 different genes for σ factors have been identified in *S. coelicolor* (Bentley et al. 2002), some of which are strictly regulated by development such as *bldN* and *sigF* (Kelemen et al. 1996; Bibb et al. 2000). In contrast, the *E. coli* genome only encodes seven σ factors (Pérez-Rueda and Collado-Vides 2000). Attempts to isolate a strong promoter from a synthetic library of randomized promoter sequences underlined the importance of guanine residues at specific position within the regulatory regions, but failed to produce promoters stronger than the currently available ones (Seghezzi et al. 2011).

The engineering of known promoters can produce a remarkable improvement in strength. A combination of rational and random mutagenesis of the strictly regulated promoter P_{kasO} resulted in a de-repressed strong promoter sequence (Wang et al. 2013). The opposite engineering was shown recently to work as well in *Streptomyces*. Introduction of riboswitches in between the promoter sequence and the translational start codon mediated ligand-dependent expression of reporter genes (Rudolph et al. 2013).

In this work, we analyzed the global transcription profiles from liquid- and solid-grown cultures of two different streptomycetes, *S. coelicolor* M145 (Świątek et al. 2013) and *S. lividans* 1326 (Dwarakanath et al. 2012) and identified new strong promoters. To screen the activity of those promoters, a reliable and quick reporter system with a good level of sensitivity and an easy temporal recording is needed. The *redD*, *xylE*, *egfp* and *lux* promoter-probe systems are commonly used for analysis of promoter activity. RedD is the transcriptional activator of the biosynthetic pathway for the pigmented antibiotic undecylprodigiosin (Red) in *Streptomyces* (Takano et al. 1992). The *redD* gene has been used as a reporter (van Wezel et al. 2000c) as it

allows a direct pigmentation of the colonies that can be followed in time, and is in contrast to most antibiotics not secreted, but the limited sensitivity of the detection method hampers an accurate quantification. The *xylE* gene from *Pseudomonas putida* encodes catechol dioxygenase, which converts the colorless substrate catechol into the bright yellow compound benzoquinone (Ingram et al. 1989). The requirement of a substrate that needs to be sprayed directly onto the plate is a disadvantage of this system. Cloning different promoters in front of the *egfp* gene from the jellyfish *Aequorea Victoria* (Chalfie et al. 1994) allows assessing gene expression in space and time, but is not suitable for large scale screenings.

In this work, we chose the LuxCDABE system optimized for GC rich bacteria (Craney et al. 2007) to test our selection of putative strong promoters. This system consists of the operon from *Photobacterium luminescens*, that includes the luciferase genes *luxA* and *luxB* in addition to three genes for the production of the substrate tetradecanal (*luxC*, *luxD*, *luxE*) which is synthesized directly in the cytosol and does not need to be added separately. The result is a spontaneous emission of light at 490 nm, potentially suitable for screening large number of samples in 96-well plates and including the collection of temporal data.

Among the 15 promoters analyzed, three were equivalent or stronger in comparison to P_{ermE} and were successfully tested for the production of a small laccase (SLAC) in *S. lividans*.

RESULTS AND DISCUSSION

Putative constitutive strong promoters

In this study, we used a modified version of the *lux* reporter plasmid, namely pMUIS*_mmrt, and a laccase reporter system to assess the strength of promoters selected on the basis of genome-wide transcript analysis data (in-house RNA-Seq and microarray analysis).

A list of putative strong promoters was compiled on the basis of our RNA-Seq data of *S. lividans* 1326 in liquid-grown cultures (Dwarakanath et al. 2012). The best hits in terms of transcriptional activity were filtered for ribosomal protein synthesis genes, because these genes are known to have a strict and growth dependent transcription control (Lindahl and Zengel 1982). Only the promoter upstream of *rpsP* (P_{sco5591}) was kept in the selection as an internal control. 15 promoters were selected, the 13 best hits from *S. lividans* and in addition the two best hits of genes present in *S. coelicolor* but not in *S. lividans* (Table 1 and Table S1). The latter data were taken from microarray data of *S. coelicolor* M145 grown on minimal media agar plates with mannitol (15 w/v) as the sole carbon source (Świątek et al. 2013). In the final list, five genes encode stress-related proteins, namely the cold-shock proteins CspD, CspG, CspA and the heat-shock proteins GroEL2 and GroES, while the others encode various membrane proteins and enzymes. Little is known about the regulation of these sequences (Table S2). When the regulatory elements are not described in literature, the sequences were analyzed by BPPROM Softberry (<http://linux1.softberry.com>) for the presence of canonical -10/-35 sequences, conforming to the consensus for the household sigma factor σ^{70} . This identified seven out of 15 sequences as likely σ^{70} -like promoters (Table S2).

Table 1. Selection of 15 potential strong promoters and relative expression levels from in-house transcription data (RNA-Seq and microarray analysis).

Annotation	SCO Gene #	SLI Gene #	sequence relative to start codon	RPKM
Cold shock protein CspD	SCO4505	SLI4786	-200/-22	40657
Membrane protein	SCO6624	SLI6984	-182/-15	14184
60 kDa chaperonin 2 GroEL protein 2	SCO4296	SLI4533	-200/-25	10076
Cold-shock protein CspG	SCO3731	SLI3978	-191/-12	9099
Cold shock protein CspA	SCO0527	SLI0486	-324/-16	7184
DNA-binding protein Hbsu	SCO2950	SLI3296	-184/-23	6658
10 kDa chaperonin GroES protein	SCO4761	SLI5031	-300/-81	5850
Uncharacterized protein SCO4253	SCO4253	SLI4489	-212/-15	2466
30S ribosomal protein 16S, RpsP	SCO5591	SLI5878	-277/-16	5167
Glyceraldehyde-3-phos- phate dehydrogenase GAPDH (EC 1.2.1.12)	SCO1947	SLI2261	-236/-25	4322
ATP synthase subunit a	SCO5367	SLI5636	-200/-13	1679
Thiosulfate sulfurtrans- ferase (EC 2.8.1.1)	SCO4164	SLI4405	-200/-27	3970
Membrane protein	SCO7636	SLI7864	-300/-10	43
Sugar binding protein	SCO3484	-	-278/-14	-
Hydrolase	SCO3487	-	-280/-10	-

Vector optimization

The vector used in this study is a derivative of pMU1, designated pMU1S* (Craney et al. 2007, JR Nodwell pers comm.). First, *S. lividans* 1326 was transformed with the empty vector and tested for background transcription when grown on several solid media (Fig. S1). The vector itself already gave high luminescence from the 30 hr time point onwards. This luminescence was assumed to be caused by promoter activity originating from the vector sequences upstream of the *lux* genes. Analysis for the presence of a putative promoter by BPROM Softberry revealed putative promoter sequences upstream of the transcriptional terminator (-10 box AGTTAGGCT and -35 box TTTTTT). To reduce transcriptional readthrough, the transcriptional terminator of the methylenomycin resistance gene of *S. coelicolor* (*mmrT*) was amplified from pMT3003 (Paget et al. 1994) and cloned as an EcoRV-BamHI fragment in the multiple cloning site of pMU1S*, generating plasmid pMU1S*_mmrT. The new

vector showed much lower background luminescence on different solid media (Fig. S1) and was therefore used in all subsequent experiments.

To eliminate translational effects, the RBS from pIJ8660 cloned in front of *luxC* in the original vector was substituted with the strong RBS from *S. ramocissimus* elongation factor *tuf1*, preceded by a 16 nucleotide linker essential for the correct recognition (Vijgenboom et al. 1994; Motamedi et al. 1995). The reference P_{ermE} including the *tuf1* RBS was taken from pHM10a (Motamedi et al. 1995). This construct typically results in high levels of protein expression (van Wezel et al. 2000).

Promoter screening

All promoter sequences were cloned in pMU1S*_mmrt directly upstream of *luxCDABE*. *S. lividans* transformants containing the constructs with the *lux* genes under the control of one of the selected promoters were first screened by growing them in 96-well microtitre plates containing minimal agar medium supplemented with mannitol (1% w/v). Luminescence was measured at eight hour intervals over a period of 72 hours (Fig. S2). All putative promoter sequences that did not result in luminescence higher than 4000 cps during exponential growth were discarded. The seven strongest promoters were $P_{sco0527}$, $P_{sco1947}$, $P_{sco3484}$, $P_{sco3487}$, $P_{sco4505}$, $P_{sco4253}$ and $P_{sco5591}$ and these were selected for further analysis (Fig. 1A). The transformants were grown in liquid minimal medium supplemented with 0.5% mannitol and 0.5% glucose (Fig. 1B). The luminescence was measured at 10 time points during exponential growth (14-23 hr) and normalized for biomass. Comparison of the luminescence/biomass values (14-20h) showed that four promoters had similar or higher strength than P_{ermE} , namely $P_{sco1947}$ (about the same strength), $P_{sco4253}$ (+33%), $P_{sco5591}$ (+125%) and $P_{sco3484}$ (+154%) (Fig. 1C). The other three promoters ($P_{sco0527}$, $P_{sco3487}$ and $P_{sco4505}$) were discarded.

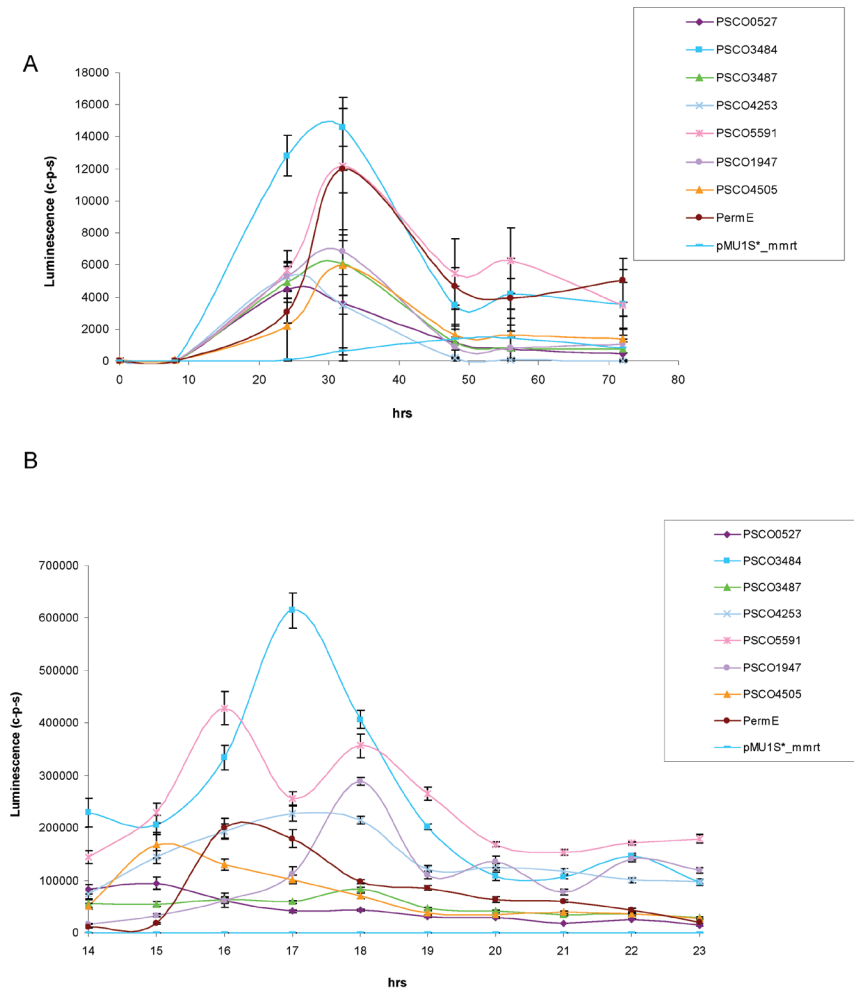


Figure 1 Pre-screening of the selected promoters. The data for the seven strongest promoters are shown together with the luminescence of the benchmark P_{ermE} and the empty vector. The strains are grown on solid MM + 1% mannitol (A) and liquid NMMP + 0.5% mannitol and 0.5% glucose (B).

	Average luminescence/biomass 14-20 hrs (%)	highest value (%)
PermE	100	100
PSCO1947	108	145
PSCO3484	254	308
PSCO4253	133	114
PSCO5591	225	179
negative control	3	0

Table 2 Comparison of promoters $P_{SCO1927}$, $P_{SCO3484}$, $P_{SCO4253}$ and $P_{SCO5591}$ from liquid culture data between 14 and 20 hr of growth. The luminescence obtained with P_{ermE} was set as 100%.

Validation of the promoters

To assess if the promoters could potentially find application in expression vectors, the four selected promoters were used to drive the transcription of a small laccase gene, encoding SLAC of *S. coelicolor* (Machczynski et al. 2004). *S. lividans* transformants containing the different promoter-*slac* expression constructs were grown in liquid TSBS and samples were taken at 24 and 48 hr. The amount of SLAC present in the spent medium was determined by an in-gel enzymatic detection, visualizing the active SLAC fraction (Fig. 2A and C) and by Western blot analysis (Fig. 2B and D), reflecting the total protein produced.

The activity assay showed that P_{sco1947}-*slac* resulted in SLAC activity comparable to P_{ermE} after 24 hr of growth, with an increase of 67% after 48 hr, while P_{sco4253}-*slac* and P_{sco3484}-*slac* resulted in slightly higher (+10%) or comparable expression of SLAC when enzyme levels were measured after 48 hr. Similar results were obtained with the Western blot analysis for P_{sco1947}-*slac* construct. The total SLAC levels for P_{sco4253}-*slac* and P_{sco3484}-*slac* as detected in the Western blots are higher than those measured by the in-gel assay. So part of the enzyme produced in transformants with these constructs is not active. However, the difference between the protein production assays is much smaller after 48 hours of growth. Nevertheless, it should be noted that P_{sco3484} was almost three-fold stronger when the transcriptional level was analyzed with the bioluminescence assay and that the transformants carrying P_{sco3484}-*slac* were strongly retarded in growth. This might be explained by a metabolic imbalance, with a deviation of the flux towards heterologous protein production versus biomass formation, resulting in growth impairment (D’Huys et al. 2011). In addition, the promoter derived from rpsP (P_{sco5591}) did not show any protein production despite the high transcriptional levels shown in the lux experiment. This difference might depend on the fact that the *slac* reporter is inserted in a multicopy vector while the lux construct is present in a single copy integrated in the genome. However, this demonstrates once more that promoters derived from ribosomal protein or rRNA genes typically are not suitable for use in multicopy expression vectors.

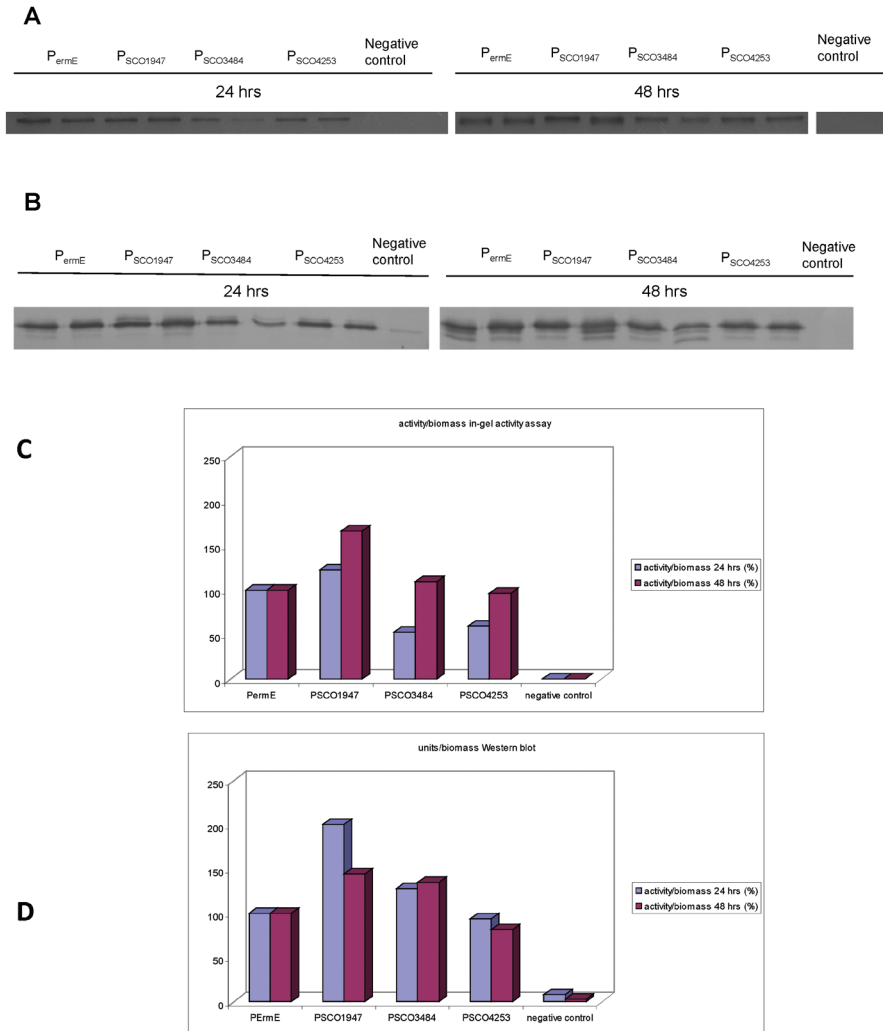


Figure 2 In-gel SLAC activity assay with DMPPDA 0.125 mg/ml and 1-naphtol 0.125 mg/ml (A) and Western blot with polyclonal antibodies raised in rabbits and GARAP as secondary antibody (B). The quantification of the signals corresponding to active SLAC as determined by the in-gel assay and the total amount fo SLAC as detected by Western blot are shown in panels C and D Band intensities were normalized for biomass and the amount of (active) protein obtained in the P_{ermE} construct was set at 100%.

The SLAC assays are all carried out on laboratory scale and in rich liquid medium, mimicking to some extent the conditions in industry where complex media are preferred. However, production pilots in a fermentation setup with optimized growth conditions and fermentation parameters are required to properly validate the potential of expression systems.

CONCLUSION

We have identified three promoters with potential use in expression systems. The transcriptional activity of these promoters could also be correlated to high level protein expression, using the versatile SLAC protein as a reporter. Currently, a limited number of promoter-vector combinations are available in *Streptomyces*. The promoters identified in this study are a welcome addition to the selection and will provide more flexibility for the design of protein production platforms. Further design of these new promoters by random or Selex methods as well as optimizing growth conditions should be employed to obtain even better levels of protein production.

MATERIALS AND METHODS

Promoter amplification and cloning in lux constructs

A modified version of plasmid pMU1 (Crane et al. 2007) named pMU1S* (JR Nodwell, personal communication) was used in this study. All 15 promoter sequences were amplified by PCR with the *S. lividans* 1326 genome as template, except for P_{sco3484} and P_{sco3487}, which were amplified from *S. coelicolor* M145 genomic DNA. The region to amplify was selected as a 200-300bp sequence upstream of the annotated translational start site for each gene, including the putative -35 and -10 regions. The ribosome binding site was identified and substituted by a 16 nucleotide linker and the RBS of *tuf1* (TACAGAACCACTCCACAGGAGGACC) included in the reverse primer of each construct. The constructs and primers used in this study are listed in Table S3 and S4. The promoters were cloned in pMU1S*_mmrt as BamHI-NdeI fragments, generating 15 different *lux* constructs. These plasmids were introduced in *S. lividans* 1326 by protoplast transformation (Kieser et al. 2000). Transformants carrying the promoterless pMU1S*_mmrt plasmid were used as negative control and transformants carrying P_{ermE} as reference (benchmark).

Bioluminescence assay

Bioluminescence assays on solid media were performed in 96 well plates made of white polystyrene (Greiner-bio-one) filled with 200 μ l of different media, including MS, R5 and Minimal Medium + 1% mannitol. Eight wells per construct were inoculated with 1000 spores and the plate was incubated at 30 °C. Measurements of the eight replicates were done every 8 hr for 72 hr with a GloMax 96 Microplate Luminometer and luminescence is expressed in counts per second (cps).

For the assay in liquid cultures, one flask per construct carrying 50 ml of liquid minimal medium (NMMP + 0.5% mannitol and 0.5% glucose) was inoculated with 2.5×10^8 spores and incubated at 30 °C in a shaking incubator. After 14 hrs of growth, sampling of each culture was done every hr up to 23 hrs of growth with eight replicates. A 1.5 mL sample was taken and the mycelium was harvested by

centrifugation and used for the biomass determination. The dry weight of each sample was determined after overnight drying at 100 °C. Eight samples of 100 µL were taken for the bioluminescence measurements. These samples were loaded in eight wells of a white polystyrene 96 well plate and bioluminescence was determined in a GloMax 96 Microplate Luminometer.

Plasmids for SLAC expression

The efficiency of the promoters in protein production was carried out with a selection of the four strongest promoters and P_{ermE} as reference. They were cloned as EcoRI-NdeI fragments in plasmid pSLAC, carrying the ORF of *slac* (SCO6712) with an NdeI site overlapping with the translational start codon and 400 nucleotides downstream. The vector used is a modified version of pHJL401 lacking all NdeI sites (pHJL401N⁻). The constructs and primers used in this study are listed in Table S3 and S4. After protoplast transformation of *S. lividans* 1326, two independent transformants were used for the enzymatic assay. Transformants carrying the promoterless pSLAC plasmid were used as negative control.

SLAC/laccase in-gel activity assay

The transformants were grown in 10 ml TSBS with 25 µM Cu(II) and 2 µg/ml thiostrepton. About 5×10^7 spores were inoculated and the flasks incubated at 30 °C in a shaking incubator. Samples of 1 ml were taken after 24 and 48 hr of growth, centrifuged for 10 min and the pellet incubated overnight at 100 °C for dry weight determination. Ten µl of the supernatant were mixed with ten µl of SDS PAGE loading buffer without the addition of β-mercaptoethanol and loaded on a 12.5% polyacrylamide gel. Enzymatic activity was essentially determined according to Endo et al. (2003) and Machczynski et al. (2004). Following electrophoresis, the gel was soaked for 1 hr in 100 mM Na-phosphate buffer pH 6.8 at room temperature on a rocking platform and for 1 hr at 30 °C. Subsequently, the substrates, 0.125 mg/ml DMPPDA and 0.125 mg/ml 1-naphtol in phosphate buffer were added. SLAC activity

becomes visible within minutes as clear blue/purple bands in the gel. A digital image was taken and the band intensities were analyzed with the software ImageJ (Schneider et al. 2012). For the calibration curve, two to 25 μ l of the most concentrated sample were loaded, revealing a linear range.

Western blot

Samples of the spent medium were mixed 1:1 with loading buffer including β -mercaptoethanol and heated at 95 °C for 4 minutes. Equal amounts of each sample were loaded on a 12.5% polyacrylamide SDS-PAGE gel. After electrophoresis, proteins were transferred to Hybond-P membrane (Amersham) using the Biorad blotting system. The membranes were washed with PBS and incubated in 5% low fat baby milk powder (Frisolac) in PBS for 30 minutes followed by overnight incubation with a 1:5000 diluted polyclonal antibodies raised against SLAC in rabbits. SLAC was detected using an anti-rabbit IgG alkaline phosphatase secondary antibody (sigma A8025), diluted 1:5000 and BCIP/NBT (5-Bromo-4-chloro-3-indolyl phosphate/ Nitro blue tetrazolium) as substrates. Band intensities were determined with ImageJ and the gel analysis option. Gels were standardized using 2 pmol of purified SLAC and one of the samples as internal controls in each Western Blot experiment. The amount of SLAC detected was normalized for the biomass (g/L). For the calibration curve, SLAC was purified as a N-terminal truncated form following expression in *E. coli* and stored as a 5 μ M stock at -20 °C (Machczynski et al 2004). Serial dilution were run on SDS PAGE followed by Western blotting. NBT/BCIP signals were quantified with ImageJ and the calibration curve showed a linear response up to 3 pmol of SLAC.

SUPPLEMENTAL MATERIAL

Table S-1 The best expression hits obtained from RNA-Seq data ordered by expression level.

<i>S.coelicolor</i> M145	<i>S.lividans</i> 1326	RPKM	Function
SCO4505	SLI4786	40657	Cold shock protein CspD
SCO4635	SLI4906	37093	LSU ribosomal protein L33p @ LSU ribosomal protein L33p, zinc-dependent
SCO4653	SLI4924	19581	LSU ribosomal protein L7/L12 (P1/P2)
SCO4662	SLI4936	17428	Translation elongation factor Tu
SCO3906	SLI4164	15191	SSU ribosomal protein S6p
SCO4652	SLI4923	14885	LSU ribosomal protein L10p (P0)
SCO6624	SLI6984	14184	hypothetical protein
SCO4725	SLI4994	12641	Translation initiation factor 1
SCO4716	SLI4985	11909	SSU ribosomal protein S8p (S15Ae)
SCO4721	SLI4990	11528	LSU ribosomal protein L15p (L27Ae)
SCO4702	SLI4971	10854	LSU ribosomal protein L3p (L3e)
SCO4717	SLI4986	10637	LSU ribosomal protein L6p (L9e)
SCO4713	SLI4982	10483	LSU ribosomal protein L24p (L26e)
SCO4296	SLI4533	10076	chaperonin GroEL
SCO4661	SLI4935	9424	Translation elongation factor G
SCO4701	SLI4970	9381	SSU ribosomal protein S10p (S20e)
SCO4711	SLI4980	9375	SSU ribosomal protein S17p (S11e)
SCO4730	SLI4999	9232	LSU ribosomal protein L17p
SCO3731	SLI3978	9099	Cold shock protein CspG
SCO4714	SLI4983	8983	LSU ribosomal protein L5p (L11e)
SCO3909	SLI4167	8730	LSU ribosomal protein L9p
SCO4706	SLI4975	8576	SSU ribosomal protein S19p (S15e)
SCO4659	SLI4933	8390	SSU ribosomal protein S12p (S23e)
SCO4709	SLI4978	8172	LSU ribosomal protein L16p (L10e)
SCO4719	SLI4988	8051	SSU ribosomal protein S5p (S2e)
SCO4720	SLI4989	8046	LSU ribosomal protein L30p (L7e)
SCO4660	SLI4934	8044	SSU ribosomal protein S7p (S5e)
SCO3908	SLI4166	7728	SSU ribosomal protein S18p @ SSU ribosomal protein S18p, zinc-dependent
SCO4704	SLI4973	7614	LSU ribosomal protein L23p (L23Ae)
SCO4708	SLI4977	7220	SSU ribosomal protein S3p (S3e)
SCO0527	SLI0486	7184	Cold shock protein CspA

SCO1998	SLI2315	7085	SSU ribosomal protein S1p
SCO4718	SLI4987	6987	LSU ribosomal protein L18p (L5e)
SCO4712	SLI4981	6979	LSU ribosomal protein L14p (L23e)
SCO4727	SLI4996	6970	SSU ribosomal protein S13p (S18e)
SCO4707	SLI4976	6742	LSU ribosomal protein L22p (L17e)
SCO2950	SLI3296	6658	Non-specific DNA-binding protein HBsu

Table S-2. Classification of sequences according to their similarities with the σ -70 like promoters.

Known elements of regulation are listed.

SCO Gene #	SLI Gene #	-35/-10 regions (based on Strohl et al.)	-35/-10 regions (Softberry)	σ 70-like promoter	Regulators
SCO4505	SLI4786	-160/-182	-60/-83	yes	
SCO6624	SLI6984	-135/-161	-	yes	
SCO4296	SLI4533	-159/-183	-		HrcA/CIRCE regulon (Duchene et al. 1994)
SCO3731	SLI3978	-	-57/-84	yes	
SCO0527	SLI0486	-	-		
SCO2950	SLI3296	-149/-167			developmentally regulat- ed (Salerno et al, 2009)
SCO4761	SLI5031	-131/-155	-133/-155	yes	HrcA/CIRCE regulon (Duchene et al. 1994)
SCO4253	SLI4489	-	-		controlled by SCO4263, BldA dependent (Kim et al, 2005)
SCO5591	SLI5878	-59/-83	-135/-184	yes	
SCO1947	SLI2261	-	-		
SCO5367	SLI5636	-	-		
SCO4164	SLI4405	-140/-163	-		
SCO7636	SLI7864	-	-		
SCO3487	-	-61/-84	-61/-84	yes	possible BldA regulation (Temuujin et al 2012)
SCO3484	-	-134/-156	-96/-120	yes	

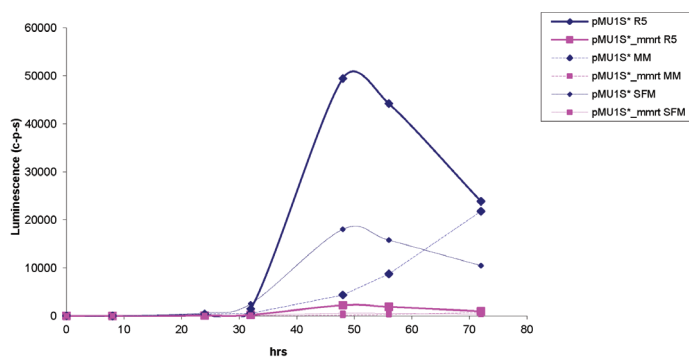


Figure S-1. Comparison of background light emission between pMU1S* and pMU1S*_mmrt on different solid media. An increase in emission can be observed starting at 30 hr for pMU1S*, while pMU1S*_mmrt shows a remarkable reduction in background.

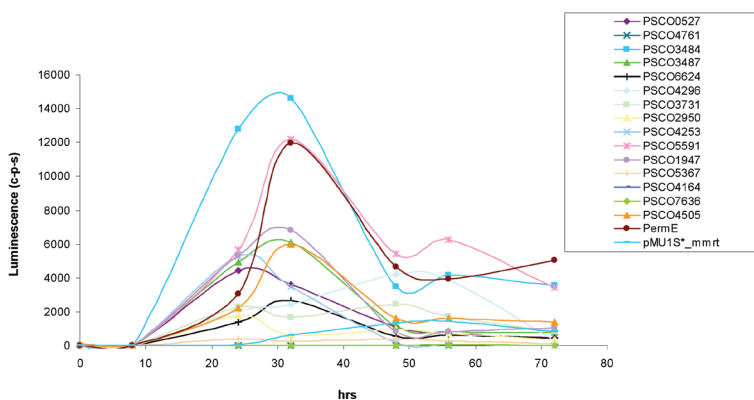


Figure S-2. Pre-screening of the 15 selected promoters compared with the benchmark P_{ermE} and the empty vector. Transformants were grown on MM agar plates with mannitol (1% w/v).

Table S-3. Plasmid used in this study

Name	Description	Reference
pMU1S*	pIJ8660 derivative carrying the luxCDABE cluster from <i>Photorhabdus luminescens</i>	(derived from Craney et al., 2007)
pMU1S*_mmrT	pMU1S* derivative with additional mmrT transcriptional terminator upstream of the MCS	This work
pTZ18R	pUC18 derivative, <i>E. coli</i> cloning vector	Pharmacia, Sweden
p18ERM	pTZ18R carrying P _{ermE} from er gene of <i>S. erythraeus</i> + 16 nucleotide linker sequence and RBS of <i>tuf1</i> from <i>S. ramocissimus</i>	(derived from Motamedi et al., 1995)
pHJL401	<i>E.coli-Streptomyces</i> shuttle vector, TsrR, AmpR	(Larson and Her-shberger, 1986)
pHJL401N-	pHJL401 derivative without NdeI sites	This work
pSLAC	pHJL401N- carrying the <i>slac</i> gene and 400 downstream nucleotides from <i>S. coelicolor</i> cloned as EcoRI/NdeI-HindIII	This work

Table S-4. Oligonucleotides used in this study

Name	Sequence 5'-3'	Restriction sites
mmrT FW	GCG GAT ATC GAA CGC CGC AGC GCC GTC AC	EcoRV
mmrT RV	CGC GGA TCC GGT CGA TAC CCG GAG TGC GTG	BamHI
4253F	GCG GAA TTC GGA TCC GAC AGT CGA CAC AAG ACG TTG AAT C	EcoRI-BamHI
4253R_RBS	CGC AAG CTT CAT ATG GGT CCT CCT GTG GAG TGG TTC TGT AGGG TAC GAG ACA GGA CGC C	HindIII-NdeI
5591F	GCG GAA TTC GGA TCC GGT CGG CGC GGG AAT GAG CTG	EcoRI-BamHI
5591R_RBS	CGC AAG CTT CAT ATG GGT CCT CCT GTG GAG TGG TTC TGT AGGT TTT GAC GTG GTT GGG CAC GG	HindIII-NdeI
1947F	GCG GAA TTC GGA TCC GAC GAG TGA ATC CCG GTG TGC G	EcoRI-BamHI
1947R_RBS	CGC AAG CTT CAT ATG GGT CCT CCT GTG GAG TGG TTC TGT AGGC CCG ATG TGC CGG CGA G	HindIII-NdeI
4505F	GCG GAA TTC GGA TCC TCT TGA CCT CTG TTG CGC TCG G	EcoRI-BamHI
4505R_RBS	CGC AAG CTT CAT ATG GGT CCT CCT GTG GAG TGG TTC TGT AGTT GCC CTG CTC CAG AAC CAG	HindIII-NdeI
6624F	GCG GAA TTC GGA TCC GTG CAG TAG AGT GAC TTG TGC TG	EcoRI-BamHI
6624R_RBS	CGC AAG CTT CAT ATG GGT CCT CCT GTG GAG TGG TTC TGT AGGT GGT GAG CAG GAA TGG TGG	HindIII-NdeI
4296F	GCG GAA TTC GGA TCC CCC GAG AGG CGC TTG CAC TC	EcoRI-BamHI
4296R_RBS	CGC AAG CTT CAT ATG GGT CCT CCT GTG GAG TGG TTC TGT AGGT GAT TCC TTC GGA CCG CGC	HindIII-NdeI
3731F	GCG GAA TTC GGA TCC GCC GTC CCG GGA ATA TTC CC	EcoRI-BamHI

3731R_RBS	CGC AAG CTT CAT ATG GGT CCT CCT GTG GAG TGG TTC TGT AGGT ACG GTG CTC GGA GTT CAC C	HindIII-NdeI
2950F	GCG GAA TTC GGA TCC GGG TGC CGG ATT GGC TTT ACC	EcoRI-BamHI
2950R_RBS	CGC AAG CTT CAT ATG GGT CCT CCT GTG GAG TGG TTC TGT AGCC GTT GAG GCG TGC CAC	HindIII-NdeI
5367F	GCG GAA TTC GGA TCC TGT GAA GTC CTG CTA TCG TCC G	EcoRI-BamHI
5367R_RBS	CGC AAG CTT CAT ATG GGT CCT CCT GTG GAG TGG TTC TGT AAGC GTG GCG CAT GGA TAC GG	HindIII-NdeI
4164F	GCG GAA TTC GGA TCC ACG AAG CGG CGG GCA GTG	EcoRI-BamHI
4164R_RBS	CGC AAG CTT CAT ATG GGT CCT CCT GTG GAG TGG TTC TGT AGGG CGT GCG GTG AGA AGG	HindIII-NdeI
4761PF	GCG GAA TTC GGA TCC TCG AGG ACG AGG CCG TCC	EcoRI-BamHI
4761R_RBS	CGC AAG CTT CAT ATG GGT CCT CCT GTG GAG TGG TTC TGT AGA CCT GCC CGT CGC GTA G	HindIII-NdeI
3487PF	GCG GAA TTC GGA TCC CTC ATC TTG TCG TCG CAG CC	EcoRI-BamHI
3487R_RBS	CGC AAG CTT CAT ATG GGT CCT CCT GTG GAG TGG TTC TGT AAT CTG GGA AGG TGC GCA GAG G	HindIII-NdeI
3484PF	GCG GAA TTC GGA TCC CGT CGA CCA GAT AGA GGG CC	EcoRI-BamHI
3484R_RBS	CGC AAG CTT CAT ATG GGT CCT CCT GTG GAG TGG TTC TGT AGAG CGT CGT TGC ATC GGG	HindIII-NdeI
7636PF	GCG GAA TTC GGA TCC CCG GAA CTC CGC GGA GCC	EcoRI-BamHI
7636R_RBS	CGC AAG CTT CAT ATG GGT CCT CCT GTG GAG TGG TTC TGT ATA CGT GCA CGC CGC CCG G	HindIII-NdeI
0527F	GCG GAA TTC GGA TCC CTC CGA CTC CGT GGG TGG ACT C	EcoRI-BamHI
0527R_RBS	CGC AAG CTT CAT ATG GGT CCT CCT GTG GAG TGG TTC TGT ACCG TTA TCG GAT TCG CAC CGC G	HindIII-NdeI

Chapter 6

Functional analysis of the SsgA-like proteins in *Streptomyces lividans* 1326

Giulia Mangiameli, Nadine Mascini, Erik Vijgenboom and Gilles P. van Wezel

ABSTRACT

SsgA-like proteins (SALPs) are a family of actinomycete-specific regulatory proteins that control sporulation-specific cell division and spore maturation in actinomycetes. We recently showed that SsgA and SsgB activate cell division by directly controlling the localization of FtsZ, while other SALPs have yet poorly characterized roles in morphogenesis and cell wall synthesis. Here we report the creation of null mutants for the genes encoding SsgA-like proteins SsgA, SsgB, SsgC, SsgD and SsgE, respectively, and show that *ssgA* and *ssgB* null mutants had a nonsporulating phenotype. Three alternative translational start sites for *ssgA* were analyzed, and it was established that of these, changing the first or the third codon into an ATC had a detrimental effect on development, whereby the first ATG is perhaps preferred over the third ATG codon. The *ssgB* null mutants of *S. lividans* lacked the large colony phenotype seen in *S. coelicolor*, which may reflect differences in the morphogenesis between these sister streptomycetes. Finally, enzyme production by several of the mutants was analyzed using the small laccase SLAC as a reporter.

INTRODUCTION

Streptomycetes have a strong potential to adapt to diverse natural habitats. This is highlighted by the presence of more than 20 clusters specifying secondary metabolites, around 65 sigma factors and an unprecedented number of sugar transporters and polysugar hydrolases on their genomes (Bentley et al. 2002; Ikeda et al. 2003; Ohnishi et al. 2008). The study of *Streptomyces* development is carried out primarily on solid-grown cultures, whereby the vegetative mycelium develops aerial hyphae which then produce chains of spores (Chater 1972). Most developmental genes that control aerial development (the so-called *whi* genes) encode transcription factors (Chater 1972; Flårdh et al. 1999; Ryding et al. 1999). Aerial hyphae are by definition not produced in submerged culture. Nonetheless, several streptomycetes also produce spores in liquid cultures, such as *S. griseus* and *S. venezuelae* (Kendrick and Ensign 1983; Glazebrook et al. 1990). Some *whi* genes also play a role in submerged sporulation. For example, overexpression of the sporulation-specific σ -factor WhiG induces some submerged sporulation in liquid-grown mycelium of *S. coelicolor* (Chater et al. 1989), and deletion of a number of *whi* gene orthologues in *S. venezuelae* (i.e. *whiA*, *whiB*, *whiD*, *whiG*, *whiH* and *whiI*) resulted in a failure to sporulate on agar plates and in liquid-grown cultures (M.J. Buttner and M.J. Bibb, pers. comm.). This suggests significant overlap between the sporulation pathways under both conditions.

The SsgA-like proteins are a family of sporulation control proteins (Traag and van Wezel 2008; Jakimowicz and van Wezel 2012). SsgA was originally identified as a suppressor of a hyper-sporulating *S. griseus* mutant (designated SY1) and was shown to be essential for submerged sporulation (Kawamoto and Ensign 1995; Kawamoto et al. 1997). Overexpression of *S. griseus* SsgA in liquid-grown mycelium of *S. coelicolor* induced mycelial fragmentation and spore formation (van Wezel et al. 2000a). The ability of SsgA to enhance fragmentation and also protein secretion was applied in industrial fermentations, revealing a significant improvement in yield and fermentation time (van Wezel et al. 2006). We recently discovered that SsgA acts by dynamically controlling the localization of its paralogue SsgB, which is a member of

the cell division complex in actinomycetes, and in turn recruits FtsZ to the septum sites to initiate sporulation-specific cell division (Willemse et al. 2011). This rare example of positive control of cell division explains the critical role of SsgAB in the sporulation process. The *ssgA*, *ssgB* and *ssgG* genes directly relate to the control of septum-site localization in *S. coelicolor*, with *ssgA* and *ssgB* essential for sporulation (van Wezel et al. 2000a; Keijser et al. 2003; Sevcikova and Kormanec 2003), while in *ssgG* mutants septa are frequently skipped, resulting in large spores containing multiple well-segregated chromosomes (Noens et al. 2005). The crystal structure of SsgB, which is the archetype of the SALP family and has functional orthologues in all sporulating actinomycetes, revealed a bell-shaped trimer with strong similarity to mitochondrial guide RNA binding proteins, although direct nucleic acid binding by SALPs is unlikely (Xu et al. 2009).

Here we look into the role of SALPs in *Streptomyces lividans*, studying the effect of deletion of either *ssgA*, *ssgB*, *ssgC*, *ssgD* or *ssgE* on growth and morphogenesis. An initial assessment of the ability of the mutants to produce enzyme is presented.

RESULTS AND DISCUSSION

Functional heterogeneity in SsgA orthologues and the ssgA translational start

The differential activity of SsgA orthologues obtained from different *Streptomyces* species is still poorly understood. For example, overexpression of *S. griseus* SsgA in liquid-grown mycelium of *S. coelicolor* induces mycelial fragmentation (van Wezel et al. 2000b), while overexpression of orthologues from *S. coelicolor* or *S. lividans* does not have a major effect on liquid-culture morphology (van Wezel et al. 2006; van Wezel et al. 2009). Apparently, the effect of SsgA is dictated by its amino acid sequence. Indeed, it was recently shown that streptomycetes may be separated phylogenetically on the basis of the SsgA sequence, where six signature amino acid residues allow discrimination between streptomycetes that sporulate in submerged culture (LSp) and those that do not (NLSp) (Girard et al. 2013).

Another controversy relates to the precise translational start site of *ssgA*. Alignment of the promoter regions of *ssgA* orthologues identified three alternative translational start sites, with the first and third possible ATG conserved in all species, including the putative ribosome binding site (RBS) upstream (Figure 1). These are therefore considered as possible alternative translational start sites. In all streptomycetes but *S. ramocissimus*, which contains duplication of the codons for VQA, the first and second ATG are separated by precisely 30 nucleotides, or ten possible codons. To further analyse which of the three alternative ATG start codons of *ssgA* may be used in vivo, clones were prepared with one of the respective ATG start codons mutated to an ATC codon (for isoleucine). For convenience, the three ATG triplets will be referred to as ATG(1), ATG(2) and ATG(3), for the first, second and third of the three candidate start codons, respectively. The *S. griseus* *ssgA* gene fully complements *ssgA* null mutants of *S. coelicolor* and the proteins have identical N-terminal regions (including the three ATG triplets). The introduction of *ssgA*^{sg} in the *S. coelicolor* *ssgA* null mutant allows us to test not only which start codons are important, but also what the effect is of the introduction of an SsgA with a “submerged sporulation signature” (LSp; (Girard et al. 2013)) on liquid-culture morphology.

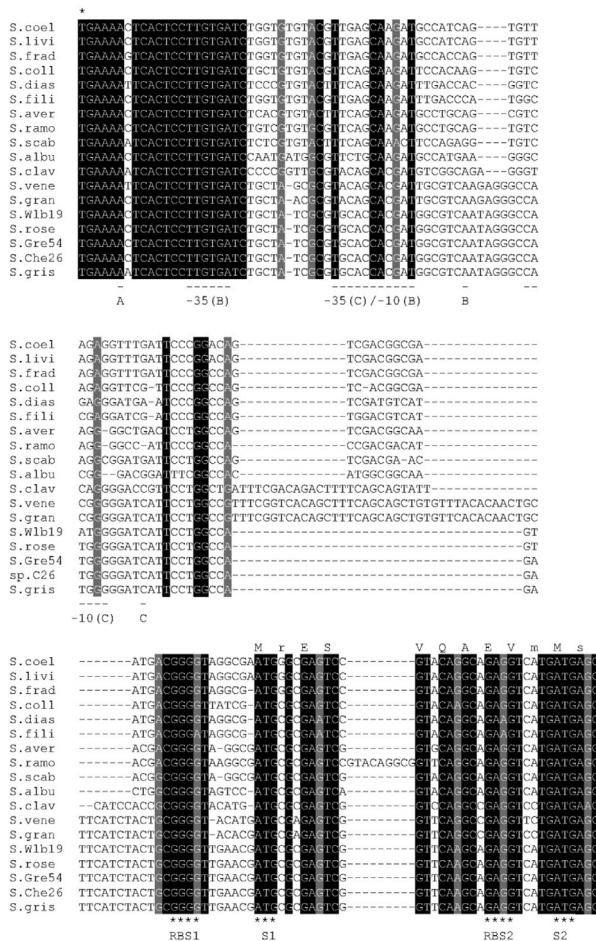


Figure 1. Multiple alignment of *ssgA* promoter regions. Only completely conserved nucleotides are shaded; nucleotides shaded in light grey refer to conserved purines. The two most likely start codons S1 (ATG(1)) and S2 (ATG(3)) for *ssgA* and their respective ribosome binding sites (RBS1 and RBS2) are indicated below the aligned sequence. The ATG immediately upstream of start codon S2 (designated ATG(2) in the text) is most likely not a true translational start codon. The two transcriptional start sites and their respective -35 and -10 recognition sequences from *S. griseus* (Yamazaki et al. 2003) and *S. coelicolor* (Traag et al. 2004) are underlined, where “A” refers to the p1 promoter from *S. griseus*, “B” to p1 from *S. coelicolor* or p2 from *S. griseus*, and “C” to p2 from *S. coelicolor*. The TGA stop codon for *ssgR* is indicated with an asterisk. The consensus amino acid sequence of the N-terminus of SsgA proteins is given above the aligned DNA sequences. Sequences were labeled by their strain of origin and abbreviated as follows: (S.albu) *S. albus*, (S.aver) *S. avermitilis*, (S.clav) *S. clavuligerus*, (S.coel) *S. coelicolor*, (S.coll) *S. collinus*, (S.dias) *S. diastatochromogenes*, (S.fili) *S. filipinensis*, (S.frad) *S. fradiae*, (S.livi) *S. lividans*, (S.gran) *S. granaticolor*, (S.gris) *S. griseus*, (S.rose) *S. roseosporus*, (S.ramo) *S. ramocissimus*, (S.scab) *S. scabies*, (S.vene) *S. venezuelae*, (S.Wlb19) *Streptomyces* species Wlb19, (S.Che26) *Streptomyces* species Che26, (S.Gre54) *Streptomyces* species Gre54.

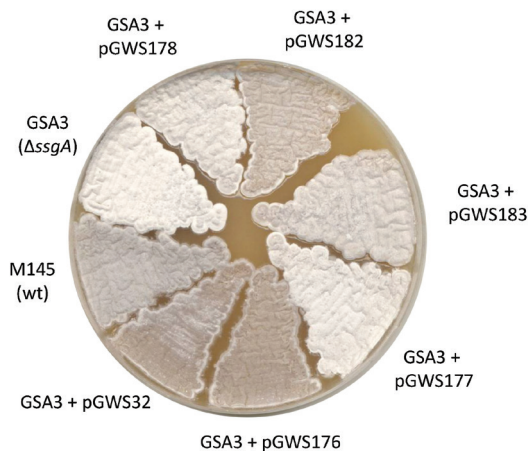


Figure 2. Complementation of the *ssgA* null mutant. Constructs carrying wild-type *ssgRA* or mutations in the first (pGWS177), second (pGWS182) and third (pGWS183) predicted start codons were introduced in the mutant and their ability to restore sporulation assessed on MS medium. M145 and the *ssgA* null mutant GSA3 harbouring pHJL401 as control plasmid are also shown.

To obtain a construct for the ready cloning and expression of *ssgA* variants from the *S. coelicolor* promoter region, around 1.5 kb of the upstream and downstream regions of *S. coelicolor* A3(2) *ssgA* were amplified by PCR and cloned into the low-copy vector pHJL401, resulting in *ssgA* exchange construct pGWS174. The *S. griseus* *ssgA* variants with mutated translational start codons were then introduced in the *ssgA* exchange construct, resulting in pGWS177 (*ssgA*-ATG(1)→ATC), pGWS182 (*ssgA*-ATG(2)→ATC), and pGWS183 (*ssgA*-ATG(3)→ATC), respectively. In this way, the *ssgA* gene of *S. griseus* (or mutants thereof) is expressed from the natural *S. coelicolor* promoter region. The *ssgR* gene was included as read-through occurs into *ssgA* from a promoter upstream of *ssgR* (Traag et al. 2004; van Wezel et al. 2000a). pGWS178, which carries a 27 nt in-frame deletion rendering *ssgA* inactive (Kawamoto et al. 1997) was used as negative control, while pGWS176 (carrying wild-type *S. griseus* *ssgA*) and pGWS32 (wild-type *S. coelicolor* *ssgA*; (Traag et al. 2007)) were used as positive controls. All constructs were introduced into the *S. coelicolor* *ssgA* mutant GSA3, and their ability to complement the non-sporulating phenotype of the *ssgA* null mutant was assessed.

The phylogenetic evidence (Figure 1) and its location relative to the upstream RBS, with only three nucleotides spacing (instead of the canonical 6-9 nt), apparently ruled out the second ATG as possible start codon. Indeed, sporulation was fully restored to *ssgA* mutants by the expression of *ssgA*- Δ ATG(2), strongly suggesting that ATG(2) is not used as translational start codon (Figure 2). Mutation of ATG(3) - which in contrast to ATG(2) is completely conserved in all *Streptomyces ssgA* genes - did not dramatically affect sporulation, although less grey spore pigment was observed for GSA3 transformants harbouring this variant than for the transformants expressing wild-type *S. griseus ssgA* or *ssgA*-ATG(2) \rightarrow ATC. No complementation of sporulation was observed when *ssgA*-ATG(1) \rightarrow ATC was introduced in the *S. coelicolor ssgA* null mutant, and this should therefore be regarded as the primary start codon for *ssgA*, at least in surface-grown cultures on MS agar plates. Interestingly, when the same *ssgA*-ATG(1) \rightarrow ATC was introduced in multiple copies, using pWHM3 instead of the low-copy vector pHJL401, sporulation was fully restored to the *ssgA* null mutant (data not shown). Apparently, ATG(3) is a less efficient start codon or full length SsgA (145 aa) is more effective in activating sporulation than the truncated SsgA (135 aa) .

Construction of null mutants of the cell division genes ssgA and ssgB in S. lividans

We then wondered if indeed the function of the cell division proteins SsgA and SsgB was the same in *S. coelicolor* and *S. lividans*. Firstly, an *ssgA* null mutant was created by replacement of the coding region of the gene by the apramycin resistance cassette *aacC4*, which confers resistance to apramycin, using the instable multi-copy vector pWHM3 as described previously (Colson et al. 2008). *S. lividans* 1326 was transformed with the disruption construct pGWS175 followed by several rounds of nonselective growth to allow loss of the vector. Double recombinants were selected by replication of the colonies to MS agar plates containing either apramycin or thiostrepton as selective markers, whereby double recombinants should be resistant to apramycin (gene replacement) and sensitive to thiostrepton (due to loss of the pWHM3 vector sequences). The putative mutant colonies were verified by PCR amplification with oligonucleotides flanking the *ssgA* gene. This showed that all

correct double recombinants have a white (nonsporulating) phenotype, similar to *ssgA* null mutants of *S. coelicolor* (Figure 3). The mutant phenotype of the *ssgA* null mutant of *S. lividans* could be restored to sporulation by the introduction of a wild-type copy of *ssgA* in the low-copy number vector pHJL401 (Figure 3).

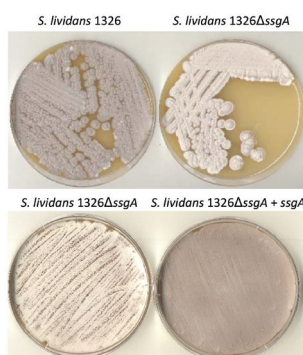


Figure 3. Phenotypic analysis of the *S. lividans ssgA* mutant and complementation with wild-type *ssgA*. The strains were incubated for five days at 30°C on MS agar plates.

In *S. coelicolor*, deletion of the gene for SsgB result in an unconditionally white (nonsporulating) phenotype on all media, resulting in the formation of long aseptate aerial hyphae (Keijser et al. 2003). Interestingly, the *ssgB* mutant colonies have a large colony phenotype, which grow on to form very large colonies as compared to those formed by the wild-type strain. This suggests that SsgB not only controls cell division, but may also be involved in the correct timing of growth cessation, which is an important checkpoint for the initiation of aerial growth (Chater 2001). To establish the role of *ssgB* in cell division and growth in *S. lividans*, a null mutant was created in similar fashion as for *ssgA*, by replacing the entire coding sequence of the gene (nt positions -6/+469 relative to the translational start of *ssgB*) by the apramycin resistance cassette *aacC4* that was flanked by *loxP* sequences to allow the removal of the cassette after double recombination. Subsequently, the apramycin resistance cassette was excised following introduction of plasmid pUWLcre (Fedoryshyn et al. 2008) expressing the Cre recombinase that recognizes the *loxP* sites, thus leaving an in-frame deletion of the gene except for a scar sequence as a result of the joined *loxP* sites.

Expectedly, colonies had a *whi* mutant phenotype, failing to sporulate in surface-grown culture, and regardless of what media were used (Figure 4). However, in *S. lividans* a large colony phenotype (LCP) was not observed. This suggests that these two functions - sporulation and LCP - are not functionally coupled. However, this cannot be due to intrinsic functional differences between the *ssgB* orthologues of *S. coelicolor* and *S. lividans*, as the genes are identical at the nucleotide level.

Deletion of ssgC, ssgD and ssgE in S. lividans

In similar fashion as described for *ssgB*, deletion mutants were also prepared for *ssgC*, *ssgD* and *ssgE*. For *ssgC*, the +1 to +425 region was removed, for *ssgD* +1/+408, and for *ssgE* -7/+367. The precise function of SsgC, SsgD and SsgE is less clear. SsgC was suggested to be involved in septum formation and peptidoglycan maintenance and the mutant in *S. coelicolor* has a phenotype that is more or less the inverse of that of *ssgA* null mutants, with increased septation for null mutants, while overexpression results in inhibition of cell division. Therefore, it was proposed that SsgC may function as an antagonist of SsgA (Noens et al. 2005). In addition, *S. coelicolor* *ssgC* null mutants produced long spore chains with spores of variable length. Direct orthologues of *ssgC* have only been found in streptomycetes of the NLSp branch (species that do not sporulate in submerged cultures), which invariably have a low SsgA expression level (Girard et al. 2013). As published previously for *S. coelicolor*, colonies of deletion mutants of *ssgC* in *S. lividans* also gave a dark grey phenotype on MS agar plates, and showed enhanced production of the antibiotic actinorhodin on R5 agar plates with added copper (Figure 4). No major effect on septum formation was observed in *S. lividans*, although closer examination is required, for example by high resolution transmission electron microscopy.

SsgD is the only SALP that is highly expressed during vegetative growth, and *ssgD* null mutants of *S. coelicolor* show major defects in lateral cell wall synthesis; it was therefore suggested to play a role in the synthesis of the lateral cell wall, perhaps by enabling the proper function of one or more penicillin binding proteins (PBPs), such as PBP2 (Den Blaauwen et al. 2003; Errington et al. 2003). The *ssgD* mutant of

S. coelicolor shows defects in integrity of the hyphae and spores, whereby the spores have a significantly thinner peptidoglycan layer than those of the wild-type strain. Deletion of *ssgD* in *S. lividans* resulted in mutants with reduced sporulation on R5 agar plates and normal sporulation on MS agar plates (Figure 4). SsgE was previously reported as being involved in spore maturation in *S. coelicolor*, with hypersporulation and in particular the formation of single spores rather than spore chains, suggesting accelerated autolytic spore separation. However, major differences between *ssgE* null mutants and the parental strain were not observed (Figure 4). The phenotypes of the mutants are currently being investigated in more detail and should reveal the extent of the morphological changes. Furthermore, growth curves should be carried out under different conditions to check for the phenotype of the mutants in liquid-grown cultures.

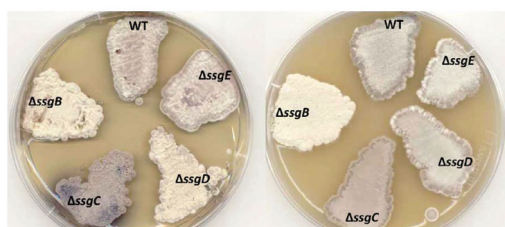


Figure 4. Phenotypic analysis of *S. lividans* mutants Δ *ssgB*, Δ *ssgC*, Δ *ssgD* and Δ *ssgE*. wt, *S. lividans* 1326. The strains were incubated for five days at 30°C on R5 agar (left) or MS agar (right).

Enzyme production in selected mutants

The *ssgB*, *ssgC*, *ssgD* and *ssgE* mutants, together with the *csIA* and *glxA* mutants (Chapter 3), were tested for productivity using the small laccase SLAC as a reporter enzyme. Laccases are multicopper oxidases with a wide variety of substrates in nature. A small laccase (SLAC) has been characterized in *S. coelicolor* (Machczynski et al. 2004) and the gene was inserted in the low copy number vector pHJL401 under the control of the strong constitutive promoter P_{ermE} to generate P_{ermE} *slac* (see Chapter 6 of this Thesis). The reproducibility of the assay using a gel-based system makes it a suitable reporter for this study. The assays were performed as described in Materials and Methods.

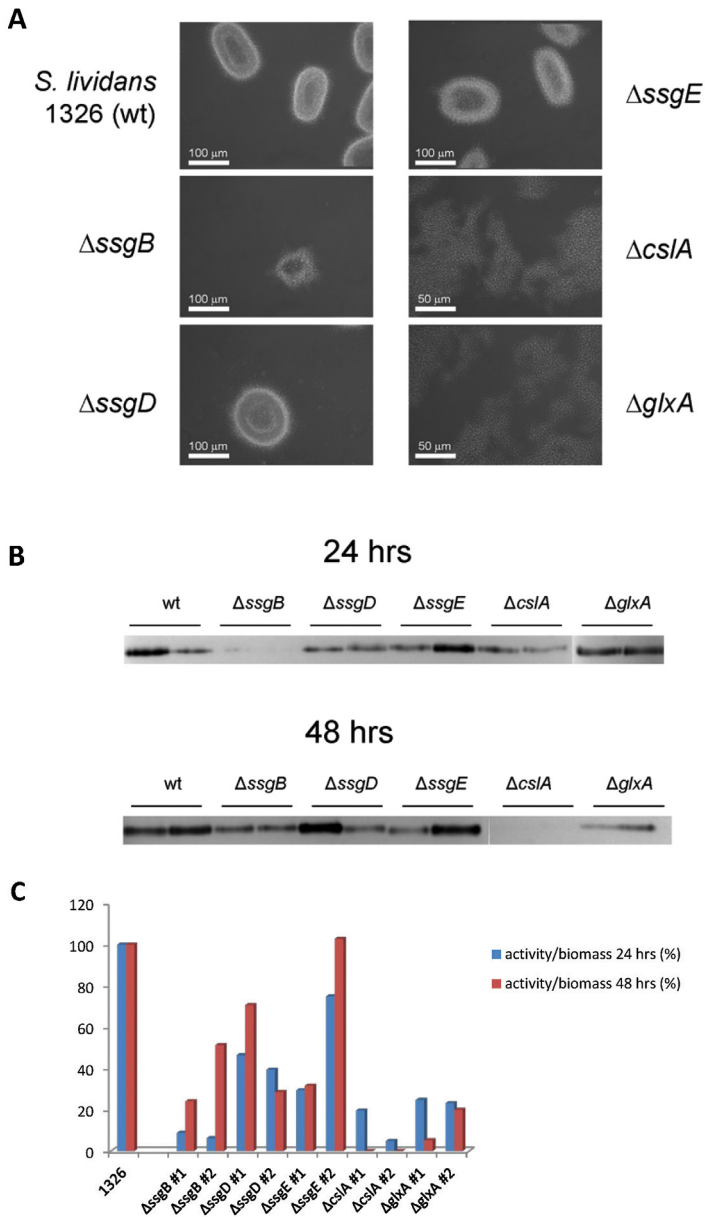


Figure 5. (A) Phenotype of SLAC-producing strains after 48 hrs growth in liquid TSBS. All strains harboured plasmid P_{ermE} -*slac*. *S. lividans* 1326 was the parent for all mutants. (B) In-gel laccase activity assay performed on samples obtained from 24 hrs (top) and 48 hrs (bottom). Activity in the *ssgC* mutants was zero (data not shown). (C) Quantification of the signals corresponding to active SLAC as determined by the in-gel assay. Band intensities were normalized for biomass and *S. lividans* 1326 harbouring P_{ermE} construct was set at 100%.

The experiments were carried out in duplicate, with samples taken at 24 and 48 hrs, analyzed on gel for their activity and normalized for dry weight. The phenotypes of the transformants were analyzed after 48 hrs of growth in TSBS cultures (containing 5 µg/ml thiostrepton for plasmid maintenance). This showed that *ssgC*, *ssgD* and *ssgE* null mutants had a phenotype similar to that of the parental strain 1326, while *ssgB* mutants harbouring the plasmid expressing laccase grew poorly and produced small pellets. In accordance with the experiments presented in Chapter 3, transformants of *cslA* and *glxA* mutants grew fast, forming open mycelial structures, often referred to as mycelial mats (Figure 5A).

In terms of laccase production, there was strong variability between the two independent transformants, for wild-type (in particular after 24 hrs of growth) and in particular also for the mutants. The *ssgB* mutant not only grew slowly but also produced only small amounts of the laccase per gram of biomass, while *ssgD* and *ssgE* mutants on average produced similar amounts of laccase as the parent but with strong variability in production between transformants (Figure 5B and C). Enzyme activity in the *ssgC* mutants was zero and will need to be confirmed further (data not shown). Transformants of the *cslA* and *glxA* mutants, which produced open mycelial mats and grew fast (Figure 5A) produced only small amounts of laccase, and in particular *cslA* mutants had completely lost their ability to produce laccase after 48 hrs of growth. This is most likely due to poor stability of the plasmid in the mutants at times when the thiostrepton pressure drops. This is supported by the fact that following sporulation on MS plates, more than 80% of the spores do not contain plasmid (unpublished results). This loss of plasmid may tentatively be explained by lack of a protective layer of the CslA-dependent polysaccharide at apical sites, resulting in plasmid leakage. This interesting phenomenon needs to be analyzed in more detail. Finally, the high variation in productivity between individual transformants is typical of streptomycetes and underlines the need to analyze a large amount of transformants, for example by prescreening using high throughput systems, such as using 96 well microtitre plates.

In conclusion, mutants deleted for the genes encoding SsgA-SsgE were created, whereby *ssgA* and *ssgB* null mutants had the same nonsporulating phenotype

as seen for *S. coelicolor*. The alternative translational start sites for *ssgA* were analyzed, which showed that two alternative start sites are used, whereby the first ATG may be preferred, with less frequent use of the third ATG. Changing the second ATG codon (annotated as the start codon in *S. coelicolor*) into an ATC had no effect on morphogenesis, and therefore most likely does not function as a start codon for translation. The *ssgB* null mutants lacked the large colony phenotype seen in *S. coelicolor*, which was unexpected and also unfortunate as an ‘immortal’ phenotype of *ssgB* null mutants seems like a promising phenotype from the perspective of growth during fermentations. More extensive study of the mutants, both phenotypically by various microscopy methods and in terms of growth and enzyme production, is required to assess the role of the SALPs in morphogenesis and productivity of *S. lividans*.

MATERIAL AND METHODS

Strains and media

The parent of all strains described in this study was *S. lividans* 1326 (also known as *S. lividans* 66; stock number 1326 from the John Innes Centre (Hopwood et al. 1985)). *Escherichia coli* JM109 was used for routine cloning and plasmid amplification (Messing et al. 1981). For growth and phenotypic characterization, soy flour mannitol (Ms) agar plates, R5 agar plates supplemented with 10 μ M copper or minimal medium (MM) agar plates with 1% (w/v) mannitol were used. For liquid-grown cultures, liquid minimal medium (NMMP) supplemented with 1% mannitol or tryptic soy broth with 10% sucrose (TSBS) were used (Kieser et al. 2000). *E. coli* strains were routinely grown on Luria-Bertani medium (LB).

Table 1. Constructs used in this study.

Constructs	Description
pWHM3	Multi-copy shuttle vector, colE1 replicon, pSG5 replicon, Tsr ^R , Amp ^R (Vara et al. 1989)
pHJL401	Low-copy shuttle vector, SCP2*, pUC19 replicon, Tsr ^R , Amp ^R (Larson and Hershberger 1986)
pGWS174	pHJL401 with 1.5 kb of the upstream (including ssg ^R) and 1.5 kb of the downstream region of <i>S. coelicolor</i> ssgA
pGWS175	pWHM3 harbouring the insert of pGWS174 and an apramycin resistance cassette cloned between the 1.5 kb flanking regions
pGWS176	pGWS174 containing ssgAsg-WT
pGWS177	pGWS174 containing ssgAsg- ATG(1) \rightarrow ATC
pGWS178	pGWS174 containing ssgAsg with a 27 bp SacI in-frame deletion (Kawamoto et al. 1997)
pGWS182	pGWS174 containing ssgAsg- ATG(2) \rightarrow ATC
pGWS183	pGWS174 containing ssgAsg- ATG(3) \rightarrow ATC
pGWS32	pHJL401 containing 2kb ssgRA region of <i>S. coelicolor</i> (Traag 2004)

Plasmids and constructs

All constructs used in this study are presented in Table 1. The gene replacement mutants were obtained by cloning the flanking regions of the genes with the apramycin resistance cassette *aacC4* flanked by *loxP* sites in the unstable multi-copy vector pWHM3 (Vara et al. 1989) as described previously (van Wezel et al. 2005).

The flanking regions were (nucleotide positions are relative to the translational start of the genes): *ssgB* -1500/-7 and +470/+1968; for *ssgC* -1497/-1 and +426/+1920; for *ssgD* -1494/-1 and +409/+1917; for *ssgE* -1500/-8 and +368/+1881. To obtain the deletion mutants, the antibiotic cassettes were removed by the Cre-lox recombinase using plasmid pUWLcre (Fedoryshyn et al. 2008), leaving a scar *loxP* site flanked by XbaI restriction sites. All the primers are presented in Table 2.

Laccase assay

The SLAC gene from *S. coelicolor* (Machczynski et al. 2004) was cloned in the low copy number vector pHJL401 (Larson and Hershberger 1986; van Wezel et al. 2000c) under the control of the strong constitutive promoter P_{ermE} as described in Chapter 5 of this Thesis. Each mutant was transformed with the construct and the spores harvested. 10⁷ spores were inoculated in 10 ml TSBS supplemented with 25µM copper and 2 µg/ml thiostrepton and grown at 30 °C for 48 hrs. Alternatively, mycelium was harvested from two MS plates and inoculated in the case of the non sporulating strain Δ*ssgB*. The experiment was carried out in duplicate, with 1 ml sample per transformant taken at 24 and 48 hrs and centrifuged for 10 min at 14000 rpm. The pellet was incubated overnight at 100 °C for dry weight determination, while 10 µl of the supernatant were mixed with an equal volume of SDS-PAGE loading buffer and loaded on a 10% acrylamide gel. The gel was incubated for 1 hr in 100mM phosphate buffer pH 6.8 at room temperature on a rocking platform refreshing the buffer every 20 min and for an additional hr at 30 °C. The activity assay is based on the conversion of N-N-Dimethyl-p-phenylenediamine (DMPPDA) into a dark blue precipitate. The gel is therefore incubated with 0.125 mg/ml DMPPDA and 0.125 mg/ml 1-naphtol until the appearance of the signal. The intensity of the bands is directly proportional to the amount of protein and can be quantified with the software ImageJ.

ACKNOWLEDGMENTS

The authors would like to acknowledge Bjorn Traag for discussion.

SUPPLEMENTAL MATERIAL

Table S1. Oligonucleotides used in this study.

Name	5'-3' sequence	Restriction sites
ssgB-1500F	CGCAGATCTCCCGCATC ACCTG CCGC	BglII
ssgB-7RV	GCGTCTAGAACATGCCACCTACGGTGCCG	XbaI
ssgB+470F	CGCTCTAGAGAAAGCTAGGGCGGGGCTC	XbaI
ssgB+1968RV	GCGAAGCTTGGTGGCACCCGCAAGCAGCG	HindIII
ssgC-1497F	GCGGAATCCGCGTACCGGGTGGTCTTCGG	EcoRI
ssgC-1RV	CGCTCTAGAGGGGGCTCCAGCAGGAC	XbaI
ssgC+426	GCGTCTAGATGAACCGCCCGGGCCGGC	XbaI
ssgC+1920RV	CGCAAGCTTGTCCGGCCTGCTGACCGG	HindIII
ssgD-1494F	CGCGAATTCTGATGTGCTCGTACTGCCGC	EcoRI
ssgD-1RV	GCGTCTAGACGCCTTGCTCCCTCGTGAC	XbaI
ssgD+409F	CGCTCTAGAGCTGCTGACCGGCTCCCG	XbaI
ssgD+1917	GCGAAGCTTGCCAGCCGCAGCAGCACC	HindIII
ssgE-1500F	CGCGAATTCGAGCACCGCAAGGCGAC	EcoRI
ssgE-8RV	GCGTCTAGACCCTTACGCTCTGCCACCTG	XbaI
ssgE+368F	CGCTCTAGAGGTGGCCCACTGAGCCGC	XbaI
ssgE+1881RV	GCGAAGCTTAGCGGTTCTGACCGCCTG	HindIII

Chapter 7

General Discussion

GENERAL DISCUSSION

Enzymes play a very important role in industrial biotechnology, and where possible are applied to replace the more traditional chemical synthesis processes. This has led to what is generally referred to as “the bio-based economy”. Examples of enzymes include amylases and glucose isomerases that are used in the starch industry, cellulases and xylanases in the paper industry, lipases for detergents, and peroxidases and laccases for, among others, bleaching denim. In addition, many therapeutic proteins are produced in the fermentation industry, typically in heterologous hosts, which started with the production of growth hormone in 1985. The increasing demand for energy from clean sources as a result of exhaustion of natural sources and an ever expanding world population has shifted the attention to more sustainable alternatives, namely the second generation biofuels, which are obtained via conversion of waste sugars into bioethanol and require a variety of degrading enzymes for the process.

The constant increase in the need of enzymes and new hosts for production has again brought *Streptomyces* in the spotlight. *Streptomyces* are well known as antibiotic producers, and were recently referred to as the *medicine makers* by Sir David Hopwood (Hopwood 2007). However, as saprophytic microorganisms, streptomycetes recycle all biologically occurring biopolymers, aimed at obtaining the necessary nutrients (Chater et al. 2010), whilst secreting antibiotics to compete with other microorganisms (van Wezel and McDowall 2011). The utilization of complex polysaccharides such as cellulose, chitin, starch, xylan, agar and lignin is possible due to the production of a massive arsenal of hydrolytic enzymes that are attractive for industry. Moreover, some species, such as the preferred host for the production of industrial enzymes *Streptomyces lividans*, couple high secretion to low proteolytic activity and thus prove to be a valuable alternative for the production of a variety of proteins when compared to traditional bacterial hosts (Anné et al. 2012).

Despite advances that have been made in the past, streptomycetes are still relatively unattractive production hosts. This is primarily due to their mycelial life style, which results in slow growth and mass transfer problems, with oxygen and

nutrient limitation inside the mycelia as a result (van Wezel et al. 2006). In liquid-grown cultures, such as during industrial fermentation, the intricate network of vegetative hyphae forms dense aggregates of different sizes (Pamboukian et al. 2002) with oxygen as the limiting nutrient (Celler et al. 2012). In these pellets, only the outer layer is metabolically active (Manteca et al. 2008). Moreover, the mycelial behavior causes high viscosity in the culture, problems in oxygen and nutrient transfer and limits the stirring speed to avoid cell lysis (Meyerhoff et al. 1995). Secondly, in contrast to the preferred production platforms, the molecular biological tools and expression systems are still relatively limited. Within the frame work of the ERA-Industrial Biotechnology (ERA-IB) project EPOS, funded by NWO-ACTS, new ways were explored to optimize *Streptomyces lividans* and to develop new vectors for efficient protein production.

The factors involved in pellet formation in *Streptomyces* have been partially identified, although the global mechanism remains unknown. Hyphal aggregation is linked to the formation of an extracellular matrix via cell surface proteins such as the chaplins (Claessen et al. 2003; Elliot et al. 2003) and a cellulose synthase-like protein CslA (Xu et al. 2008). The chaplins form amyloid structures (Sawyer et al. 2011; Bokhove et al. 2013) which organize into a network, perhaps in conjunction with the polysaccharide synthesized by CslA, and allow attachment of the hyphae to surfaces (de Jong et al. 2009). Deletion of either the chaplin genes or *cslA* leads to pellets of reduced size or open mycelial structures in liquid cultures (Xu et al. 2008; van Veluw et al. 2012). Another protein that influences pellet aggregation is SsgA. As a cell division protein responsible for septum localization and initiation (Jakimowicz and van Wezel 2012), its overexpression leads to hyper septation and fragmentation in liquid cultures with consequent higher enzyme production (van Wezel et al. 2006), perhaps due to the increase of the number of tips, which are active sites for secretion (Willemse et al. 2012). Changing *Streptomyces* morphology through a rational genetic approach is an attractive concept. This guided the investigation to study in more detail the function of CslA and its functional partner, a copper oxidase GlxA, and the effect on liquid morphology of null mutants in *S. lividans*.

Moreover, analysis of global transcript profiles by RNA-seq of *cslA* and *glxA* mutants identified novel proteins potentially involved in morphogenesis. Considering their major impact on mycelial morphology, a pilot study was initiated to study the effect of the *ssg* genes in *S. lividans*, to see if this could potentially be an attractive target for altering mycelial morphology and protein production. Therefore, several *ssg* genes for SsgA-like proteins (SsgA-G) were deleted to analyze the phenotype of the mutants and compare it to the data obtained in *S. coelicolor* (Traag and van Wezel 2008). This showed similarities but also some noteworthy differences between *S. lividans* and *S. coelicolor*, which should be analyzed in more detail in the future.

The data presented in this thesis show that both CslA and GlxA are required for the synthesis and correct deposition at the hyphal tips of a polysaccharide involved in matrix formation, aerial development on rich media, agar invasion and pellet aggregation. That means the proteins have a major impact on the morphology of the mycelia. We were able to detect thin fibrils of the polysaccharide with a fluorescent chitin binding protein as probe, which suggests that the glycan may at least in part consist of chitin. This represents a novel aspect in *Streptomyces* morphology, and is a feature more akin to the fungal cell wall than to that of bacteria (Bowman and Free 2006). The localization of CslA and GlxA to in particular the hyphal tips again stresses that this may be a hub for the expression proteins involved in growth and development (Holmes et al. 2013). RNA-Seq analysis of the *cslA* and *glxA* null mutants revealed that a cluster of 17 adjacent genes (SCO4242-SCO4260 and SLI_4479-SLI_4495) showed a two- to five- fold increase in the mutants. The function of these genes in bacteria is not known, but their products show similarity with phage tail proteins and a role in virulence and biofilm formation has been suggested in some species (Chen et al. 2010; Ghosh et al. 2012; Du et al. 2012). It is intriguing that one or more of these proteins may assemble into amyloid-like fibrils, which have an important role in *Streptomyces* morphogenesis (Claessen et al. 2003; de Jong et al. 2009; Gras and Claessen, 2014). In a recent study in our laboratory on the spontaneous nonpelleting mutant *S. lividans* 1326MR, phage tail proteins were also among the most significantly deregulated proteins (D. van Dissel and G.P. van

Wezel, unpublished), and this further supports the notion that these proteins may be pivotal for maintaining the typical pellet morphology. More extensive analysis of these proteins is required to establish their precise function and if indeed these proteins may be a target for strain engineering. One important aspect of this work that awaits to be resolved is the exact nature of the polysaccharide produced by the concerted action of CslA and GlxA. Fibrils that were suggested to consist of cellulose were previously identified as dependent on CslA in *S. coelicolor* (de Jong et al. 2009) and, although it is known that bacteria can synthesize polysaccharides with different composition according to the growth conditions (Lee et al. 2001), characterizing the polysaccharide in detail will be of great interest for both basic and applied research. Moreover, it will be compelling to unravel the links between CslA, GlxA and all the proteins described so far as involved in matrix formation, aerial development and pellet aggregation, namely the chaplins, SapB and HyaS, in addition to identifying the specific role of the phage tail related proteins in this organism.

In addition to the study of genes involved in matrix formation, several genes belonging to the SALP group were also analyzed for their involvement in cell division and morphology. Mutants of the *ssg* genes *ssgA*, *ssgB*, *ssgC*, *ssgD* and *ssgE* were studied in *S. lividans* and compared to the corresponding *S. coelicolor* mutants, demonstrating functional overlaps but also some differences between the function of the genes in the two strains. This awaits further analysis.

Besides the analysis of genes involved in the control of morphogenesis, a search was also initiated for new strong and constitutive promoters for use in *Streptomyces* expression vectors that should allow higher level expression of industrial enzyme genes. Through the analysis of in-house transcription data (RNA-Seq and microarray data obtained previously), three promoters were identified, namely $P_{SCO1947}$, $P_{SCO4253}$ and $P_{SCO3484}$, with higher or comparable strength than the benchmark P_{ermE} and validated for the production in *S. lividans* of a small laccase SLAC from *S. coelicolor*. This represents an improvement in respect to reported studies, which failed to produce promoters stronger than the currently known ones (Seghezzi et al. 2011).

Based on the data described in this thesis as well as in the literature, advances can be envisioned for both morphology and expression systems. As mentioned previously, *Streptomyces* are able to decompose various substrates such as chitin, cellulose, lignin and xylan to obtain nutrients (Chater et al. 2010). Their capacity as hosts would be therefore exploited at best in the production of these proteins, with clear advantages, for example, in the production of second generation biofuels.

The most effective change in morphology has so far been achieved by the overexpression of the SsgA protein, which enhances cell division resulting in mycelial fragmentation, which leads to enhanced expression and secretion of proteins (van Wezel et al. 2006). However, other mutants with an open mycelial morphology might present good alternatives, either in terms of producing higher yield per kg of biomass, as well as in improving the secretion efficiency. This is among others achieved by increasing the number of apical sites, as this is the place in the mycelia where secretion may primarily take place (Willemse et al. 2012). Targeting cell surface (Claessen et al. 2006) or cytoskeleton-related genes (Celler et al. 2013) should be considered and in particular the application of *csIA* and *glxA* need to be analyzed further. For example, while deletion mutants produce less dense pellets, we do not have sufficient insight into the stress resistance of the hyphae that lack the CslA-produced polysaccharide. Such stress resistance is also an important factor during industrial fermentations as extensive lysis in the often heavily stirred cultures would be detrimental for the production process.

New ways need to be found to create a morphology that circumvents viscosity issues while allowing high growth rate and maintaining production and secretion capacity. Preliminary studies have shown that null mutants of *sco1*, encoding the copper chaperon suggested to deliver the metal to GlxA, show the same open mycelial phenotype as *glxA* null mutants, while the addition of copper to the medium restores pellet growth. Perhaps positioning *glxA* under the control of an inducible promoter is an option as it will allow temporally changing the expression of the gene without disrupting the production of the structural polysaccharide during growth phases where this is undesirable.

In terms of expression vectors, the development of tailor-made promoter-expression combinations for expression of genes in *Streptomyces* is continuing to be an important issue. Such an expression system should encompass a stable multi-copy vector, a strong constitutive or inducible promoter, an efficient ribosome binding site such as that for the elongation factor EF-Tu (Vijgenboom et al. 1994) and a signal sequence for efficient secretion, such as *vsi* or *xlnC* (Schaerlaekens et al. 2004; Pimienta et al. 2007). In terms of promoter sequences, this thesis revealed the possible applicability of the promoters P_{SCO1947}, P_{SCO3484} and P_{SCO4253} for strong and constitutive gene expression. To further improve their transcriptional activity, random mutagenesis and/or SELEX methods (Zimmermann et al. 2010) should be investigated. Thus, the thesis presents new ideas towards developing enabling technologies for the improved production of enzymes by *Streptomyces* in general and by *S. lividans* in particular. The availability of the *S. lividans* genome sequence is thereby very useful for among others genomics-based global strain improvement approaches. For example, production hosts have been generated by random strain improvement programs over the years, by companies that use *Streptomyces* for industrial enzyme production. Comparison of these strains by genomics approaches should reveal new genes that correlate to the achieved improved productivity. Such novel insight in combination with a morphology-optimized host and excellent expression systems should make streptomycetes a preferred industrial platform for heterologous protein production.

NEDERLANDSE SAMEVATTING

Enzymen spelen een belangrijke rol in de Biotechnologie industrie waar ze indien mogelijk toegepast worden om de traditionele chemisch synthetische processen te vervangen. Dit heeft geleid tot wat nu in het algemeen de “bio-based economy” wordt genoemd. Voorbeelden van deze enzymen zijn: amylasen en glucose isomerasen die gebruikt worden in de zetmeelindustrie, cellulasen en xylanasen in de papierindustrie, lipasen in waspoeders en peroxidasen en laccasen in ondermeer het blekingsproces van denim. Verder zijn er vele therapeutische eiwitten die geproduceerd worden in de fermentatie-industrie, over het algemeen in heterologe gastheren. De productie van groeihormoon in 1985 is één van de eerste voorbeelden. De toegenomen vraag naar energie uit schone grondstoffen als gevolg van de uitputting van natuurlijke bronnen en de zich alsmaar uitbreidende wereldbevolking, heeft de aandacht verlegd naar meer duurzame alternatieven zoals de tweede generatie biobrandstoffen. Deze energiebron wordt verkregen via de omzetting van o.a. plantaardig agrarisch afval in bio-ethanol waarvoor een diversiteit aan enzymen nodig is.

De constante toename in de vraag naar enzymen en nieuwe gastheren voor hun productie heeft de filamenteuze bacterie *Streptomyces* weer naar de voorgrond gebracht. Streptomyceten zijn bekend als antibiotica producenten en zijn aangeduid als de “medicine makers” door Sir David Hopwood (Hopwood 2007). Echter, streptomyceten hergebruiken als saprofytische micro-organismen alle biopolymeren om de benodigde nutriënten te verkrijgen (Chater et al. 2010) en scheiden tegelijkertijd antibiotica uit om de strijd aan te gaan met andere micro-organismen (van Wezel en McDowal 2011). Hun gebruik van complexe polysacchariden zoals cellulose, chitine, zetmeel, xyloaan, agar en lignine is mogelijk vanwege de productie van een zeer grote verscheidenheid aan hydrolytische enzymen die ook aantrekkelijk zijn voor de industrie. Sommige streptomyceten, zoals de industrieel geprefereerde productiegastheer *Streptomyces lividans*, koppelen een grote secretiecapaciteit aan een lage proteolytische activiteit. Daarmee is deze streptomyceet een waardevol alternatief voor de productie van diverse enzymen ten opzichte van de traditionele bacteriële gastheren (Anné et al. 2012).

Ondanks de vooruitgang die in het verleden is geboekt, blijven streptomyceten relatief onaantrekkelijke gastheren voor enzymproductie. De voornaamste oorzaak is de filamenteuze groeiwijze welke resulteert in langzame groei en limitatie van onder andere zuurstof en nutriënten in het mycelium (van Wezel et al. 2006). In vloeibare cultures, zoals tijdens industriële fermentaties, vormt het complexe netwerk van myceliumdraden compacte aggregaten van verschillende grootte (Pamboukian et al. 2002) waarbij zuurstof de limiterende nutriënt is (Celler et al. 2012). In deze pellets heeft alleen de buitenste laag metabole activiteit (Manteca et al. 2008). Bovendien resulteert de filamenteuze groei in een hoge viscositeit van de cultuur, problemen met zuurstof- en nutriëntenoverdracht en wordt de roersnelheid gelimiteerd om cellysis te voorkomen (Meyerhoff et al. 1995). In tegenstelling tot de geprefereerde productiesystemen zijn de moleculair biologische gereedschappen en expressiesystemen voor *Streptomyces* nog niet optimaal. In het project EPOS binnen het kader van het ERA netwerk Industrial Biotechnology (ERA-IB), gefinancierd door NWO-ACTS, zijn nieuwe wegen onderzocht om *Streptomyces lividans* te optimaliseren als gastheer voor enzymproductie inclusief de ontwikkeling van nieuwe expressieplasmiden.

De factoren betrokken bij de pelletvorming van *Streptomyces* zijn deels geïdentificeerd maar het volledige mechanisme dat eraan ten grondslag ligt is nog onopgehelderd. Aggregatie van hyfen is gekoppeld aan de vorming van een extracellulaire matrix waar oppervlakte-eiwitten zoals chaplins deel van uit maken (Claessen et al. 2003; Elliot et al. 2003) en waarbij een cellulose synthase-achtig enzym, CslA, betrokken is (Xu et al. 2008). De chaplins vormen amyloïde structuren (Sawyer et al. 2011; Bokhove et al. 2013) die zich organiseren in een netwerk, mogelijk in samenhang met het polysaccharide dat gemaakt wordt door CslA, waardoor hyfen zich kunnen hechten aan oppervlakken (de Jong et al. 2009). Verwijderen van één van de chaplin genen of van *cslA* resulteert in kleinere pellets of open myceliumstructuren in vloeibare cultures (Xu et al. 2008; van Veluw et al. 2012). Een ander eiwit dat pelletaggregatie beïnvloedt is SsgA, een celdelingseiwit verantwoordelijk voor de septumlokalisatie en initiatie (Jakimowicz and van Wezel 2012). Overexpressie van SsgA leidt tot hyper septumvorming, fragmentatie in vloeibare cultures en een hogere

enzymproductie (van Wezel et al. 2006). Mogelijk is de verhoogde enzymproductie het gevolg van meer myceliumtips waar de secretie van eiwitten plaats heeft (Willemse et al. 2012).

De *Streptomyces* morfologie veranderen op basis van een rationele genetische benadering is een aantrekkelijk concept. Op basis hiervan werd onderzoek gedaan naar de functie van CslA en de functionele partner GlxA, een radicaalkperoxidase, en het effect van de deletie van de genen op de morfologie in vloeibare cultures van *S. lividans*. De analyse van het transcriptieprofiel van de *cslA* en *glxA* mutanten met RNA-Seq resulteerde in de identificatie van een aantal nieuwe eiwitten dat mogelijk betrokken is bij de morfogenese. In het kader van deze rationele genetische benadering is ook gekeken naar de *ssg* genen, die een grote impact hebben op de morfologie op vaste voedingsbodems. De onderzoeksvraag was of deze genen potentiële doelen zijn om de morfologie in vloeistofcultures te veranderen en de eiwitproductie te verhogen. Diverse *ssg* genen die coderen voor SsgA-achtige eiwitten in *S. lividans* zijn verwijderd en het fenotype van de mutanten is vergeleken met dat van de data verkregen met dezelfde mutanten in *S. coelicolor* (Traag en van Wezel 2008). Hier kwamen overeenkomsten uit maar ook noemenswaardige verschillen die in een vervolgonderzoek nader uitgezocht moeten worden.

De resultaten gepresenteerd in deze thesis laten zien dat zowel CslA als GlxA nodig zijn voor de synthese en de correcte plaatsing van een polysaccharide in de tips van de hyfen. Dit polymeer, een glycaan, is betrokken bij de matrix vorming, luchtmycelium ontwikkeling op rijke media, invasie van de agar en aggregatie van het mycelium tot pellets. De eiwitten CslA en GlxA hebben dus een grote invloed op de morfologie. Dunne fibrillen van het polysaccharide konden gedetecteerd worden met een fluorescent chitine bindingsdomein, hetgeen suggereert dat de glycaan deels uit chitine bestaat. Dit is een geheel nieuw aspect in de morfologie van Streptomyceten en is meer verwant aan de celwand van schimmels dan die van bacteriën (Bowman and Free 2006). De localisatie van CslA en GlxA in de uiteinden van de hyfen onderstreept dat een centrum voor eiwitten betrokken bij groei en ontwikkeling hier is gelegen (Holmes et al. 2013).

Expressie analyse met RNA-Seq in de *cslA* en *glxA* mutanten laat zien dat

zeventien naast elkaar gelegen genen (SCO4242-4260 en SLI_4479-4495) een twee tot vijf maal hogere expressie hebben in de mutanten. De functie van de eiwitten gecodeerd door deze genen is in bacteriën niet bekend maar de eiwitten vertonen overeenkomsten met de “phage tail proteins”. Voor deze eiwitten is een rol in virulentie en biofilmvorming voorgesteld (Chen et al. 2010; Ghosh et al. 2012; Du et al. 2012). Het is fascinerend dat één of meerdere van deze “phage tail proteins” zich kunnen samenvoegen tot amyloïde-achtige fibrillen. Dit type fibrillen speelt een belangrijke rol in de *Streptomyces* morfogenese (Claessen et al. 2003; de Jong et al. 2009; Gras and Claessen 2014). In een recent onderzoek in ons laboratorium aan de spontane niet-pelleterende *S. lividans* mutant 1326MR bleek dat de “phage tail proteins” ook sterk gedereguleerd zijn (D. Van Dissel and G.P. van Wezel, unpublished). Dit onderbouwt de stelling dat deze eiwitten van doorslaggevend belang zijn voor de handhaving van de typische pelletmorfologie. Een meer gedetailleerde analyse van deze eiwitten is nodig om de exacte functie vast te stellen en om te bepalen of deze eiwitten geschikte doelen zijn voor stamontwikkeling.

Een belangrijk aspect van dit onderzoek dat nog opgehelderd moet worden is de karakterisatie van het polysaccharide dat geproduceerd wordt door de gezamenlijke activiteit van CslA en GlxA. Fibrillen die verondersteld werden uit cellulose te bestaan zijn eerder in *S. coelicolor* als CslA-afhankelijk geïdentificeerd (de Jong et al. 2009). Aangezien het bekend is dat bacteriën polysacchariden kunnen produceren waarvan de samenstelling afhankelijk is van de groeiomstandigheden (Lee et al. 2001), is de karakterisatie van dit polysaccharide van belang voor zowel fundamenteel onderzoek als de toegepaste wetenschap. Bovendien is het fascinerend het verband tussen CslA, GlxA en alle andere eiwitten, o.a. chaplins, SapB en HyaS, betrokken bij de matrixvorming, luchtmycelium ontwikkeling en mycelium aggregatie aan te tonen. Hierbij dient ook de rol van de “phage tail proteins” meegenomen te worden.

Naast de analyse van de genproducten betrokken bij de controle van de morfogenese werd ook een onderzoek opgestart naar sterke constitutieve promotors. Deze zijn nodig in *Streptomyces* plasmiden voor het produceren van industrieel relevante enzymen in zo groot mogelijke hoeveelheden. Deze promotors zijn geïdentificeerd met de transcriptiegegevens verkregen uit RNA-Seq en micro-

arrays. Drie promotors zijn geselecteerd, P_{SCO1947}, P_{SCO4253} en P_{SCO3484}, met een hogere of gelijkwaardige transcriptieactiviteit als de referentie P_{ermE}. Met de productie van een laccase (SLAC) in *S. lividans*, is aangetoond dat deze promotors daadwerkelijk een verbetering in de productie opleveren ten opzichte van de referentie. Dit is een vooruitgang in vergelijking met eerder onderzoek waar men niet slaagde in het verkrijgen van sterkere promotors (Seghezzi et al. 2011).

Gebaseerd op de resultaten beschreven in deze thesis en in de literatuur kan een vooruitgang in de ontwikkeling van zowel aangepaste morfologie als expressiesystemen voorzien worden. Zoals eerder genoemd zijn Streptomyceten in staat tot het afbreken van een verscheidenheid aan substraten zoals chitine, cellulose, lignine en xyloaan om nutriënten te verkrijgen (Chater et al. 2010). Daarom kan hun capaciteit als productiegastheer het best tot zijn recht komen bij de productie van de enzymen die voor de afbraak van deze substraten nodig zijn bijvoorbeeld voor de productie van de tweede generatie biobrandstoffen.

De meest effectieve verandering van de morfologie is tot nu toe verkregen door de overexpressie van SsgA. Dit eiwit verhoogt de frequentie van celdeling hetgeen resulteert in fragmentatie bij *Streptomyces* en een verhoogde opbrengst bij de productie van gesecreteerde eiwitten (van Wezel et al. 2006). Echter, mutanten met een open myceliumstructuur zijn mogelijk goede alternatieven voor zowel de productiecapaciteit per kilogram biomassa als de verhoogde secretie-efficiëntie. Dit laatste wordt onder meer bereikt door de toename van het aantal groeipunten aangezien dit de plekken zijn waar eiwitsecretie voornamelijk plaatsvindt (Willemse et al. 2012). Gericht onderzoek aan celoppervlakte (Claessen et al. 2006) en cytoskelet gerelateerde genen (Celler et al. 2012) dient overwogen te worden en in het bijzonder de toepassing van *csIA* en *glxA* mutanten behoeft verder onderzoek. Hoewel de *csIA* en *glxA* mutanten minder compacte pellets maken, hebben we niet voldoende inzicht in de stressbestendigheid van de hyfen waar het door CslA geproduceerde polysaccharide ontbreekt. Tijdens industriële fermentaties speelt stressbestendigheid een voorname rol omdat uitgebreide lysis van de hyfen, in de vaak intensief geroerde cultures, zeer ongunstig is voor het productieproces. Nieuwe wegen moeten gevonden worden om een morfologie te creëren die problemen met

de viscositeit omzeilt en tegelijkertijd een hoge groeisnelheid, productiecapaciteit en eiwitsecretie handhaaft. Voorbereidende experimenten hebben laten zien dat mutanten met een deletie van *sco1*, een gen coderend voor de koperchaperone van GlxA, dezelfde open myceliumgroei heeft als de *glxA* mutant. Toevoegen van koper aan het medium tijdens de groei herstelt de pelletvorming weer in de *sco1* mutant. Mogelijk biedt een stam met *glxA* of *sco1* onder de controle van een induceerbare promotor de mogelijkheid de morfologie in een cultuur tijdelijk te wijzigen al naar gelang de morfologie die nodig is voor groei of eiwitproductie.

De ontwikkeling van op maat gemaakte expressieplasmiden voor de productie van enzymen in *Streptomyces* is nog steeds een belangrijke zaak. Zulke expressieplasmiden bestaan uit een stabiele vector met meerdere kopiën per cel, een sterke constitutieve of induceerbare promotor, een sterke bindingsplaats voor ribosomen zoals die voor de translatie van EF-Tu (Vijgenboom et al. 1994) en een efficiënt secretiesignaal zoals gevonden voor Vsi en XlnC (Schaerlakens et al. 2004; Pimienta et al. 2007). De resultaten in deze thesis laten zien dat een drietal constitutieve promotors goede kandidaten zijn voor gebruik in een expressieplasmide. De transcriptie-activiteit zou nog verbeterd kunnen worden met willekeurige mutagenese en/of SELEX methoden (Zimmerman et al. 2010).

Deze thesis beschrijft nieuwe ideeën gericht op de ontwikkeling van technologie voor de verbetering van enzymproductie in *Streptomyces* in het algemeen en in *S. lividans* in het bijzonder. De volledige genoomsequentie van *S. lividans*, die recent beschikbaar is gekomen, is daarbij zeer bruikbaar voor bijvoorbeeld globale op de genoomsequentie gebaseerde stamverbeteringsmethoden. Een voorbeeld daarvan is dat in de productiegastheren, die door de jaren heen door diverse bedrijven via algemene mutagenese methoden zijn geïsoleerd, de wijzigingen ten opzichte van de ouderstam nu bepaald kunnen worden. Deze genoomvergelijkingen zullen nieuwe genen aan het licht brengen die van belang zijn voor verdere enzymproductieverhoging in *S. lividans*. Zulke nieuwe inzichten zullen in combinatie met optimalisatie van de morfologie en excellente expressievectoren resulteren in een competitief industrieel platform voor enzymproductie.

References

REFERENCES

- Amore A, Pepe O, Ventrino V, Birolo L, Giangrande C, Faraco V (2012) Cloning and recombinant expression of a cellulase from the cellulolytic strain *Streptomyces* sp. G12 isolated from compost. *Microb Cell Fact* 11:164.
- Anné J, Maldonado B, Van Impe J, Van Mellaert L, Bernaerts K (2012) Recombinant protein production and streptomycetes. *J Biotechnol* 158:159–67.
- Arias E, Li H, Morosoli R (2007) Effect of protease mutations on the production of xylanases in *Streptomyces lividans*. *Can J Microbiol* 53:695–701.
- Beloin C, Roux A, Ghigo JM (2008) *Escherichia coli* biofilms. *Curr Top Microbiol Immunol* 322:249–89.
- Bentley SD, Chater KF, Cerdeño-Tárraga A-M, Challis GL, Thomson NR, James KD, Harris DE, Quail MA, Kieser H, Harper D, Bateman A, Brown S, Chandra G, Chen CW, Collins M, Cronin A, Fraser A, Goble A, Hidalgo J, Hornsby T, Howarth S, Huang C-H, Kieser T, Larke L, Murphy L, Oliver K, O’Neil S, Rabinowitz E, Rajandream M-A, Rutherford K, Rutter S, Seeger K, Saunders D, Sharp S, Squares R, Squares S, Taylor K, Warren T, Wietzorrek A, Woodward J, Barrell BG, Parkhill J, Hopwood DA (2002) Complete genome sequence of the model actinomycete *Streptomyces coelicolor* A3(2). *Nature* 417:141–7.
- Bibb MJ, Janssen GR, Ward JM (1985) Cloning and analysis of the promoter region of the erythromycin resistance gene (*ermE*) of *Streptomyces erythraeus*. *Gene* 38:215–26.
- Bibb MJ, Molle V, Buttner MJ (2000) sigma(BldN), an extracytoplasmic function RNA polymerase sigma factor required for aerial mycelium formation in *Streptomyces coelicolor* A3(2). *J Bacteriol* 182:4606–16.
- Bibb MJ, White J, Ward JM, Janssen GR (1994) The mRNA for the 23S rRNA methylase encoded by the *ermE* gene of *Saccharopolyspora erythraea* is translated in the absence of a conventional ribosome-binding site. *Mol Microbiol* 14:533–45.
- Bierman M, Logan R, O’Brien K, Seno ET, Rao RN, Schoner BE (1992) Plasmid cloning vectors for the conjugal transfer of DNA from *Escherichia coli* to *Streptomyces* spp. *Gene* 116:43–9.
- Binnie C, Butler MJ, Aphale JS, Bourgault R, DiZonno MA, Krygsman P, Liao L, Walczyk E, Malek LT (1995) Isolation and characterization of two genes encoding proteases associated with the mycelium of *Streptomyces lividans* 66. *J Bacteriol* 177:6033–40.
- Blundell KLIM, Wilson MT, Svistunenka DA, Vijgenboom E, Worrall JAR (2013) Morphological development and cytochrome c oxidase activity in *Streptomyces lividans* are dependent on the action of a copper bound Sco protein. *Open Biol* 3:120163.
- Bokhove M, Claessen D, Jong W de, Dijkhuizen L, Boekema EJ, Oostergetel GT (2013) Chaplins of *Streptomyces coelicolor* self-assemble into two distinct functional amyloids. *J Struct Biol* 184:301–309.
- Borodina I, Krabben P, Nielsen J (2005) Genome-scale analysis of *Streptomyces coelicolor* A3(2) metabolism. *Genome Res* 15:820–9.
- Bourn WR, Babb B (1995) Computer assisted identification and classification of streptomycete promoters. *Nucleic Acids Res* 23:3696–703.
- Bowman SM, Free SJ (2006) The structure and synthesis of the fungal cell wall. *Bioessays* 28:799–808.
- Bringmann M, Landrein B, Schudoma C, Hamant O, Hauser M-T, Persson S (2012) Cracking the elusive alignment hypothesis: the microtubule-cellulose synthase nexus unraveled. *Trends Plant Sci* 17:666–74.
- Buist G, Steen A, Kok J, Kuipers OP (2008) LysM, a widely distributed protein motif for binding to (peptido) glycans. *Mol Microbiol* 68:838–47.
- Burns KE, Darwin KH (2010) Pupylation versus ubiquitylation: tagging for proteasome-dependent degradation. *Cell Microbiol* 12:424–31.
- Bursy J, Kuhlmann AU, Pittelkow M, Hartmann H, Jebbar M, Pierik AJ, Bremer E (2008) Synthesis and uptake of the compatible solutes ectoine and 5-hydroxyectoine by *Streptomyces coelicolor* A3(2) in response to salt and heat stresses. *Appl Environ Microbiol* 74:7286–96.
- Butler MJ, Aphale JS, DiZonno MA, Krygsman P, Walczyk E, Malek LT (1994) Intracellular aminopeptidases in *Streptomyces lividans* 66. *J Ind Microbiol* 13:24–9.
- Butler MJ, Binnie C, DiZonno MA, Krygsman P, Soltes GA, Soostmeyer G, Walczyk E, Malek LT (1995) Cloning and characterization of a gene encoding a secreted tripeptidyl aminopeptidase from *Streptomyces lividans* 66. *Appl Environ Microbiol* 61:3145–50.
- Celler K, Koning RI, Koster AJ, van Wezel GP (2013) A multi-dimensional view of the bacterial cytoskeleton. *J Bacteriol* 195:1627–36.

- Celler K, Picioareanu C, van Loosdrecht MCM, van Wezel GP (2012) Structured morphological modeling as a framework for rational strain design of *Streptomyces* species. *Antonie Van Leeuwenhoek* 409–423.
- Celler K, van Wezel GP, Willemsse J (2013) Single particle tracking of dynamically localizing TatA complexes in *Streptomyces coelicolor*. *Biochem Biophys Res Commun* 1:38–42.
- Chalfie M, Tu Y, Euskirchen G, Ward WW, Prasher DC (1994) Green fluorescent protein as a marker for gene expression. *Science* 263:802–5.
- Chater KF (1972) A Morphological and Genetic Mapping Study of White Colony Mutants of *Streptomyces coelicolor*. *J Gen Microbiol* 72:9–28.
- Chater KF (2001) Regulation of sporulation in *Streptomyces coelicolor* A3(2): a checkpoint multiplex? *Curr Opin Microbiol* 4:667–73.
- Chater KF, Biró S, Lee KJ, Palmer T, Schrempf H (2010) The complex extracellular biology of *Streptomyces*. *FEMS Microbiol Rev* 34:171–98.
- Chater KF, Bruton CJ, Plaskitt KA, Buttner MJ, Méndez C, Helmann JD (1989) The developmental fate of *S. coelicolor* hyphae depends upon a gene product homologous with the motility sigma factor of *B. subtilis*. *Cell* 59:133–43.
- Cheah IK, Halliwell B (2012) Ergothioneine; antioxidant potential, physiological function and role in disease. *Biochim Biophys Acta* 1822:784–93.
- Chen S-M, Tsai Y-S, Wu C-M, Liao S-K, Wu L-C, Chang C-S, Liu Y-H, Tsai P-J (2010) Streptococcal collagen-like surface protein 1 promotes adhesion to the respiratory epithelial cell. *BMC Microbiol* 10:320.
- Cho KH, Caparon MG (2005) Patterns of virulence gene expression differ between biofilm and tissue communities of *Streptococcus pyogenes*. *Mol Microbiol* 57:1545–56.
- Chong S, Mersha FB, Comb DG, Scott ME, Landry D, Vence LM, Perler FB, Benner J, Kucera RB, Hirvonen CA, Pelletier JJ, Paulus H, Xu M (1997) Single-column purification of free recombinant proteins using a self-cleavable affinity tag derived from a protein splicing element. *Gene* 192:271–281.
- Claessen D, de Jong W, Dijkhuizen L, Wösten HAB (2006) Regulation of *Streptomyces* development: reach for the sky! *Trends Microbiol* 14:313–9.
- Claessen D, Rink R, de Jong W, Siebring J, de Vreugd P, Boersma FGH, Dijkhuizen L, Wösten HAB (2003) A novel class of secreted hydrophobic proteins is involved in aerial hyphae formation in *Streptomyces coelicolor* by forming amyloid-like fibrils. *Genes Dev* 17:1714–26.
- Claessen D, Stokroos I, Deelstra HJ, Penninga NA, Bormann C, Salas JA, Dijkhuizen L, Wösten HAB (2004) The formation of the rodlet layer of streptomycetes is the result of the interplay between rodlines and chaplins. *Mol Microbiol* 53:433–43.
- Claessen D, Wösten HAB, Keulen G van, Faber OG, Alves AMCR, Meijer WG, Dijkhuizen L (2002) Two novel homologous proteins of *Streptomyces coelicolor* and *Streptomyces lividans* are involved in the formation of the rodlet layer and mediate attachment to a hydrophobic surface. *Mol Microbiol* 44:1483–1492.
- Colson S, Stephan J, Hertrich T, Saito A, van Wezel GP, Titgemeyer F, Rigali S (2007) Conserved cis-acting elements upstream of genes composing the chitinolytic system of streptomycetes are DasR-responsive elements. *J Mol Microbiol Biotechnol* 12:60–6.
- Colson S, van Wezel GP, Craig M, Noens EEE, Nothaft H, Mommaas AM, Titgemeyer F, Joris B, Rigali S (2008) The chitobiose-binding protein, DasA, acts as a link between chitin utilization and morphogenesis in *Streptomyces coelicolor*. *Microbiology* 154:373–82.
- Combes P, Till R, Bee S, Smith MCM (2002) The *Streptomyces* genome contains multiple pseudo-attB sites for the (phi)C31-encoded site-specific recombination system. *J Bacteriol* 184:5746–52.
- Craney A, Hohenauer T, Xu Y, Navani NK, Li Y, Nodwell J (2007) A synthetic *luxCDABE* gene cluster optimized for expression in high-GC bacteria. *Nucleic Acids Res* 35:e46.
- Cruz-Morales P, Vijgenboom E, Iruegas-Bocardo F, Girard G, Yañez-Guerra LA, Ramos-Aboites HE, Pernodet J-L, Anné J, van Wezel GP, Barona-Gómez F (2013) The genome sequence of *Streptomyces lividans* 66 reveals a novel tRNA-dependent peptide biosynthetic system within a metal-related genomic island. *Genome Biol Evol* 5:1165–75.
- D’Huys P-J, Lule I, Van Hove S, Vercammen D, Wouters C, Bernaerts K, Anné J, Van Impe JFM (2011) Amino acid uptake profiling of wild type and recombinant *Streptomyces lividans* TK24 batch fermentations. *J Biotechnol* 152:132–43.
- D’Huys P-J, Lule I, Vercammen D, Anné J, Van Impe JF, Bernaerts K (2012) Genome-scale metabolic flux analysis of *Streptomyces lividans* growing on a complex medium. *J Biotechnol* 161:1–13.
- Damveld RA, vanKuyk PA, Arentshorst M, Klis FM, van den Hondel CAMJJ, Ram AFJ (2005) Expression of *agsA*, one of five 1,3-a-D-glucan synthase-encoding genes in *Aspergillus niger*, is induced in response to cell wall stress. *Fungal Genet Biol* 42:165–77.

- Davis LL, Bartnicki-Garcia S (1984) The co-ordination of chitosan and chitin synthesis in *Mucor rouxii*. J Gen Microbiol 130:2095–102.
- De Jong W, Vijgenboom E, Dijkhuizen L, Wösten HAB, Claessen D (2012) SapB and the rodlinins are required for development of *Streptomyces coelicolor* in high osmolarity media. FEMS Microbiol Lett 329:154–9.
- De Jong W, Wösten HAB, Dijkhuizen L, Claessen D (2009) Attachment of *Streptomyces coelicolor* is mediated by amyloid fimbriae that are anchored to the cell surface via cellulose. Mol Microbiol 73:1128–40.
- De Keersmaecker S, Van Mellaert L, Schaerlaekens K, Van Dessel W, Vrancken K, Lammertyn E, Anné J, Geukens N (2005) Structural organization of the twin-arginine translocation system in *Streptomyces lividans*. FEBS Lett 579:797–802.
- De Keersmaecker S, Vrancken K, Van Mellaert L, Anné J, Geukens N (2007) The Tat pathway in *Streptomyces lividans*: interaction of Tat subunits and their role in translocation. Microbiology 153:1087–94.
- De Keersmaecker S, Vrancken K, Van Mellaert L, Lammertyn E, Anné J, Geukens N (2006) Evaluation of TatABC overproduction on Tat- and Sec-dependent protein secretion in *Streptomyces lividans*. Arch Microbiol 186:507–12.
- Demain AL, Vaishnav P (2009) Production of recombinant proteins by microbes and higher organisms. Biotechnol Adv 27:297–306.
- Den Blaauwen T, Aarsman MEG, Vischer NOE, Nanninga N (2003) Penicillin-binding protein PBP2 of *Escherichia coli* localizes preferentially in the lateral wall and at mid-cell in comparison with the old cell pole. Mol Microbiol 47:539–47.
- Dilks K, Rose RW, Hartmann E, Pohlschroder M (2003) Prokaryotic Utilization of the Twin-Arginine Translocation Pathway: a Genomic Survey. J Bacteriol 185:1478–1483.
- Ditkowski B, Holmes N, Ryzak J, Donczew M, Bezulska M, Ginda K, Kedzierski P, Zakrzewska-Czerwinska J, Kelemen GH, Jakimowicz D (2013) Dynamic interplay of ParA with the polarity protein, Scy, coordinates the growth with chromosome segregation in *Streptomyces coelicolor*. Open Biol 3:130006.
- Dobson LF, O'Cleirigh CC, O'Shea DG (2008) The influence of morphology on geldanamycin production in submerged fermentations of *Streptomyces hygroscopicus* var. *geldanus*. Appl Microbiol Biotechnol 79:859–66.
- Douville K, Price A, Eichler J, Economou A, Wickner W (1995) SecYEG and SecA are the stoichiometric components of preprotein translocase. J Biol Chem 270:20106–11.
- Du Plessis DJF, Berrelkamp G, Nouwen N, Driessen AJM (2009) The lateral gate of SecYEG opens during protein translocation. J Biol Chem 284:15805–14.
- Du Plessis DJF, Nouwen N, Driessen AJM (2011) The Sec translocase. Biochim Biophys Acta 1808:851–65.
- Driessen AJ (1992) Bacterial protein translocation: kinetic and thermodynamic role of ATP and the protonmotive force. Trends Biochem Sci 17:219–23.
- Du X, Wang F, Lu X, Rasco BA, Wang S (2012) Biochemical and genetic characteristics of *Cronobacter sakazakii* biofilm formation. Res Microbiol 163:448–56.
- Dwarakanath S, Chaplin AK, Hough MA, Rigali S, Vijgenboom E, Worrall JAR (2012) Response to Copper Stress in *Streptomyces lividans* Extends beyond Genes under Direct Control of a Copper-sensitive Operon Repressor Protein (CsoR). J Biol Chem 287:17833–47.
- Elliot MA, Karoonthaisiri N, Huang J, Bibb MJ, Cohen SN, Kao CM, Buttner MJ (2003) The chaplins: a family of hydrophobic cell-surface proteins involved in aerial mycelium formation in *Streptomyces coelicolor*. Genes Dev 17:1727–40.
- Endo K, Hayashi Y, Hibi T, Hosono K, Beppu T, Ueda K (2003) Enzymological characterization of EpoA, a laccase-like phenol oxidase produced by *Streptomyces griseus*. J Biochem 133:671–7.
- Errington J, Daniel RA, Scheffers D-J (2003) Cytokinesis in bacteria. Microbiol Mol Biol Rev 67:52–65, table of contents.
- Fedorushyn M, Welle E, Bechthold A, Luzhetskyy A (2008) Functional expression of the Cre recombinase in actinomycetes. Appl Microbiol Biotechnol 78:1065–70.
- Fernández Martínez L, Bishop A, Parkes L, Del Sol R, Salerno P, Sevcikova B, Mazurakova V, Kormanec J, Dyson P (2009) Osmoregulation in *Streptomyces coelicolor*: modulation of SigB activity by OsaC. Mol Microbiol 71:1250–62.
- Flärdh K, Findlay KC, Chater KF (1999) Association of early sporulation genes with suggested developmental decision points in *Streptomyces coelicolor* A3(2). Microbiology 145:2229–43.
- Flärdh K, Richards DM, Hempel AM, Howard M, Buttner MJ (2012) Regulation of apical growth and hyphal branching in *Streptomyces*. Curr Opin Microbiol 15:736–743.
- Flemming H-C, Wingender J (2010) The biofilm matrix. Nat Rev Microbiol 8:623–33.

- Fuchino K, Bagchi S, Cantlay S, Sandblad L, Wu D, Bergman J, Kamali-Moghaddam M, Flårdh K, Ausmees N (2013) Dynamic gradients of an intermediate filament-like cytoskeleton are recruited by a polarity landmark during apical growth. *Proc Natl Acad Sci U S A* 110:E1889–E1897.
- Fujimoto M, Yamada A, Kurosawa J, Kawata A, Beppu T, Takano H, Ueda K (2012) Pleiotropic role of the Sco1/SenC family copper chaperone in the physiology of *Streptomyces*. *Microb Biotechnol* 5:477–88.
- Gamboa-Suasnavart RA, Marin-Palacio LD, Martínez-Sotelo JA, Espitia C, Servín-González L, Valdez-Cruz NA, Trujillo-Roldán MA (2013) Scale-up from shake flasks to bioreactor, based on power input and *Streptomyces lividans* morphology, for the production of recombinant APA (45/47 kDa protein) from *Mycobacterium tuberculosis*. *World J Microbiol Biotechnol* 1421–1429.
- Gamboa-Suasnavart RA, Valdez-Cruz NA, Cordova-Dávalos LE, Martínez-Sotelo JA, Servín-González L, Espitia C, Trujillo-Roldán MA (2011) The O-mannosylation and production of recombinant APA (45/47 kDa) protein from *Mycobacterium tuberculosis* in *Streptomyces lividans* is affected by culture conditions in shake flasks. *Microb Cell Fact* 10:110.
- Gatesy J, Hayashi C, Motriuk D, Woods J, Lewis R (2001) Extreme diversity, conservation, and convergence of spider silk fibroin sequences. *Science* 291:2603–5.
- Gauthier C, Li H, Morosoli R (2005) Increase in xylanase production by *Streptomyces lividans* through simultaneous use of the Sec- and Tat-dependent protein export systems. *Appl Environ Microbiol* 71:3085–92.
- Gebbink MFBG, Claessen D, Bouma B, Dijkhuizen L, Wösten HAB (2005) Amyloids--a functional coat for microorganisms. *Nat Rev Microbiol* 3:333–41.
- Gerin PA, Dufrene Y, Bellon-Fontaine MN, Asther M, Rouxhet PG (1993) Surface properties of the conidiospores of *Phanerochaete chrysosporium* and their relevance to pellet formation. *J Bacteriol* 175:5135–5144.
- Ghosh N, McKillop TJ, Jowitt TA, Howard M, Davies H, Holmes DF, Roberts IS, Bella J (2012) Collagen-like proteins in pathogenic *E. coli* strains. *PLoS One* 7:e37872.
- Gill RT, Valdes JJ, Bentley WE (2000) A comparative study of global stress gene regulation in response to overexpression of recombinant proteins in *Escherichia coli*. *Metab Eng* 2:178–89.
- Girard G, Traag BA, Sangal V, Mascini N, Hoskisson PA, Goodfellow M, van Wezel GP (2013) A novel taxonomic marker that discriminates between morphologically complex actinomycetes. *Open Biol* 3:130073.
- Glazebrook MA, Doull JL, Stuttard C, Vining LC (1990) Sporulation of *Streptomyces venezuelae* in submerged cultures. *J Gen Microbiol* 136:581–8.
- Gomes RC, Soares RMA, Nakamura CV, Souto-Pradón T, de Souza RF, de Azevedo Soares Semêdo LT, Alviano CS, Rodrigues Coelho RR (2008) *Streptomyces lunalinharesii* spores contain chitin on the outer sheath. *FEMS Microbiol Lett* 286:118–23.
- Görgens JF, Passoth V, van Zyl WH, Knoetze JH, Hahn-Hägerdal B (2005) Amino acid supplementation, controlled oxygen limitation and sequential double induction improves heterologous xylanase production by *Pichia stipitis*. *FEMS Yeast Res* 5:677–83.
- Görgens JF, van Zyl WH, Knoetze JH, Hahn-Hägerdal B (2005) Amino acid supplementation improves heterologous protein production by *Saccharomyces cerevisiae* in defined medium. *Appl Microbiol Biotechnol* 67:684–91.
- Gruber TM, Gross C a (2003) Multiple sigma subunits and the partitioning of bacterial transcription space. *Annu Rev Microbiol* 57:441–66.
- Guimond J, Morosoli R (2008) Identification of *Streptomyces lividans* proteins secreted by the twin-arginine translocation pathway following growth with different carbon sources. *Can J Microbiol* 54:549–58.
- Gustafsson C, Govindarajan S, Minshull J (2004) Codon bias and heterologous protein expression. *Trends Biotechnol* 22:346–53.
- Hempel AM, Cantlay S, Molle V, Wang S-B, Naldrett MJ, Parker JL, Richards DM, Jung Y-G, Buttner MJ, Flårdh K (2012) The Ser/Thr protein kinase AfsK regulates polar growth and hyphal branching in the filamentous bacteria *Streptomyces*. *Proc Natl Acad Sci U S A* 109:E2371–E2379.
- Herth W, Schnepf E (1980) The fluorochrome, calcofluor white, binds oriented to structural polysaccharide fibrils. *Protoplasma* 133:129–133.
- Hicks MG, Guymier D, Buchanan G, Widdick DA, Caldelari I, Berks BC, Palmer T (2006) Formation of functional Tat translocases from heterologous components. *BMC Microbiol* 6:64.
- Holmes DJ, Caso JL, Thompson CJ (1993) Autogenous transcriptional activation of a thiostrepton-induced gene in *Streptomyces lividans*. *EMBO J* 12:3183–91.
- Holmes NA, Walshaw J, Leggett RM, Thibessard A, Dalton KA, Gillespie MD, Hemmings AM, Gust B, Kelemen GH (2013) Coiled-coil protein Scy is a key component of a multiprotein assembly controlling polarized growth in *Streptomyces*. *Proc Natl Acad Sci U S A* 110:E397–406.

- Hong B, Wang L, Lammertyn E, Geukens N, Van Mellaert L, Li Y, Anné J (2005) Inactivation of the 20S proteasome in *Streptomyces lividans* and its influence on the production of heterologous proteins. *Microbiology* 151:3137–45.
- Hook-Barnard IG, Hinton DM (2007) Transcription initiation by mix and match elements: flexibility for polymerase binding to bacterial promoters. *Gene Regul Syst Bio* 1:275–93.
- Hopwood DA (2007) *Streptomyces* in Nature and Medicine. Oxford University Press, New York
- Hopwood DA, Bibb MJ, Chater KF, Kieser T, Lydiate DJ, Smith CP, Ward JM, Schrempf H (1985) Genetic manipulation of *Streptomyces* — A laboratory manual. Cold Spring Harbor Laboratory Press, New York.
- Ikeda H, Ishikawa J, Hanamoto A, Shinose M, Kikuchi H, Shiba T, Sakaki Y, Hattori M, Omura S (2003) Complete genome sequence and comparative analysis of the industrial microorganism *Streptomyces avermitilis*. *Nat Biotechnol* 21:526–31.
- Ingram C, Brawner ME, Youngman P, Westpheling J (1989) xylE functions as an efficient reporter gene in *Streptomyces* spp.: use for the study of *galP1*, a catabolite-controlled promoter. *J Bacteriol* 171:6617–24.
- Jakimowicz D, van Wezel GP (2012) Cell division and DNA segregation in *Streptomyces*: how to build a septum in the middle of nowhere? *Mol Microbiol* 85:393–404.
- Jiang X, Oohira K, Iwasaki Y, Nakano H, Ichihara S, Yamane T (2002) Reduction of protein degradation by use of protease-deficient mutants in cell-free protein synthesis system of *Escherichia coli*. *J Biosci Bioeng* 93:151–6.
- Jing D (2010) Improving the simultaneous production of laccase and lignin peroxidase from *Streptomyces lavendulae* by medium optimization. *Bioresour Technol* 101:7592–7.
- Joly N, Engl C, Jovanovic G, Huvet M, Toni T, Sheng X, Stumpf MPH, Buck M (2010) Managing membrane stress: the phage shock protein (Psp) response, from molecular mechanisms to physiology. *FEMS Microbiol Rev* 34:797–827.
- Joshi M V, Mann SG, Antelmann H, Widdick DA, Fyans JK, Chandra G, Hutchings MI, Toth I, Hecker M, Loria R, Palmer T (2010) The twin arginine protein transport pathway exports multiple virulence proteins in the plant pathogen *Streptomyces scabies*. *Mol Microbiol* 77:252–71.
- Kappes RM, Kempf B, Kneip S, Boch J, Gade J, Meier-Wagner J, Bremer E (1999) Two evolutionarily closely related ABC transporters mediate the uptake of choline for synthesis of the osmoprotectant glycine betaine in *Bacillus subtilis*. *Mol Microbiol* 32:203–16.
- Kassama Y, Xu Y, Dunn WB, Geukens N, Anné J, Goodacre R (2010) Assessment of adaptive focused acoustics versus manual vortex/freeze-thaw for intracellular metabolite extraction from *Streptomyces lividans* producing recombinant proteins using GC-MS and multi-block principal component analysis. *Analyst* 135:934–42.
- Katz E, Thompson CJ, Hopwood D a (1983) Cloning and expression of the tyrosinase gene from *Streptomyces antibioticus* in *Streptomyces lividans*. *J Gen Microbiol* 129:2703–14.
- Kawamoto S, Ensign JC (1995) Isolation of mutants of *Streptomyces griseus* that sporulate in nutrient rich media: cloning of DNA fragments that suppress the mutations. *Actinomycetologica* 9:124–135.
- Kawamoto S, Watanabe H, Hesketh A, Ensign JC, Ochi K (1997) Expression analysis of the *ssgA* gene product, associated with sporulation and cell division in *Streptomyces griseus*. *Microbiology* 143:1077–86.
- Keijser BJE, Noens EE., Kraal B, Koerten HK, van Wezel GP (2003) The *Streptomyces coelicolor ssgB* gene is required for early stages of sporulation. *FEMS Microbiol Lett* 225:59–67.
- Keijser BJE, van Wezel GP, Canters GW, Kieser T, Vijgenboom E (2000) The ram-dependence of *Streptomyces lividans* differentiation is bypassed by copper. *J Mol Microbiol Biotechnol* 2:565–74.
- Kelemen GH, Brown GL, Kormanec J, Potúcková L, Chater KF, Buttner MJ (1996) The positions of the sigma-factor genes, *whiG* and *sigF*, in the hierarchy controlling the development of spore chains in the aerial hyphae of *Streptomyces coelicolor* A3(2). *Mol Microbiol* 21:593–603.
- Kendrick KE, Ensign JC (1983) Sporulation of *Streptomyces griseus* in submerged culture. *J Bacteriol* 155:357–66.
- Kenney JM, Knight D, Wise MJ, Vollrath F (2002) Amyloidogenic nature of spider silk. *Eur J Biochem* 269:4159–4163.
- Kieser T, Bibb MJ, Buttner MJ, Chater KF, Hopwood DA (2000) *Practical Streptomyces Genetics*. John Innes Centre, Norwich, United Kingdom
- Kikuchi Y, Itaya H, Date M, Matsui K, Wu L-F (2009) TatABC overexpression improves *Corynebacterium glutamicum* Tat-dependent protein secretion. *Appl Environ Microbiol* 75:603–7.
- Kim D-W, Chater KF, Lee K-J, Hesketh A (2005) Effects of growth phase and the developmentally significant bldA-specified tRNA on the membrane-associated proteome of *Streptomyces coelicolor*. *Microbiology* 151:2707–20.

- Kim Y-M, Kim J (2004) Formation and dispersion of mycelial pellets of *Streptomyces coelicolor* A3(2). *J Microbiol* 42:64–7.
- Kimura Y, Kawasaki S, Yoshimoto H, Takegawa K (2010) Glycine betaine biosynthesized from glycine provides an osmolyte for cell growth and spore germination during osmotic stress in *Myxococcus xanthus*. *J Bacteriol* 192:1467–70.
- Knipfer N, Shrader TE (1997) Inactivation of the 20S proteasome in *Mycobacterium smegmatis*. *Mol Microbiol* 25:375–83.
- Kodani S, Hudson ME, Durrant MC, Buttner MJ, Nodwell JR, Willey JM (2004) The SapB morphogen is a lantibiotic-like peptide derived from the product of the developmental gene *ramS* in *Streptomyces coelicolor*. *Proc Natl Acad Sci U S A* 101:11448–53.
- Koebisch I, Overbeck J, Piepmeyer S, Meschke H, Schrempf H (2009) A molecular key for building hyphae aggregates: the role of the newly identified *Streptomyces* protein HyaS. *Microb Biotechnol* 2:343–60.
- Kuznetsov VD, Filippova SN, Kudryavtseva A V (1992) Intrapopulation variability of antibiotic biosynthesis in streptomycetes. *Folia Microbiol (Praha)* 37:283–5.
- Lamark T, Kaasen I, Eshoo MW, Falkenberg P, McDougall J, Strøm AR (1991) DNA sequence and analysis of the bet genes encoding the osmoregulatory choline-glycine betaine pathway of *Escherichia coli*. *Mol Microbiol* 5:1049–64.
- Lammertyn E, Van Mellaert L, Schacht S, Dillen C, Sablon E, Van Broekhoven A, Anné J (1997) Evaluation of a novel subtilisin inhibitor gene and mutant derivatives for the expression and secretion of mouse tumor necrosis factor alpha by *Streptomyces lividans*. *Appl Environ Microbiol* 63:1808–13.
- Landfald B, Strøm AR (1986) Choline-glycine betaine pathway confers a high level of osmotic tolerance in *Escherichia coli*. *J Bacteriol* 165:849–55.
- Larson JL, Hershberger CL (1986) The minimal replicon of a streptomycete plasmid produces an ultrahigh level of plasmid DNA. *Plasmid* 15:199–209.
- Latgé J-P (2007) The cell wall: a carbohydrate armour for the fungal cell. *Mol Microbiol* 66:279–90.
- Lee JW, Deng F, Yeomans WG, Allen AL, Gross RA, Kaplan DL (2001) Direct incorporation of glucosamine and N-acetylglucosamine into exopolymers by *Gluconacetobacter xylinus* (= *Acetobacter xylinum*) ATCC 10245: production of chitosan-cellulose and chitin-cellulose exopolymers. *Appl Environ Microbiol* 67:3970–5.
- Leiman PG, Arisaka F, van Raaij MJ, Kostyuchenko VA, Aksyuk AA, Kanamaru S, Rossmann MG (2010) Morphogenesis of the T4 tail and tail fibers. *Virology* 407:355–66.
- Lenarcic R, Halbedel S, Shaw M, Wu LJ, Errington J, Marenduzzo D, Hamoen LW (2009) Localisation of DivIVA by targeting to negatively curved membranes. *EMBO J* 28:2272–2282.
- Lenardon MD, Munro C A, Gow NAR (2010) Chitin synthesis and fungal pathogenesis. *Curr Opin Microbiol* 13:416–23.
- Levitz SM (2010) Innate recognition of fungal cell walls. *PLoS Pathog* 6:e1000758.
- Leyh-Bouille M, Dusart J, Nguyen-Distèche M, Ghuysen JM, Reynolds PE, Perkins HR (1977) The peptidoglycan crosslinking enzyme system in *Streptomyces* strains R61, K15 and rimosus. *Eur J Biochem* 81:19–28.
- Li H, Faury D, Morosoli R (2006) Impact of amino acid changes in the signal peptide on the secretion of the Tat-dependent xylanase C from *Streptomyces lividans*. *FEMS Microbiol Lett* 255:268–74.
- Li H, Jacques P-E, Ghinet MG, Brzezinski R, Morosoli R (2005) Determining the functionality of putative Tat-dependent signal peptides in *Streptomyces coelicolor* A3(2) by using two different reporter proteins. *Microbiology* 151:2189–98.
- Li J-X, Zhao L-M, Wu R-J, Zheng Z-J, Zhang R-J (2013) High-Level Overproduction of Thermobifida Enzyme in *Streptomyces lividans* Using a Novel Expression Vector. *Int J Mol Sci* 14:18629–39.
- Lichenstein HS, Busse LA, Smith GA, Narhi LO, McGinley MO, Rohde MF, Katzowitz JL, Zukowski MM (1992) Cloning and characterization of a gene encoding extracellular metalloprotease from *Streptomyces lividans*. *Gene* 111:125–30.
- Liman R, Facey PD, van Keulen G, Dyson PJ, Del Sol R (2013) A Laterally Acquired Galactose Oxidase-Like Gene Is Required for Aerial Development during Osmotic Stress in *Streptomyces coelicolor*. *PLoS One* 8:e54112.
- Lindahl L, Zengel JM (1982) Expression of ribosomal genes in bacteria. *Adv Genet* 21:53–121.
- Linder MB, Szilvay GR, Nakari-Setälä T, Penttilä ME (2005) Hydrophobins: the protein-amphiphiles of filamentous fungi. *FEMS Microbiol Rev* 29:877–96.
- Lussier F-X, Denis F, Sharek F (2010) Adaptation of the highly productive T7 expression system to *Streptomyces lividans*. *Appl Environ Microbiol* 76:967–70.
- Machczynski MC, Vijgenboom E, Samyn B, Canters GW (2004) Characterization of SLAC: a small laccase from *Streptomyces coelicolor* with unprecedented activity. *Protein Sci* 13:2388–97.

- Manteca A, Alvarez R, Salazar N, Yagüe P, Sanchez J (2008) Mycelium differentiation and antibiotic production in submerged cultures of *Streptomyces coelicolor*. *Appl Environ Microbiol* 74:3877–86.
- Martin SM, Bushell ME (1996) Effect of hyphal micromorphology on bioreactor performance of antibiotic-producing *Saccharopolyspora erythraea* cultures. *Microbiology* 142:1783–1788.
- Martinez JP, Pilar Falomir M, Gozalbo D (2009) Chitin: A Structural Biopolysaccharide. eLS
- Maupin-Furlow J (2012) Proteasomes and protein conjugation across domains of life. *Nat Rev Microbiol* 10:100–11.
- Mehner D, Osadnik H, Lünsdorf H, Brüser T (2012) The Tat System for Membrane Translocation of Folded Proteins Recruits the Membrane-stabilizing Psp Machinery in *Escherichia coli*. *J Biol Chem* 287:27834–42.
- Merzendorfer H (2011) The cellular basis of chitin synthesis in fungi and insects: common principles and differences. *Eur J Cell Biol* 90:759–69.
- Messing J, Crea R, Seeburg PH (1981) A system for shotgun DNA sequencing. *Nucleic Acids Res* 9:309–21.
- Metz B, Kossen NWF (1977) The growth of molds in the form of pellets—a literature review. *Biotechnol Bioeng* 19:781–799.
- Meyerhoff J, Tiller V, Bellgardt K-H (1995) Two mathematical models for the development of a single microbial pellet. *Bioprocess Eng* 12:305–313.
- Miyazaki T, Noda S, Tanaka T, Kondo A (2013) Hyper secretion of *Thermobifida fusca* beta-glucosidase via a Tat-dependent signal peptide using *Streptomyces lividans*. *Microb Cell Fact* 12:88.
- Morosoli R, Shareck F, Kluepfel D (2006) Protein secretion in streptomycetes. *FEMS Microbiol Lett* 146:167–174.
- Mortazavi A, Williams BA, McCue K, Schaeffer L, Wold B (2008) Mapping and quantifying mammalian transcriptomes by RNA-Seq. *Nat Methods* 5:621–8.
- De Mot R, Nagy I, Walz J, Baumeister W (1999) Proteasomes and other self-compartmentalizing proteases in prokaryotes. *Trends Microbiol* 7:88–92.
- Motamedi H, Shafiee A, Cai S (1995) Integrative vectors for heterologous gene expression in. *Gene* 160:25–31.
- Murakami T, Holt TG, Thompson CJ (1989) Thiostrepton-induced gene expression in *Streptomyces lividans*. *J Bacteriol* 171:1459–66.
- Nagy I, Banerjee T, Tamura T, Schoofs G, Gils A, Proost P, Tamura N, Baumeister W, De Mot R (2003) Characterization of a novel intracellular endopeptidase of the alpha/beta hydrolase family from *Streptomyces coelicolor* A3(2). *J Bacteriol* 185:496–503.
- Nakashima N, Mitani Y, Tamura T (2005) Actinomycetes as host cells for production of recombinant proteins. *Microb Cell Fact* 4:7.
- Noda S, Ito Y, Shimizu N, Tanaka T, Ogino C, Kondo A (2010) Over-production of various secretory-form proteins in *Streptomyces lividans*. *Protein Expr Purif* 73:198–202.
- Noda S, Kawai Y, Miyazaki T, Tanaka T, Kondo A (2013) Creation of endoglucanase-secreting *Streptomyces lividans* for enzyme production using cellulose as the carbon source. *Appl Microbiol Biotechnol* 97:5711–20.
- Noens EE, Mersinias V, Willems J, Traag BA, Laing E, Chater KF, Smith CP, Koerten HK, van Wezel GP (2007) Loss of the controlled localization of growth stage-specific cell-wall synthesis pleiotropically affects developmental gene expression in an *ssgA* mutant of *Streptomyces coelicolor*. *Mol Microbiol* 64:1244–59.
- Noens EEE, Mersinias V, Traag BA, Smith CP, Koerten HK, van Wezel GP (2005) SsgA-like proteins determine the fate of peptidoglycan during sporulation of *Streptomyces coelicolor*. *Mol Microbiol* 58:929–44.
- Novozyme (2012) The Novozymes Report 2012. 8–12.
- Nowruzi K, Elkamel A, Schärer JM, Cossar D, Moo-Young M. (2008) Development of a minimal defined medium for recombinant human interleukin-3 production by *Streptomyces lividans* 66. *Biotechnol Bioeng* 99:214–22.
- Ohnishi Y, Ishikawa J, Hara H, Suzuki H, Ikenoya M, Ikeda H, Yamashita A, Hattori M, Horinouchi S (2008) Genome sequence of the streptomycin-producing microorganism *Streptomyces griseus* IFO 13350. *J Bacteriol* 190:4050–60.
- Olmos E, Mehmood N, Haj Husein L, Goergen J-L, Fick M, Delaunay S (2012) Effects of bioreactor hydrodynamics on the physiology of *Streptomyces*. *Bioprocess Biosyst Eng* 3:259–72.
- Pagé N, Kluepfel D, Shareck F, Morosoli R (1996) Increased xylanase yield in *Streptomyces lividans*: dependence on number of ribosome-binding sites. *Nat Biotechnol* 14:756–9.
- Paget M, Hintermann G, Smith C (1994) Construction and application of streptomycete promoter probe vectors which employ the *Streptomyces glaucescens* tyrosinase-encoding gene as reporter. *Gene* 146:105–110.
- Palacín A, de la Fuente R, Valle I, Rivas LA, Mellado RP (2003) *Streptomyces lividans* contains a minimal functional signal recognition particle that is involved in protein secretion. *Microbiology* 149:2435–42.
- Palmer T, Berks BC (2012) The twin-arginine translocation (Tat) protein export pathway. *Nat Rev Microbiol* 10:483–96.

- Pamboukian CRD, Guimarães LM, Facciotti MCR, Politécnic E, Paulo DS, Química DDE, Paulo S (2002) Application of image analysis in the characterization of *Streptomyces olidiensis* in submerged culture. 17–21.
- Papagianni M (2004) Fungal morphology and metabolite production in submerged mycelial processes. *Biotechnol Adv* 22:189–259.
- Papagianni M, Moo-Young M. (2002) Protease secretion in glucoamylase producer *Aspergillus niger* cultures: fungal morphology and inoculum effects. *Process Biochem* 37:8.
- Payne GE, Delacruz N, Coppella SJ (1990) Improved production of heterologous protein from *Streptomyces lividans*. *Appl Microbiol Biotechnol* 33:395–400.
- Pérez-Rueda E, Collado-Vides J (2000) The repertoire of DNA-binding transcriptional regulators in *Escherichia coli* K-12. *Nucleic Acids Res* 28:1838–47.
- Pernodet JL, Simonet JM, Guérineau M (1984) Plasmids in different strains of *Streptomyces ambofaciens*: free and integrated form of plasmid pSAM2. *Mol Gen Genet* 198:35–41.
- Pimienta E, Ayala JC, Rodríguez C, Ramos A, Van Mellaert L, Vallín C, Anné J (2007) Recombinant production of *Streptococcus equisimilis* streptokinase by *Streptomyces lividans*. *Microb Cell Fact* 6:20.
- Pozidis C, Lammertyn E, Politou AS, Tsiftoglou AS, Sianidis G, Economou A (2001) Protein secretion biotechnology using *Streptomyces lividans*: large-scale production of functional trimeric tumor necrosis factor alpha. *Biotechnol Bioeng*. 72:611–9.
- Richards DM, Hempel AM, Flårdh K, Buttner MJ, Howard M (2012) Mechanistic Basis of Branch-Site Selection in Filamentous Bacteria. *PLoS Comput Biol* 8:e1002423.
- Rokem JS, Lantz AE, Nielsen J (2007) Systems biology of antibiotic production by microorganisms. *Nat Prod Rep* 24:1262–87.
- Römling U (2002) Molecular biology of cellulose production in bacteria. *Res Microbiol* 153:205–12.
- Ross P, Mayer R, Benziman M (1991) Cellulose biosynthesis and function in bacteria. *Microbiol Rev* 55:35–58.
- Roubos JA, Krabben P, Luiten RG, Verbruggen HB, Heijnen JJ (2001) A quantitative approach to characterizing cell lysis caused by mechanical agitation of *Streptomyces clavuligerus*. *Biotechnol Prog* 17:336–47.
- Rudolph MM, Vockenhuber M-P, Suess B (2013) Synthetic riboswitches for the conditional control of gene expression in *Streptomyces coelicolor*. *Microbiology* 7:1416–22.
- Ruiz-Arribas A, Sánchez P, Calvete JJ, Raida M, Fernández-Abalos JM, Santamaría RI (1997) Analysis of *xysA*, a gene from *Streptomyces halstedii* JM8 that encodes a 45-kilodalton modular xylanase, Xys1. *Appl Environ Microbiol* 63:2983–8.
- Ryding NJ, Bibb MJ, Molle V, Findlay KC, Chater KF, Buttner MJ (1999) New sporulation loci in *Streptomyces coelicolor* A3(2). *J Bacteriol* 181:5419–25.
- Saldaña Z, Xicohtencatl-Cortes J, Avelino F, Phillips AD, Kaper JB, Puente JL, Girón JA (2009) Synergistic role of curli and cellulose in cell adherence and biofilm formation of attaching and effacing *Escherichia coli* and identification of Fis as a negative regulator of curli. *Environ Microbiol* 11:992–1006.
- Santini CL, Bernadac A, Zhang M, Chanal A, Ize B, Blanco C, Wu LF (2001) Translocation of jellyfish green fluorescent protein via the Tat system of *Escherichia coli* and change of its periplasmic localization in response to osmotic up-shock. *J Biol Chem* 276:8159–64.
- Sarrà M, Casas C, Gòdia F (1997) Continuous production of a hybrid antibiotic by *Streptomyces lividans* TK21 pellets in a three-phase fluidized-bed bioreactor. *Biotechnol Bioeng* 53:601–10.
- Sawyer EB, Claessen D, Haas M, Hurgobin B, Gras SL (2011) The assembly of individual chaplin peptides from *Streptomyces coelicolor* into functional amyloid fibrils. *PLoS One* 6:e18839.
- Schaerlaekens K (2004) The importance of the Tat-dependent protein secretion pathway in *Streptomyces* as revealed by phenotypic changes in tat deletion mutants and genome analysis. *Microbiology* 150:21–31.
- Schaerlaekens K, Lammertyn E, Geukens N, De Keersmaeker S, Anné J, Van Mellaert L (2004) Comparison of the Sec and Tat secretion pathways for heterologous protein production by *Streptomyces lividans*. *J Biotechnol* 112:279–88.
- Schneider CA, Rasband WS, Eliceiri KW (2012) NIH Image to ImageJ: 25 years of image analysis. *Nat Methods* 9:671–675.
- Schrempf H (2001) Recognition and degradation of chitin by streptomycetes. *Antonie Van Leeuwenhoek* 79:285–9.
- Schügerl K, Wittler R, Lorenz T (1983) The use of molds in pellet form. *Trends Biotechnol* 1:120–123.
- Seebeck FP (2013) Thiohistidine biosynthesis. *Chimia (Aarau)* 67:333–6.
- Seghezzi N, Amar P, Koebmann B, Jensen PR, Virolle M-J (2011) The construction of a library of synthetic promoters revealed some specific features of strong *Streptomyces* promoters. *Appl Microbiol Biotechnol* 90:615–23.
- Serganov A, Nudler E (2013) A decade of riboswitches. *Cell* 152:17–24.

- Sevcikova B, Kormanec J (2003) The *ssgB* gene, encoding a member of the regulon of stress-response sigma factor sigmaH, is essential for aerial mycelium septation in *Streptomyces coelicolor* A3(2). *Arch Microbiol* 180:380–4.
- Sevillano L, Díaz M, Santamaría RI (2013) Stable expression plasmids for *Streptomyces* based on a toxin-antitoxin system. *Microb Cell Fact* 12:39.
- Sevillano L, Díaz M, Yamaguchi Y, Inouye M, Santamaría RI (2012) Identification of the First Functional Toxin-Antitoxin System in *Streptomyces*. *PLoS One* 7:e32977.
- Sianidis G, Pozidis C, Becker F, Vrancken K, Sjoeholm C, Karamanou S, Takamiya-Wik M, van Mellaert L, Schaefer T, Anné J, Economou A (2006) Functional large-scale production of a novel Jonesia sp. xyloglucanase by heterologous secretion from *Streptomyces lividans*. *J Biotechnol* 121:498–507.
- Siegl T, Luzhetskyy A (2012) Actinomycetes genome engineering approaches. *Antonie Van Leeuwenhoek* 102:503–16.
- Silakowski B, Pospiech A, Neumann B, Schairer HU (1996) *Stigmatella aurantiaca* fruiting body formation is dependent on the *fbfA* gene encoding a polypeptide homologous to chitin synthases. *J Bacteriol* 178:6706–13.
- Smit G, Swart S, Lugtenberg BJ, Kijne JW (1992) Molecular mechanisms of attachment of Rhizobium bacteria to plant roots. *Mol Microbiol* 6:2897–903.
- Smokvina T, Mazodier P, Boccard F, Thompson CJ, Guérineau M (1990) Construction of a series of pSAM2-based integrative vectors for use in actinomycetes. *Gene* 94:53–9.
- Smucker R, Pfister R (1978) Characteristics of *Streptomyces coelicolor* A3 (2) aerial spore rodlet mosaic. *Can J Microbiol* 24:397–408.
- Strohl WR (1992) Compilation and analysis of DNA sequences associated with apparent streptomycete promoters. *Nucleic Acids Res* 20:961–74.
- Sun J, Kelemen GH, Fernandez-Abalos JM, Bibb MJ (1999) Green fluorescent protein as a reporter for spatial and temporal gene expression in *Streptomyces coelicolor* A3(2). *Microbiology* 145:2221–2227.
- Sun N, Wang Z-B, Wu H-P, Mao X-M, Li Y-Q (2012) Construction of over-expression shuttle vectors in *Streptomyces*. *Ann Microbiol* 62:1541–1546.
- Świątek MA, Gubbens J, Bucca G, Song E, Yang Y-H, Laing E, Kim B-G, Smith CP, van Wezel GP (2013) The ROK family regulator Rok7B7 pleiotropically affects xylose utilization, carbon catabolite repression, and antibiotic production in *Streptomyces coelicolor*. *J Bacteriol* 195:1236–48.
- Takano E, Gramajo HC, Strauch E, Andres N, White J, Bibb MJ (1992) Transcriptional regulation of the *redD* transcriptional activator gene accounts for growth-phase-dependent production of the antibiotic undecylprodigiosin in *Streptomyces coelicolor* A3(2). *Mol Microbiol* 6:2797–804.
- Takano E, Tao M, Long F, Bibb MJ, Wang L, Li W, Buttner MJ, Bibb MJ, Deng ZX, Chater KF (2003) A rare leucine codon in *adpA* is implicated in the morphological defect of *bldA* mutants of *Streptomyces coelicolor*. *Mol Microbiol* 50:475–86.
- Tamura S, Park Y, Toriyama M, Okabe M (1997) Change of mycelial morphology in tylosin production by batch culture of *Streptomyces fradiae* under various shear conditions. *J Ferment Bioeng* 83:523–528.
- Thomas JD, Daniel RA, Errington J, Robinson C (2001) Export of active green fluorescent protein to the periplasm by the twin-arginine translocase (Tat) pathway in *Escherichia coli*. *Mol Microbiol* 39:47–53.
- Traag BA, Kelemen GH, Van Wezel GP (2004) Transcription of the sporulation gene *ssgA* is activated by the IelR-type regulator SsgR in a whi-independent manner in *Streptomyces coelicolor* A3(2). *Mol Microbiol* 53:985–1000.
- Traag BA, Seghezzi N, Vijgenboom E, van Wezel GP (2007) Characterization of the sporulation control protein SsgA by use of an efficient method to create and screen random mutant libraries in streptomycetes. *Appl Environ Microbiol* 73:2085–92.
- Traag BA, van Wezel GP (2008) The SsgA-like proteins in actinomycetes: small proteins up to a big task. *Antonie Van Leeuwenhoek* 94:85–97.
- Ueda K, Tomaru Y, Endoh K, Beppu T (1997) Stimulatory effect of copper on antibiotic production and morphological differentiation in *Streptomyces tanashiensis*. *J Antibiot (Tokyo)* 50:693–5.
- Van Wezel GP, van der Meulen J, Kawamoto S, Luiten RG, Koerten HK, Kraal B (2000a) *ssgA* is essential for sporulation of *Streptomyces coelicolor* A3(2) and affects hyphal development by stimulating septum formation. *J Bacteriol* 182:5653–62.
- Van Wezel GP, White J, Hoogvliet G, Bibb MJ (2000b) Application of *redD*, the transcriptional activator gene of the undecylprodigiosin biosynthetic pathway, as a reporter for transcriptional activity in *Streptomyces coelicolor* A3(2) and *Streptomyces lividans*. *J Mol Microbiol Biotechnol* 2:551–6.

- Van Wezel GP, Vijgenboom E (2003) Improved growth characteristics of filamentous microorganisms. Patent Application WO 2004/041858 A1.
- Van Wezel GP, Mahr K, König M, Traag BA, Pimentel-Schmitt EF, Willimek A, Titgemeyer F (2005) GlcP constitutes the major glucose uptake system of *Streptomyces coelicolor* A3(2). *Mol Microbiol* 55:624–36.
- Van Wezel GP, Krabben P, Traag BA, Keijser BJF, Kerste R, Vijgenboom E, Heijnen JJ, Kraal B (2006) Unlocking *Streptomyces* spp. for use as sustainable industrial production platforms by morphological engineering. *Appl Environ Microbiol* 72:5283–8.
- Van Wezel GP, McKenzie NL, Nodwell JR (2009) Chapter 5. Applying the genetics of secondary metabolism in model actinomycetes to the discovery of new antibiotics., 1st ed. *Methods Enzymol* 458:117–41.
- Van Veluw GJ, Petrus MLC, Gubbens J, de Graaf R, de Jong IP, van Wezel GP, Wösten HAB, Claessen D (2012) Analysis of two distinct mycelial populations in liquid-grown *Streptomyces* cultures using a flow cytometry-based proteomics approach. *Appl Microbiol Biotechnol* 96:1301–12.
- Van Wezel GP, McDowall KJ (2011) The regulation of the secondary metabolism of *Streptomyces*: new links and experimental advances. *Nat Prod Rep* 28:1311–33.
- Vara J, Lewandowska-Skarbek M, Wang YG, Donadio S, Hutchinson CR (1989) Cloning of genes governing the deoxysugar portion of the erythromycin biosynthesis pathway in *Saccharopolyspora erythraea* (*Streptomyces erythreus*). *J Bacteriol* 171:5872–81.
- Vecht-Lifshitz SE, Sasson Y, Braun S (1992) Nikkomycin production in pellets of *Streptomyces tendae*. *J Appl Bacteriol* 72:195–200.
- Vijgenboom E, Woudt LP, Heinstra PW, Rietveld K, van Haarlem J, van Wezel GP, Shochat S, Bosch L (1994) Three *tuf*-like genes in the kirromycin producer *Streptomyces ramocissimus*. *Microbiology* 140 (Pt 4):983–98.
- Vrancken K, Anné J (2009) Secretory production of recombinant proteins by *Streptomyces*. *Future Microbiol* 4:181–188.
- Vrancken K, De Keersmaecker S, Geukens N, Lammertyn E, Anné J, Van Mellaert L (2007) *pspA* overexpression in *Streptomyces lividans* improves both Sec- and Tat-dependent protein secretion. *Appl Microbiol Biotechnol* 73:1150–7.
- Vrancken K, Van Mellaert L, Anné J (2010) Cloning and expression vectors for a Gram-positive host, *Streptomyces lividans*. *Methods Mol Biol* 668:97–107.
- Walisko R, Krull R, Schrader J, Wittmann C (2012) Microparticle based morphology engineering of filamentous microorganisms for industrial bio-production. *Biotechnol Lett* 11:1975–82.
- Wall D (2014) Molecular recognition in myxobacterial outer membrane exchange: Functional, social and evolutionary implications. *Mol Microbiol* 91: 209–220.
- Wang W, Li X, Wang J, Xiang S, Feng X, Yang K (2013) An engineered strong promoter for streptomycetes. *Appl Environ Microbiol* 14:4484–92.
- Wang YY, Fu ZB, Ng KL, Lam CC, Chan AKN, Sze KF, Wong WKR (2011) Enhancement of excretory production of an exoglucanase from *Escherichia coli* with phage shock protein A (PspA) overexpression. *J Microbiol Biotechnol* 21:637–45.
- Ward JM, Janssen GR, Kieser T, Bibb MJ, Buttner MJ (1986) Construction and characterisation of a series of multi-copy promoter-probe plasmid vectors for *Streptomyces* using the aminoglycoside phosphotransferase gene from Tn5 as indicator. *Mol Gen Genet* 203:468–78.
- Wardell JN, Stocks SM, Thomas CR, Bushell ME (2002) Decreasing the hyphal branching rate of *Saccharopolyspora erythraea* NRRL 2338 leads to increased resistance to breakage and increased antibiotic production. *Biotechnol Bioeng* 78:141–6.
- Watanabe T, Ito Y, Yamada T, Hashimoto M, Sekine S, Tanaka H (1994) The roles of the C-terminal domain and type III domains of chitinase A1 from *Bacillus circulans* WL-12 in chitin degradation. *J Bacteriol* 176:4465–72.
- Wen Su W, Jun He B (1997) Secreted enzyme production by fungal pellets in a perfusion bioreactor. *J Biotechnol* 54:43–52.
- Whitaker A (1992) Actinomycetes in submerged culture. *Appl Biochem Biotechnol* 32:23–35.
- Whitchurch CB, Tolker-Nielsen T, Ragas PC, Mattick JS (2002) Extracellular DNA required for bacterial biofilm formation. *Science* 295:1487.
- White AP, Gibson DL, Collinson SK, Banser PA, Kay WW (2003) Extracellular polysaccharides associated with thin aggregative fimbriae of *Salmonella enterica* serovar enteritidis. *J Bacteriol* 185:5398–407.
- Whittaker MM, Whittaker JW (2006) *Streptomyces coelicolor* oxidase (SCO2837p): a new free radical metalloenzyme secreted by *Streptomyces coelicolor* A3(2). *Arch Biochem Biophys* 452:108–18.

- Widdick DA, Dilks K, Chandra G, Bottrill A, Naldrett M, Pohlschröder M, Palmer T (2006) The twin-arginine translocation pathway is a major route of protein export in *Streptomyces coelicolor*. *Proc Natl Acad Sci U S A* 103:17927–32.
- Willemse J, Borst JW, de Waal E, Bisseling T, van Wezel GP (2011) Positive control of cell division: FtsZ is recruited by SsgB during sporulation of *Streptomyces*. *Genes Dev* 25:89–99.
- Willemse J, Ruban-Osmialowska B, Widdick D, Celler K, Hutchings MI, van Wezel GP, Palmer T (2012) Dynamic localization of Tat protein transport machinery components in *Streptomyces coelicolor*. *J Bacteriol* 194:6272–81.
- Willemse J, van Wezel GP (2009) Imaging of *Streptomyces coelicolor* A3(2) with reduced autofluorescence reveals a novel stage of FtsZ localization. *PLoS One* 4:e4242.
- Willey J, Santamaria R, Guijarro J, Geistlich M, Losick R (1991) Extracellular complementation of a developmental mutation implicates a small sporulation protein in aerial mycelium formation by *S. coelicolor*. *Cell* 65:641–50.
- Willey J, Schwedock J, Losick R (1993) Multiple extracellular signals govern the production of a morphogenetic protein involved in aerial mycelium formation by *Streptomyces coelicolor*. *Genes Dev* 7:895–903.
- Williams KP (2002) Integration sites for genetic elements in prokaryotic tRNA and tmRNA genes: sublocation preference of integrase subfamilies. *Nucleic Acids Res* 30:866–875.
- Wolanski M, Wali R, Tilley E, Jakimowicz D, Zakrzewska-Czerwinska J, Herron P (2011) Replisome trafficking in growing vegetative hyphae of *Streptomyces coelicolor* A3(2). *J Bacteriol* 193:1273–5.
- Wösten HA, Richter M, Willey JM (1999) Structural proteins involved in emergence of microbial aerial hyphae. *Fungal Genet Biol* 27:153–60.
- Wright HT, Sandrasegaram G, Wright CS (1991) Evolution of a family of N-acetylglucosamine binding proteins containing the disulfide-rich domain of wheat germ agglutinin. *J Mol Evol* 33:283–94.
- Xu H, Chater KF, Deng Z, Tao M (2008) A cellulose synthase-like protein involved in hyphal tip growth and morphological differentiation in *Streptomyces*. *J Bacteriol* 190:4971–8.
- Xu Q, Traag BA, Willemse J, McMullan D, Miller MD, Elslinger M-A, Abdubek P, Astakhova T, Axelrod HL, Bakolitsa C, Carlton D, Chen C, Chiu H-J, Chruszcz M, Clayton T, Das D, Deller MC, Duan L, Ellrott K, Ernst D, Farr CL, Feuerhelm J, Grant JC, Grzechnik A, Grzechnik SK, Han GW, Jaroszewski L, Jin KK, Klock HE, Knuth MW, Kozbial P, Krishna SS, Kumar A, Marciano D, Minor W, Mommaas A, Morse AT, Nigoghossian E, Nopakun A, Okach L, Oommachen S, Paulsen J, Puckett C, Reyes R, Rife CL, Sefcovic N, Tien HJ, Trame CB, van den Bedem H, Wang S, Weekes D, Hodgson KO, Wooley J, Deacon AM, Godzik A, Lesley SA, Wilson IA, van Wezel GP (2009) Structural and functional characterizations of SsgB, a conserved activator of developmental cell division in morphologically complex actinomycetes. *J Biol Chem* 284:25268–79.
- Yamazaki H, Ohnishi Y, Horinouchi S (2003) Transcriptional switch on of *ssgA* by A-factor, which is essential for spore septum formation in *Streptomyces griseus*. *J Bacteriol* 185:1273–83.
- Yen H-W, Hsiao H-P (2013) Effects of dissolved oxygen level on rapamycin production by pellet-form of *Streptomyces hygroscopicus*. *J Biosci Bioeng* 116:366–70.
- Zhou X, Wu H, Li Z, Zhou X, Bai L, Deng Z (2011) Over-expression of UDP-glucose pyrophosphorylase increases validamycin A but decreases validoxylamine A production in *Streptomyces hygroscopicus* var. *jinggangensis* 5008. *Metab Eng* 13:768–76.
- Zhu Y, Wang L, Du Y, Wang S, Yu T, Hong B (2011) Heterologous expression of human interleukin-6 in *Streptomyces lividans* TK24 using novel secretory expression vectors. *Biotechnol Lett* 33:253–61.
- Zimmer J, Nam Y, Rapoport TA (2008) Structure of a complex of the ATPase SecA and the protein-translocation channel. *Nature* 455:936–43.
- Zimmermann B, Bilusic I, Lorenz C, Schroeder R (2010) Genomic SELEX: a discovery tool for genomic aptamers. *Methods* 52:125–32.
- Zogaj X, Bokranz W, Nimtz M, Römling U (2003) Production of cellulose and curli fimbriae by members of the family Enterobacteriaceae isolated from the human gastrointestinal tract. *Infect Immun* 71:4151–8.

APPENDIX

RNA-Seq DATA

Table S1-A. Genes expressed higher in both *csIA* and *glxA*

Gene # <i>S. coelicolor</i>	Gene # <i>S. lividans</i>	1326 (RPKM)	<i>csIA</i> (RPKM)	<i>glxA</i> (RPKM)	<i>csIA</i> /1326	<i>glxA</i> /1326	Annotation
SCO0187	SLI0127	6,4	15,5	13,2	2,4	2,1	Phytoene synthase
SCO0188	SLI0128	5,2	13,1	13,0	2,5	2,5	CrtV-methyltransferase-like protein
	SLI0138	9,9	26,5	20,6	2,7	2,1	hypothetical protein
SCO0231	SLI0175	41,8	99,3	97,1	2,4	2,3	small hydrophobic protein
SCO0426	SLI0384	4,9	16,6	10,3	3,4	2,1	hypothetical protein
SCO0508	SLI0468	6,5	14,1	13,3	2,2	2,0	Transcriptional regulator, TetR family
	SLI0944	5,3	11,3	12,4	2,1	2,3	Transcriptional regulator XRE family
	SLI0994	5,7	11,8	13,0	2,1	2,3	CopZ-like Copper chaperone
	SLI1041	3,8	10,0	8,3	2,7	2,2	putative lipoprotein
	SLI1076	4,7	11,5	9,6	2,4	2,0	hypothetical protein
SCO6808	SLI1107	11,9	32,5	29,7	2,7	2,5	ArsR regulator
	SLI1228	4,5	10,1	11,7	2,2	2,6	Non-heme chloroperoxidase
SCO1134	SLI1410	3,1	14,6	8,5	4,7	2,8	Aromatic aldehyde oxidoreductase, YagT
	SLI1425	9,2	27,6	24,6	3,0	2,7	hypothetical protein
SCO1250	SLI1531	4,8	12,8	13,5	2,7	2,8	putative acetyltransferase
	SLI1606	6,4	29,2	19,2	4,5	3,0	hypothetical protein
SCO1620	SLI1923	31,5	193,9	117,3	6,2	3,7	<i>opuABC</i> glycine betaine transport system permease
SCO1621	SLI1924	28,7	153,3	106,7	5,3	3,7	<i>opuAA</i> glycine betaine transport ATP-binding protein
SCO1866	SLI2177	67,7	666,0	139,3	9,8	2,1	L-ectoine synthase, <i>ectC</i>
SCO2631	SLI2974	6,1	14,2	17,4	2,3	2,9	putative amino acid permease
SCO2828	SLI3177	27,1	124,4	62,2	4,6	2,3	amino acid ABC transporter, amino acid-binding protein
SCO2829	SLI3178	17,6	99,8	46,0	5,7	2,6	amino acid ABC transporter, permease
SCO2830	SLI3179	19,6	106,2	52,2	5,4	2,7	amino acid ABC transporter, integral membrane protein
SCO2831	SLI3180	23,7	118,8	54,8	5,0	2,3	amino acid ABC transporter, ATP-binding protein
SCO3121	SLI3478	3,8	9,0	19,2	2,4	5,1	hypothetical protein
SCO3428	SLI3771	2,4	7,5	13,5	3,1	5,6	LSU ribosomal protein L33p, zinc-independent
	SLI3944	4,0	9,2	12,3	2,3	3,1	hypothetical protein
SCO4243	SLI4480	24,9	98,3	60,7	3,9	2,4	secreted protein
SCO4244	SLI4481	39,3	146,7	85,3	3,7	2,2	hypothetical protein
SCO4245	SLI4482	40,4	146,1	87,9	3,6	2,2	hypothetical protein
SCO4246	SLI4483	38,4	165,0	93,3	4,3	2,4	hypothetical protein
SCO4247	SLI4484	56,0	249,4	138,1	4,5	2,5	hypothetical protein
SCO4248	SLI4485	37,2	174,2	94,9	4,7	2,5	hypothetical protein
SCO4252	SLI4488	845,1	4425,2	2045,2	5,2	2,4	hypothetical protein

Appendix

SCO4255	SLI4491	20,7	73,8	42,5	3,6	2,1	hypothetical protein
SCO4257	SLI4492	73,4	236,8	192,1	3,2	2,6	Hydrolytic protein
SCO4514	SLI4795	29,8	94,3	64,5	3,2	2,2	integral membrane protein
	SLI4831	3,6	10,2	12,0	2,8	3,3	type IV peptidase
SCO4663	SLI4937	1074,9	3617,6	2612,2	3,4	2,4	hypothetical protein
SCO4828	SLI5101	20,9	49,8	48,8	2,4	2,3	Betaine aldehyde dehydrogenase
SCO4829	SLI5102	17,8	62,4	48,6	3,5	2,7	Choline dehydrogenase
SCO4830	SLI5103	8,2	41,1	26,2	5,0	3,2	Glycine betaine ABC transporter, ATP-binding protein
SCO4831	SLI5104	8,1	33,2	22,0	4,1	2,7	Glycine betaine ABC transporter, permease
SCO4832	SLI5105	24,4	67,4	50,1	2,8	2,1	Glycine betaine ABC transporter, substrate binding protein
SCO4947	SLI5222	5,2	11,4	11,2	2,2	2,2	Respiratory nitrate reductase alpha chain
SCO4994	SLI5269	33,4	122,9	70,8	3,7	2,1	hypothetical protein
	SLI5784	83,6	320,1	198,4	3,8	2,4	hypothetical protein
SCO5522	SLI5797	116,8	482,6	242,5	4,1	2,1	3-isopropylmalate dehydrogenase
	SLI6177	26,4	57,4	62,6	2,2	2,4	hypothetical protein
	SLI6330	17,5	40,0	52,9	2,3	3,0	hypothetical protein
SCO6073	SLI6466	3,4	12,0	7,0	3,5	2,0	germacradienol/germacrene D synthase
SCO6509	SLI6857	6,6	22,9	18,9	3,5	2,9	hydrophobic protein
SCO6980	SLI7182	6,0	19,1	12,4	3,2	2,1	Inositol transport system permease
SCO7428	SLI7648	6,2	15,4	14,4	2,5	2,3	Flavoheomprotein, hmpA1
	SLI7822	3,0	36,0	12,0	12,1	4,0	hypothetical protein
	SLI8052	1,1	14,0	16,3	13,0	15,1	hypothetical protein

Table S1-B. Genes expressed higher in *glxA* only

Gene # <i>S. coelicolor</i>	Gene # <i>S. lividans</i>	1326 (RPKM)	<i>csIA</i> (RPKM)	<i>glxA</i> (RPKM)	<i>csIA</i> /1326	<i>glxA</i> /1326	Annotation
SCO0569	SLI0532	9,1	13,3	20,4	1,5	2,2	LSU ribosomal protein L36p
SCO0672	SLI0644	8,9	8,1	18,3	0,9	2,1	anti-sigma factor antagonist
	SLI1189	5,7	8,9	13,9	1,6	2,4	hypothetical protein
SCO1423	SLI1720	179,6	136,4	370,5	0,8	2,1	Dolichol-phosphate mannosyltransferase
SCO1700	SLI2004	47,0	33,7	106,1	0,7	2,3	putative membrane protein
SCO1702	SLI2006	5,0	7,4	10,2	1,5	2,0	Transcriptional regulator, TetR family
	SLI2561	14,1	19,6	35,2	1,4	2,5	hypothetical protein
SCO2336	SLI2667	6,7	5,2	14,4	0,8	2,2	L-Proline/Glycine betaine transporter ProP
	SLI2831	7,9	10,2	20,0	1,3	2,6	hypothetical protein
	SLI2934	225,1	284,1	477,1	1,3	2,1	hypothetical protein
SCO2827	SLI3176	7,2	14,1	15,5	2,0	2,2	hypothetical protein
SCO2976	SLI3320	6,1	10,6	12,9	1,8	2,1	hypothetical protein
SCO3167	SLI3521	54,3	63,9	116,0	1,2	2,1	Transcriptional regulator, TetR family
SCO3271	SLI3617	5,3	5,2	16,8	1,0	3,2	dehydrogenase
	SLI4035	17,9	20,4	43,8	1,1	2,4	hypothetical protein
	SLI4041	68,3	129,8	190,7	1,9	2,8	hypothetical protein

	SLI4370	204,9	281,1	424,9	1,4	2,1	hypothetical protein
	SLI4571	37,0	58,8	132,2	1,6	3,6	hypothetical protein
SCO4640	SLI4911	70,0	67,5	159,9	1,0	2,3	Transcriptional regulator, TetR family
SCO4816	SLI5087	5,9	7,7	11,9	1,3	2,0	hypothetical protein
SCO5225	SLI5514	478,0	533,1	967,9	1,1	2,0	Ribonucleotide reductase, beta subunit
SCO5467	SLI5736	4,9	9,5	11,7	1,9	2,4	Zinc D-Ala-D-Ala carboxypeptidase
	SLI5781	13,2	6,2	30,2	0,5	2,3	hypothetical protein
SCO5908	SLI6183	8,1	7,7	20,8	1,0	2,6	hypothetical protein
SCO3525	SLI6348	6,1	5,9	14,2	1,0	2,3	transmembrane protein
	SLI6555	6,3	8,4	14,7	1,3	2,3	hypothetical protein
SCO6259	SLI6648	14,5	16,5	29,1	1,1	2,0	Inositol transport system, ATP-binding protein
SCO6524	SLI6872	7,2	10,8	15,6	1,5	2,2	putative integral membrane protein
SCO6728	SLI7072	34,3	35,6	70,6	1,0	2,1	hypothetical protein
SCO7146	SLI7361	34,8	55,4	84,3	1,6	2,4	Transcriptional regulator, ArsR family
SCO7196	SLI7413	4,7	5,5	10,0	1,2	2,1	possible ion transport integral membrane protein
SCO7271	SLI7489	35,8	57,5	71,9	1,6	2,0	putative ion channel subunit
SCO7506	SLI7727	5,0	7,5	11,0	1,5	2,2	Beta-galactosidase
	SLI7900	4,7	5,5	10,5	1,2	2,2	hypothetical protein
	SLI7991	4,9	9,7	12,0	2,0	2,5	hypothetical protein
SCO7754	SLI7994	7,6	12,1	16,8	1,6	2,2	anti-sigma factor antagonist
SCO7826	SLI8076	4,6	7,5	10,2	1,6	2,2	hypothetical protein

Table S1-C. Genes expressed higher in *csIA* only

Gene # <i>S. coelicolor</i>	Gene # <i>S. lividans</i>	1326 (RPKM)	<i>csIA</i> (RPKM)	<i>glxA</i> (RPKM)	<i>csIA</i> /1326	<i>glxA</i> /1326	Annotation
SCO0148	SLI0077	12,6	25,6	23,1	2,0	1,8	Transcriptional regulator, Cro/C1 family
SCO0346	SLI0303	4,4	12,9	8,6	2,9	1,9	putative 2-hydroxyhepta-2,4-diene-1,7- dioate isomerase
SCO0379	SLI0337	50,0	122,1	49,8	2,4	1,0	Catalase
SCO0408	SLI0366	11,1	27,0	9,9	2,4	0,9	Methyltransferase
SCO0409	SLI0367	5,6	21,8	7,5	3,9	1,3	Spore-associated protein A precursor
SCO0427	SLI0385	11,4	25,2	15,4	2,2	1,4	Beta-ketoadipate enol-lactone hydrolase
SCO0442	SLI0400	11,0	27,7	14,9	2,5	1,3	Allophanate hydrolase 2 subunit 1
SCO0443	SLI0401	5,9	21,2	10,6	3,6	1,8	Allophanate hydrolase 2 subunit 2
SCO0461	SLI0419	6,8	14,9	8,3	2,2	1,2	putative hydrolase
SCO0484	SLI0443	6,9	19,4	11,4	2,8	1,6	putative monooxygenase
SCO0494	SLI0454	59,7	141,6	53,8	2,4	0,9	iron-siderophore binding lipoprotein
SCO0498	SLI0458	9,8	21,8	7,1	2,2	0,7	Siderophore biosynthesis, monooxygenase
	SLI0487	2624,6	5701,9	3530,0	2,2	1,3	hypothetical protein
SCO0543	SLI0504	6,9	26,7	12,8	3,9	1,9	hypothetical protein
	SLI0587	5,0	13,7	9,8	2,7	2,0	hypothetical protein
SCO0682	SLI0655	46,2	92,3	57,2	2,0	1,2	hypothetical protein

Appendix

SCO0701	SLI0677	5,2	10,8	6,7	2,1	1,3	hypothetical protein
SCO0760	SLI0741	38,7	98,2	30,6	2,5	0,8	putative methyltransferase
SCO0795	SLI0778	8,3	19,6	7,4	2,4	0,9	hypothetical protein
SCO0825	SLI0809	6,6	14,9	11,0	2,2	1,7	putative transmembrane transport protein
SCO0834	SLI0818	5,4	13,7	7,8	2,6	1,5	hypothetical protein
	SLI0916	8,8	22,5	13,0	2,6	1,5	hypothetical protein
SCO6914	SLI0941	5,4	11,1	8,9	2,1	1,7	hypothetical protein SC1B2.20
SCO3698	SLI1077	7,0	14,2	11,2	2,0	1,6	ArsB heavy metal resistance transport membrane protein
SCO6821	SLI1094	6,3	15,7	5,1	2,5	0,8	hypothetical protein
SCO6819	SLI1096	1,9	10,5	2,6	5,5	1,3	5-Enolpyruvylshikimate-3-phosphate synthase
SCO6818	SLI1097	2,9	11,5	4,0	3,9	1,4	putative phosphoglycerate mutase
SCO6814	SLI1101	3,8	11,2	6,5	2,9	1,7	ABC transporter ATP-binding protein
SCO0912	SLI1141	6,4	13,1	6,8	2,0	1,1	Glutamine amidotransferases class-II
SCO0913	SLI1142	6,4	18,0	9,8	2,8	1,5	ABC transporter ATP-binding protein
SCO0922	SLI1153	2,1	14,1	2,8	6,7	1,3	Succinate dehydrogenase iron-sulfur protein
SCO0923	SLI1154	4,0	23,8	4,0	6,0	1,0	Succinate dehydrogenase flavoprotein subunit
SCO0924	SLI1155	19,8	43,0	17,4	2,2	0,9	Succinate dehydrogenase cytochrome b subunit
SCO1131	SLI1407	6,9	15,9	9,1	2,3	1,3	Xanthine and CO dehydrogenases accessory protein
SCO1132	SLI1408	8,5	19,7	11,0	2,3	1,3	aromatic aldehyde oxidoreductase, YagR
SCO1133	SLI1409	3,2	10,7	4,7	3,3	1,4	aromatic aldehyde oxidoreductase, YagS
SCO1147	SLI1423	7,2	23,8	5,8	3,3	0,8	putative ABC transporter transmembrane subunit
SCO1148	SLI1424	3,2	26,0	6,0	8,1	1,9	putative ABC transporter ATP-binding protein
SCO1293	SLI1575	6,8	15,9	7,5	2,3	1,1	hypothetical protein
SCO1294	SLI1576	2,5	29,9	4,5	12,1	1,8	Methionine gamma-lyase
SCO1357	SLI1649	8,2	17,1	10,9	2,1	1,3	hypothetical protein
SCO1570	SLI1873	32,1	133,9	54,4	4,2	1,7	Argininosuccinate lyase
SCO1577	SLI1880	32,2	116,5	34,3	3,6	1,1	Acetylornithine aminotransferase
SCO1578	SLI1881	17,0	96,9	28,8	5,7	1,7	Acetylglutamate kinase
SCO1579	SLI1882	24,8	100,2	35,6	4,0	1,4	putative glutamate N-acetyltransferase, argJ
SCO1580	SLI1883	26,1	77,1	43,7	3,0	1,7	N-acetyl-gamma-glutamyl-phosphate reductase, argC
SCO1864	SLI2175	32,4	94,2	52,1	2,9	1,6	L-2,4-diaminobutyric acid acetyltransferase
SCO1865	SLI2176	31,3	167,0	61,8	5,3	2,0	Diaminobutyrate-pyruvate aminotransferase
SCO1867	SLI2178	72,5	614,8	125,1	8,5	1,7	Ectoine hydroxylase
SCO1898	SLI2209	14,8	32,7	11,1	2,2	0,8	possible sugar binding protein
SCO1899	SLI2210	8,7	26,5	8,7	3,0	1,0	possible integral membrane sugar transport protein
SCO1900	SLI2211	8,2	40,3	9,5	4,9	1,2	possible integral membrane sugar transport protein
SCO1901	SLI2212	18,2	69,3	18,0	3,8	1,0	Sorbitol dehydrogenase
	SLI2217	29,3	125,6	39,2	4,3	1,3	hypothetical protein
SCO1987	SLI2304	10,5	25,2	10,3	2,4	1,0	Translation initiation inhibitor
SCO1988	SLI2305	22,3	51,7	16,6	2,3	0,7	hypothetical protein
SCO2011	SLI2332	29,2	65,6	32,6	2,2	1,1	Branched-chain amino acid transport ATP-binding protein LivG
SCO2012	SLI2333	39,9	86,9	49,5	2,2	1,2	Branched-chain amino acid transport ATP-binding protein LivF

SCO2025	SLI2346	90,4	235,5	106,5	2,6	1,2	Glutamate synthase (NADPH) small chain
SCO2026	SLI2347	80,5	182,1	104,2	2,3	1,3	Glutamate synthase (NADPH) large chain
SCO2270	SLI2596	7,5	16,6	4,3	2,2	0,6	hypothetical protein
SCO2372	SLI2706	11,7	40,2	21,6	3,4	1,8	Antiholin-like protein LrgA
SCO2449	SLI2785	18,6	46,4	24,6	2,5	1,3	MoxR-like ATPases
SCO2464	SLI2800	19,3	43,3	25,4	2,2	1,3	Lipid A export ATP-binding/permease protein MsbA
SCO2492	SLI2826	57,7	144,7	35,4	2,5	0,6	hypothetical protein
SCO2493	SLI2827	7,8	17,6	10,8	2,3	1,4	hypothetical protein
SCO2591	SLI2930	663,2	1353,8	612,4	2,0	0,9	hypothetical protein
SCO2633	SLI2975	406,1	2553,7	609,1	6,3	1,5	superoxide dismutase, Fe-Zn
SCO2637	SLI2979	59,5	127,2	61,0	2,1	1,0	Serine protease
SCO2776	SLI3123	15,8	198,8	15,1	12,6	1,0	Methylcrotonyl-CoA carboxylase carboxyl transferase
SCO2777	SLI3124	11,6	172,3	9,6	14,8	0,8	Methylcrotonyl-CoA carboxylase biotin-containing
SCO2778	SLI3125	10,6	228,0	8,0	21,6	0,8	Hydroxymethylglutaryl-CoA lyase
SCO2779	SLI3126	16,5	344,2	15,7	20,9	1,0	Isovaleryl-CoA dehydrogenase
SCO2783	SLI3130	11,1	26,8	15,9	2,4	1,4	Desferrioxamine E biosynthesis, monooxygenase, DesB
SCO2785	SLI3132	13,6	28,8	15,1	2,1	1,1	Desferrioxamine E biosynthesis, ligase, DesD
SCO2837	SLI3188	188,4	3460,9	1,1	18,4	0,0	Radical Cu-oxidase, glxA
SCO2838	SLI3189	172,9	529,4	312,0	3,1	1,8	putative secreted endoglucanase
SCO2839	SLI3190	4,7	20,5	8,5	4,3	1,8	lipoprotein
	SLI3212	11,8	24,0	11,1	2,0	0,9	hypothetical protein
	SLI3213	17,2	37,7	25,7	2,2	1,5	hypothetical protein
	SLI3214	92,6	200,2	140,8	2,2	1,5	hypothetical protein
SCO2879	SLI3224	27,8	70,9	21,3	2,5	0,8	conserved hypothetical secreted protein
SCO2880	SLI3225	32,3	83,6	38,2	2,6	1,2	hypothetical protein
SCO2881	SLI3226	29,2	61,8	24,1	2,1	0,8	hypothetical protein
SCO2882	SLI3227	21,1	61,6	21,3	2,9	1,0	conserved ATP/GTP-binding protein
SCO2883	SLI3228	22,1	55,5	24,5	2,5	1,1	cytochrome P450 monooxygenase
SCO2884	SLI3229	41,3	136,1	42,5	3,3	1,0	putative cytochrome P450 hydroxylase
SCO2885	SLI3230	26,4	93,5	31,3	3,5	1,2	hypothetical protein
SCO2920	SLI3264	68,1	264,5	85,4	3,9	1,3	Serine protease 3 precursor
SCO3051	SLI3400	164,9	399,8	190,1	2,4	1,2	Butyryl-CoA dehydrogenase
SCO3160	SLI3514	36,6	75,3	71,6	2,1	2,0	possible integral membrane transport protein, Co transport
SCO3614	SLI3857	219,8	460,1	241,2	2,1	1,1	Aspartate-semialdehyde dehydrogenase
SCO3811	SLI4062	213,3	568,2	197,7	2,7	0,9	D-alanyl-D-alanine carboxypeptidase
SCO3831	SLI4083	5,6	13,8	10,0	2,4	1,8	Branched-chain alpha-keto acid dehydrogenase, E1 alpha subunit, bkdA2
SCO4020	SLI4254	20,3	81,4	20,3	4,0	1,0	putative two-component system response regulator
SCO4021	SLI4255	3,1	32,3	4,5	10,5	1,5	Osmosensitive K ⁺ channel histidine kinase KdpD
SCO4108	SLI4338	100,5	244,1	106,0	2,4	1,1	putative peptidase
SCO4157	SLI4395	6,8	14,7	6,9	2,2	1,0	putative protease
SCO4242	SLI4479	46,5	155,0	80,4	3,3	1,7	hypothetical protein
SCO4249	SLI4486	18,2	57,5	30,0	3,2	1,7	hypothetical protein

Appendix

SCO4251	SLI4487	575,8	2311,7	1137,6	4,0	2,0	secreted protein
SCO4253	SLI4489	550,1	2388,0	1065,2	4,3	1,9	Phage tail sheath protein FI
SCO4254	SLI4490	12,2	25,2	20,0	2,1	1,6	hypothetical protein
SCO4258	SLI4493	101,4	325,3	193,6	3,2	1,9	hydrolytic protein
SCO4259	SLI4494	29,0	94,4	54,5	3,3	1,9	ATPase, AAA family
SCO4336	SLI4574	236,9	477,1	394,9	2,0	1,7	Transcriptional regulator, MarR family
SCO4512	SLI4793	56,2	122,7	95,3	2,2	1,7	hypothetical protein
SCO4513	SLI4794	35,1	96,4	56,7	2,7	1,6	hypothetical protein
SCO4515	SLI4796	39,5	110,4	63,2	2,8	1,6	hypothetical protein
SCO4683	SLI4956	79,3	168,8	90,5	2,1	1,1	NADP-specific glutamate dehydrogenase
SCO4784	SLI5054	58,4	162,4	70,0	2,8	1,2	Chorismate mutase I
SCO4896	SLI5168	20,9	57,3	32,6	2,7	1,6	putative transport integral membrane protein
SCO4930	SLI5203	12,0	31,2	9,8	2,6	0,8	Methylglutaconyl-CoA hydratase
SCO4931	SLI5204	7,1	23,8	6,3	3,4	0,9	putative secreted protein
SCO4936	SLI5210	7,6	18,6	7,2	2,5	1,0	putative ABC transporter ATP-binding protein
SCO4937	SLI5211	3,8	13,4	3,3	3,5	0,9	hypothetical protein
SCO4951	SLI5223	8,8	18,2	10,3	2,1	1,2	putative oxidoreductase
SCO4995	SLI5270	12,9	35,5	19,9	2,8	1,5	hypothetical protein
SCO5012	SLI5288	9,2	19,9	12,0	2,2	1,3	hypothetical protein
SCO5013	SLI5289	4,6	11,9	7,8	2,6	1,7	secreted protein
SCO5014	SLI5290	4,7	12,6	8,6	2,7	1,8	hypothetical protein
SCO5240	SLI5531	600,9	1401,1	689,7	2,3	1,1	transcription regulator, WhiB-like
SCO5249	SLI5540	5,0	15,6	8,3	3,1	1,7	putative nucleotide-binding protein
SCO5389	SLI5658	185,0	583,3	161,6	3,2	0,9	hypothetical protein
SCO5390	SLI5659	20,3	48,0	16,5	2,4	0,8	putative alkanal monooxygenase (luciferase)
SCO5448	SLI5717	4,7	14,3	7,2	3,0	1,5	putative ABC transporter ATP-binding protein
SCO5449	SLI5718	7,1	18,2	11,1	2,6	1,6	putative ABC transporter transmembrane protein
SCO5450	SLI5719	6,5	22,6	12,0	3,5	1,8	putative ABC transporter ATP-binding protein
	SLI5785	189,0	584,0	315,4	3,1	1,7	hypothetical protein
SCO5512	SLI5786	111,5	311,5	173,7	2,8	1,6	Acetolactate synthase large subunit
SCO5513	SLI5787	51,7	233,3	72,4	4,5	1,4	Acetolactate synthase small subunit
SCO5514	SLI5788	472,1	1735,1	613,3	3,7	1,3	Ketol-acid reductoisomerase
SCO5530	SLI5806	6,4	12,9	9,3	2,0	1,5	putative membrane protein
SCO5553	SLI5830	51,4	141,1	70,9	2,7	1,4	3-isopropylmalate dehydratase large subunit
SCO5554	SLI5831	38,3	137,2	50,7	3,6	1,3	3-isopropylmalate dehydratase small subunit
	SLI6006	104,6	225,4	193,3	2,2	1,8	hypothetical protein
SCO5774	SLI6036	561,1	1300,9	779,6	2,3	1,4	glutamate permease
SCO5776	SLI6038	1414,2	2997,5	1975,9	2,1	1,4	glutamate-binding protein of ABC transporter system
	SLI6109	31,7	75,6	49,8	2,4	1,6	hypothetical protein
SCO5976	SLI6258	25,0	77,2	40,1	3,1	1,6	Ornithine carbamoyltransferase
	SLI6370	5,6	15,2	10,2	2,7	1,8	hypothetical protein
	SLI6371	38,5	82,8	55,1	2,1	1,4	hypothetical protein
	SLI6372	53,9	110,0	80,5	2,0	1,5	hypothetical protein.
	SLI6482	8,9	22,0	16,7	2,5	1,9	hypothetical protein

SCO6090	SLI6484	6,8	18,2	9,5	2,7	1,4	hypothetical protein
SCO6096	SLI6490	5,1	11,6	3,4	2,3	0,7	ABC-transporter, probable sulfate transport
SCO6097	SLI6492	9,8	22,0	7,0	2,3	0,7	Sulfate adenylyltransferase subunit 1
SCO6196	SLI6585	14,5	50,8	19,0	3,5	1,3	putative long-chain-fatty-acid-CoA ligase
SCO6197	SLI6586	272,7	632,1	209,3	2,3	0,8	secreted protein
SCO6198	SLI6587	10,6	51,5	11,8	4,8	1,1	hypothetical protein
SCO6199	SLI6588	14,2	54,1	15,5	3,8	1,1	hypothetical protein
SCO6200	SLI6589	6,4	13,2	3,8	2,1	0,6	hypothetical protein
SCO6243	SLI6631	7,7	15,9	12,3	2,1	1,6	Malate synthase
SCO6295	SLI6688	4,8	14,1	5,8	3,0	1,2	Transport ATP-binding protein CydCD
SCO6298	SLI6690	5,6	14,0	10,6	2,5	1,9	hypothetical protein
	SLI6712	4,5	11,0	5,0	2,4	1,1	hypothetical protein
SCO6344	SLI6741	14,7	29,8	20,3	2,0	1,4	amidotransferase-related protein
SCO6451	SLI6797	45,2	263,1	53,4	5,8	1,2	Nickel ABC transporter, nickel-binding protein, nikA
SCO6452	SLI6798	24,7	192,3	39,3	7,8	1,6	Nickel ABC transporter, permease, nikB
SCO6453	SLI6799	16,7	108,0	22,2	6,4	1,3	Nickel ABC transporter, permease, nikC
SCO6454	SLI6800	11,9	56,9	16,5	4,8	1,4	Nickel ABC transporter, ATP-binding protein, nikD
SCO6455	SLI6801	17,1	65,6	29,0	3,8	1,7	Nickel ABC transporter, ATP-binding protein, nikE
SCO6470	SLI6816	35,2	70,8	51,9	2,0	1,5	Mesaconyl-CoA hydratase
	SLI6822	10,6	27,7	16,8	2,6	1,6	hypothetical protein
SCO6550	SLI6900	6,9	15,6	12,4	2,3	1,8	Short-chain dehydrogenase/reductase SDR
SCO6590	SLI6947	190,0	387,6	107,6	2,0	0,6	hypothetical protein
SCO6644	SLI6989	60,6	141,5	109,2	2,3	1,8	Oligopeptide ABC transporter, solute binding protein
SCO6646	SLI6991	15,4	30,9	21,7	2,0	1,4	putative transport system permease
SCO6658	SLI7003	89,1	223,9	176,2	2,5	2,0	6-phosphogluconate dehydrogenase, decarboxylating
SCO6659	SLI7004	70,9	173,7	131,9	2,5	1,9	Glucose-6-phosphate isomerase
SCO6682	SLI7026	7,4	16,2	7,5	2,2	1,0	Lanthionine precursor peptide LanA
SCO6695	SLI7039	48,5	103,8	55,3	2,1	1,1	hypothetical protein
SCO6715	SLI7059	18,5	59,1	21,6	3,2	1,2	transcriptional regulator, WhiB-type
SCO6717	SLI7061	133,2	405,4	162,9	3,0	1,2	putative acyl-[acyl-carrier protein] desaturase
SCO6766	SLI7114	14,2	31,4	17,2	2,2	1,2	hopanoid biosynthesis associated radical SAM protein HpnH
SCO6767	SLI7115	8,7	23,9	15,7	2,8	1,8	GcpE protein homolog, lipid metabolism
SCO6778	SLI7126	8,8	17,8	15,7	2,0	1,8	hypothetical protein
SCO6981	SLI7183	6,1	14,0	9,7	2,3	1,6	Inositol transport system ATP-binding protein
SCO6982	SLI7184	7,3	16,1	12,6	2,2	1,7	Inosose dehydratase
SCO6989	SLI7191	7,1	18,5	8,0	2,6	1,1	hypothetical protein
SCO6990	SLI7192	12,0	34,5	17,2	2,9	1,4	Sodium-dependent transporter
SCO7002	SLI7204	5,1	12,3	6,5	2,4	1,3	amino acid permease (GABA permease)
SCO7036	SLI7241	36,5	232,4	67,7	6,4	1,9	Argininosuccinate synthase (EC 6.3.4.5)
SCO7040	SLI7245	21,5	50,3	26,9	2,3	1,3	NADPH-dependent glyceraldehyde-3-phosphate dehydrogenase
SCO7047	SLI7252	11,6	35,4	11,4	3,1	1,0	Undecaprenyl-diphosphatase
SCO7251	SLI7467	87,4	201,3	68,5	2,3	0,8	hypothetical protein
SCO7252	SLI7468	69,5	141,1	62,0	2,0	0,9	putative regulatory protein

Appendix

SCO7253	SLI7469	17,4	40,1	19,4	2,3	1,1	hypothetical protein
	SLI7481	7,5	19,7	9,9	2,6	1,3	hypothetical protein
SCO7399	SLI7618	35,8	76,3	36,8	2,1	1,0	Ferric hydroxamate ABC transporter, substrate binding protein FhuD
SCO7420	SLI7640	27,7	57,2	34,0	2,1	1,2	hypothetical protein
SCO7421	SLI7641	35,7	74,2	47,3	2,1	1,3	hypothetical protein
SCO7467	SLI7684	39,7	122,0	51,0	3,1	1,3	hypothetical protein
SCO7659	SLI7886	58,7	129,5	112,0	2,2	1,9	hypothetical protein
	SLI7935	10,0	20,4	15,8	2,0	1,6	hypothetical protein
SCO7722	SLI7953	3,5	10,0	5,5	2,9	1,6	hypothetical protein
SCO7733	SLI7969	12,9	26,1	21,6	2,0	1,7	hypothetical protein
SCO7772	SLI8015	14,6	33,1	22,9	2,3	1,6	hypothetical protein
	SLI8060	8,7	24,2	15,6	2,8	1,8	hypothetical protein
SCO7814	SLI8061	15,4	35,5	22,0	2,3	1,4	putative oxidoreductase (pseudogene)

Table S2-A. Genes expressed lower in both *csIA* and *glxA*

Gene # <i>S. coelicolor</i>	Gene # <i>S. lividans</i>	1326 (RPKM)	<i>csIA</i> (RPKM)	<i>glxA</i> (RPKM)	<i>csIA</i> /1326	<i>glxA</i> /1326	Annotation
	SLI0003	23,0	11,1	11,1	0,5	0,5	hypothetical protein
	SLI0174	37,1	14,6	11,2	0,4	0,3	hypothetical protein
	SLI0229	35,0	15,2	15,1	0,4	0,4	hypothetical protein
SCO0558	SLI0520	40,1	9,5	19,3	0,2	0,5	hypothetical protein
SCO0793	SLI0776	12,4	5,3	5,7	0,4	0,5	hypothetical protein
	SLI11219	13,1	1,9	1,5	0,1	0,1	hypothetical protein
	SLI1372	15,9	4,4	6,9	0,3	0,4	hypothetical protein
	SLI1891	21,9	8,6	10,5	0,4	0,5	Transcriptional regulator, GntR family
SCO1602	SLI1906	144,5	51,5	39,2	0,4	0,3	hypothetical protein
	SLI1910	108,5	43,6	54,2	0,4	0,5	hypothetical protein
	SLI1955	36,7	10,4	8,2	0,3	0,2	hypothetical protein
SCO1708	SLI2012	15,0	6,4	6,4	0,4	0,4	hypothetical protein
SCO1748	SLI2052	77,5	32,7	38,0	0,4	0,5	putative regulator, highly similar to metallo-thionein-like proteins
	SLI2174	94,6	28,3	30,8	0,3	0,3	hypothetical protein
	SLI2277	10,0	3,2	2,5	0,3	0,2	hypothetical protein
	SLI2499	28,1	10,2	12,2	0,4	0,4	hypothetical protein
SCO2185	SLI2512	264,0	76,0	92,6	0,3	0,4	hypothetical protein
SCO2224	SLI2550	168,1	65,7	64,4	0,4	0,4	hypothetical protein
	SLI2615	15,5	7,6	5,2	0,5	0,3	hypothetical protein
SCO2530	SLI2866	11,3	2,5	4,2	0,2	0,4	hypothetical protein
SCO2636	SLI2978	106,0	24,4	50,6	0,2	0,5	hypothetical protein
SCO2887	SLI3232	298,6	101,8	141,8	0,3	0,5	membrane protein
SCO3071	SLI3421	87,9	13,2	33,1	0,1	0,4	Formiminoglutamic iminohydrolase
SCO3072	SLI3422	65,1	6,5	12,2	0,1	0,2	putative amino acid hydrolase
SCO3073	SLI3423	74,5	12,8	10,6	0,2	0,1	Urocanate hydratase

SCO3075	SLI3425	52,3	6,8	8,9	0,1	0,2	Transcriptional regulator, ArsR family
SCO3081	SLI3431	202,7	61,7	101,7	0,3	0,5	hypothetical protein
SCO3088	SLI3440	133,6	19,5	63,5	0,1	0,5	hypothetical protein
SCO3196	SLI3550	45,0	23,4	20,9	0,5	0,5	PTS system, putative fructose-specific permease
SCO3285	SLI3630	30,5	14,0	12,6	0,5	0,4	hypothetical protein
SCO3386	SLI3729	30,8	13,2	7,9	0,4	0,3	hypothetical protein
SCO3431	SLI3775	98,9	26,5	37,2	0,3	0,4	membrane protein
SCO3620	SLI3864	13,8	5,0	6,1	0,4	0,4	putative membrane protein
	SLI3865	78,5	39,0	33,1	0,5	0,4	serine-threonine protein kinase
SCO3657	SLI3904	361,0	61,2	101,4	0,2	0,3	loricrin
SCO3750	SLI3994	28,0	8,0	13,8	0,3	0,5	two-component sensor histidine kinase
SCO3784	SLI4028	130,4	36,7	60,8	0,3	0,5	hypothetical protein
	SLI4074	204,7	81,0	80,2	0,4	0,4	hypothetical protein
SCO3942	SLI4190	23,1	6,2	8,6	0,3	0,4	hypothetical protein
	SLI4248	44,8	7,1	14,8	0,2	0,3	hypothetical protein
	SLI4284	12,9	5,5	5,9	0,4	0,5	penicillin amidase family protein
SCO4174	SLI4415	17,9	7,6	7,5	0,4	0,4	integral membrane protein
	SLI4557	25,5	13,1	12,6	0,5	0,5	probable DNA-binding protein
	SLI4681	33,9	10,0	9,6	0,3	0,3	hypothetical protein
SCO4802	SLI5073	49,8	7,3	21,2	0,1	0,4	hypothetical protein
SCO4803	SLI5075	81,8	13,7	35,4	0,2	0,4	hypothetical protein
SCO4867	SLI5140	20,6	6,3	8,7	0,3	0,4	hypothetical protein
	SLI5201	152,7	65,5	66,8	0,4	0,4	hypothetical protein
SCO4932	SLI5205	499,2	24,5	59,7	0,0	0,1	Histidine ammonia-lyase
	SLI5220	1099,7	498,8	385,4	0,5	0,4	hypothetical protein
	SLI5247	18,8	2,4	5,5	0,1	0,3	hypothetical protein
	SLI5409	287,2	132,4	144,2	0,5	0,5	hypothetical protein
	SLI5426	25,1	10,3	9,4	0,4	0,4	hypothetical protein
SCO5228	SLI5517	55,6	17,4	28,0	0,3	0,5	putative acetyltransferase
SCO5462	SLI5731	12,4	3,3	4,9	0,3	0,4	hypothetical protein
SCO5581	SLI5863	211,7	91,1	96,8	0,4	0,5	hypothetical protein
SCO5680	SLI5940	155,4	14,7	68,4	0,1	0,4	Cytidine deaminase
	SLI6080	459,5	163,8	137,0	0,4	0,3	hypothetical protein
	SLI6081	292,0	141,5	147,4	0,5	0,5	hypothetical protein
SCO5853	SLI6124	29,4	14,7	12,6	0,5	0,4	SgaA homolog
	SLI6195	10,6	2,7	4,8	0,3	0,5	hypothetical protein
SCO6421	SLI6765	13,3	4,7	6,2	0,4	0,5	putative two-component system sensor kinase
SCO6538	SLI6886	20,6	5,7	9,7	0,3	0,5	integral membrane protein
SCO7247	SLI7463	12,6	5,2	5,5	0,4	0,4	Usp-like, universal stress protein family
SCO7284	SLI7502	258,7	86,0	125,4	0,3	0,5	Ribonuclease HI

Table S2-B. Genes expressed lower in *glxA* only

Gene # <i>S. coelicolor</i>	Gene # <i>S. lividans</i>	1326 (RPKM)	<i>csIA</i> (RPKM)	<i>glxA</i> (RPKM)	<i>csIA/1326</i>	<i>glxA/1326</i>	Annotation
SCO0286	SLI0239	10,7	7,3	4,8	0,7	0,4	secreted peptidoglycan binding protein
SCO0761	SLI0742	281,0	356,8	104,5	1,3	0,4	hypothetical protein
	SLI1233	10,7	6,2	5,3	0,6	0,5	hypothetical protein
	SLI1346	87,5	52,4	43,6	0,6	0,5	hypothetical protein
SCO1682	SLI1987	14,9	9,6	7,5	0,6	0,5	L-idonate 5-dehydrogenase
	SLI2083	78,8	41,5	34,5	0,5	0,4	hypothetical protein
SCO1902	SLI2213	11,4	9,2	4,7	0,8	0,4	hypothetical hydrophilic protein
SCO2038	SLI2360	362,8	334,5	156,1	0,9	0,4	FIG01124547: hypothetical protein
SCO2159	SLI2485	24,7	13,9	11,5	0,6	0,5	SC6G10.32, unknown, len: 69aa
	SLI2771	28,3	24,8	14,1	0,9	0,5	FIG01121890: hypothetical protein
	SLI3141	49,1	34,5	22,8	0,7	0,5	hypothetical protein
SCO2837	SLI3188	188,4	3460,9	1,1	18,4	0,0	Radical Cu-oxidase, <i>glxA</i>
	SLI3223	35,8	57,4	17,8	1,6	0,5	hypothetical protein
SCO3074	SLI3424	149,3	238,5	66,6	1,6	0,4	putative integral membrane protein
SCO3362	SLI3704	19,5	31,1	8,6	1,6	0,4	putative membrane protein
SCO5100	SLI5378	73,7	63,8	35,2	0,9	0,5	Transcriptional regulator, GntR family
SCO6099	SLI6494	20,4	24,1	9,3	1,2	0,5	Adenylylsulfate kinase
SCO6100	SLI6495	36,9	20,1	16,9	0,5	0,5	phosphoadenosine phosphosulfate reductase, <i>cysH</i>
	SLI6946	18,8	13,1	3,9	0,7	0,2	hypothetical protein
	SLI6951	66,5	88,5	32,7	1,3	0,5	hypothetical protein
SCO6716	SLI7060	54,5	93,9	21,4	1,7	0,4	hypothetical protein
	SLI7157	11,8	7,4	5,3	0,6	0,4	hypothetical protein
SCO7257	SLI7473	25,0	14,0	12,1	0,6	0,5	ChpB
SCO7279	SLI7497	32,9	19,2	16,6	0,6	0,5	DNA-binding protein

Table S2-C. Genes expressed lower in *csIA* only. Only hints that are three-fold down or more are shown in the table.

Gene # <i>S. coelicolor</i>	Gene # <i>S. lividans</i>	1326 (RPKM)	<i>csIA</i> (RPKM)	<i>glxA</i> (RPKM)	<i>csIA/1326</i>	<i>glxA/1326</i>	Annotation
SCO0084	SLI0010	11,3	3,7	6,6	0,3	0,6	hypothetical protein
SCO0536	SLI0496	49,6	14,7	35,3	0,3	0,7	hypothetical protein
SCO0953	SLI1186	158,0	33,1	107,9	0,2	0,7	regulatory protein, <i>LacI</i>
SCO0954	SLI1187	62,8	19,2	44,4	0,3	0,7	putative acetyltransferase
SCO0977	SLI1212	111,1	29,8	94,3	0,3	0,8	hypothetical protein
SCO1000	SLI0872	27,4	1,8	36,3	0,1	1,3	Integrase
SCO1087	SLI1361	469,9	36,9	483,7	0,1	1,0	threonine aldolase
SCO1088	SLI1362	647,8	32,2	697,2	0,0	1,1	putative oxidoreductase
SCO1089	SLI1363	955,2	80,1	947,5	0,1	1,0	hypothetical protein
SCO1090	SLI1364	76,7	17,4	58,6	0,2	0,8	Glycerophosphoryl diester phosphodiesterase
SCO1109	SLI1382	104,9	26,8	91,2	0,3	0,9	2,4-dienoyl-CoA reductase (NADPH)

SCO1377	SLI1670	24,7	6,0	21,6	0,2	0,9	Molybdate-binding domain of ModE
SCO1378	SLI1671	235,7	31,1	229,2	0,1	1,0	putative glycine dehydrogenase
SCO1379	SLI1672	13,1	3,0	8,1	0,2	0,6	hypothetical protein
SCO1454	SLI1752	47,9	14,9	53,6	0,3	1,1	Lysine 2-monooxygenase
SCO1455	SLI1753	73,2	16,5	70,1	0,2	1,0	hydrolase
SCO1459	SLI1756	15,4	4,5	13,2	0,3	0,9	putative amino acid transporter
SCO1541	SLI1842	41,9	11,8	38,8	0,3	0,9	putative regulator
SCO1749	SLI2053	557,5	147,5	507,8	0,3	0,9	hypothetical protein
SCO1788	SLI2096	96,3	31,9	65,1	0,3	0,7	4-nitrophenylphosphatase
SCO1799	SLI2107	22,0	5,8	13,7	0,3	0,6	hypothetical protein
SCO1908	SLI2220	50,6	14,8	33,5	0,3	0,7	putative large secreted protein
SCO1982	SLI2298	83,0	26,1	66,1	0,3	0,8	hypothetical protein
SCO2099	SLI2423	52,8	12,7	27,1	0,2	0,5	hypothetical protein
SCO2107	SLI2431	171,7	53,1	101,2	0,3	0,6	glycine oxidase
SCO2255	SLI2582	107,3	36,7	79,5	0,3	0,7	putative membrane protein
SCO2256	SLI2583	113,1	29,1	109,9	0,3	1,0	3-methyl-2-oxobutanoate hydroxymethyltransferase
SCO2297	SLI2625	64,7	17,6	61,2	0,3	0,9	hypothetical protein
SCO2320	SLI2650	30,0	8,4	19,5	0,3	0,7	hypothetical protein
SCO2352	SLI2683	82,5	25,1	54,0	0,3	0,7	hypothetical protein
SCO2353	SLI2684	121,0	19,2	63,7	0,2	0,5	hypothetical protein
SCO2472	SLI2808	12,2	4,2	6,4	0,3	0,5	SanA protein
SCO2538	SLI2874	318,7	95,8	199,7	0,3	0,6	hypothetical protein
SCO2574	SLI2911	113,7	38,4	102,5	0,3	0,9	hypothetical protein
SCO2939	SLI3283	237,5	71,7	143,9	0,3	0,6	hypothetical protein
SCO2942	SLI3287	459,5	147,5	245,4	0,3	0,5	oxidoreductase
SCO2953	SLI3299	71,8	18,6	37,9	0,3	0,5	putative membrane protein
SCO2954	SLI3300	15,6	5,4	13,7	0,3	0,9	RNA polymerase sigma-70 factor, ECF subfamily
SCO3048	SLI3396	505,7	156,3	435,5	0,3	0,9	putative membrane protein
SCO3070	SLI3420	81,3	14,3	42,5	0,2	0,5	Imidazolonepropionase
SCO3084	SLI3434	13,8	4,0	8,4	0,3	0,6	P-hydroxybenzoate hydroxylase
SCO3086	SLI3437	1554,2	207,9	1456,8	0,1	0,9	putative lipoprotein
SCO3087	SLI3438	981,7	114,2	702,9	0,1	0,7	hypothetical protein
SCO3114	SLI3471	11,7	3,8	10,9	0,3	0,9	putative cellulose-binding protein
SCO3157	SLI3511	210,8	71,4	147,0	0,3	0,7	putative penicillin-binding protein
SCO3194	SLI3548	681,7	198,5	490,6	0,3	0,7	putative lipoprotein
SCO3197	SLI3551	59,1	16,6	44,3	0,3	0,7	Putative sugar kinase
SCO3293	SLI3638	10,1	2,8	7,0	0,3	0,7	hypothetical protein
SCO3330	SLI3673	40,0	10,3	36,9	0,3	0,9	NAD-independent protein deacetylase AcuC
SCO3341	SLI3684	440,5	114,7	258,4	0,3	0,6	hypothetical protein
SCO3342	SLI3685	894,5	129,6	539,8	0,1	0,6	glycine-rich secreted protein
SCO3343	SLI3686	121,6	29,7	71,8	0,2	0,6	hypothetical protein
SCO3356	SLI3698	2083,9	664,0	1835,7	0,3	0,9	ECF sigma factor
SCO3432	SLI3776	41,2	13,0	26,9	0,3	0,7	hypothetical protein
SCO3577	SLI3820	198,4	67,4	144,8	0,3	0,7	Arsenical pump-driving ATPase

Appendix

SCO3601	SLI3844	240,8	73,4	218,7	0,3	0,9	ligand-binding protein related to C-terminal domains of K ⁺ channels
SCO3621	SLI3866	156,8	28,1	86,5	0,2	0,6	serine-threonine protein kinase
SCO3626	SLI3871	75,5	25,7	53,2	0,3	0,7	putative RNA polymerase sigma factor
SCO3656	SLI3903	67,3	21,0	41,4	0,3	0,6	hypothetical protein
SCO3676	SLI3924	830,2	212,4	502,6	0,3	0,6	hypothetical protein
SCO3686	SLI3934	58,6	16,8	39,3	0,3	0,7	hypothetical protein
SCO3703	SLI3952	70,6	19,6	71,2	0,3	1,0	Molybdate-binding domain of ModE
SCO3710	SLI3959	240,8	67,2	242,8	0,3	1,0	hypothetical protein
SCO3712	SLI3961	719,2	135,4	469,0	0,2	0,7	hydrolase
SCO3772	SLI4016	32,8	8,1	22,3	0,2	0,7	hypothetical protein
SCO3783	SLI4027	46,7	14,9	28,4	0,3	0,6	putative lipoprotein
SCO3786	SLI4030	24,2	6,0	17,8	0,2	0,7	integral membrane protein
SCO3817	SLI4068	617,2	206,3	532,2	0,3	0,9	Branched-chain alpha-keto acid dehydrogenase, E1 alpha subunit
SCO3840	SLI4092	264,3	84,6	209,8	0,3	0,8	hypothetical protein
SCO3866	SLI4120	40,2	14,0	25,8	0,3	0,6	hypothetical protein
SCO3905	SLI4163	158,9	52,1	161,3	0,3	1,0	hypothetical protein
SCO3914	SLI4172	289,6	87,9	264,0	0,3	0,9	Transcriptional regulator, MarR family
SCO3915	SLI4173	261,2	21,9	189,6	0,1	0,7	putative transmembrane efflux protein
SCO3943	SLI4191	21,4	6,6	13,0	0,3	0,6	putative LacI-family transcriptional regulator
SCO3975	SLI4226	208,8	32,0	128,9	0,2	0,6	putative regulatory protein
SCO3976	SLI4227	91,9	26,2	75,1	0,3	0,8	Glycerophosphoryl diester phosphodiesterase
SCO4015	SLI4249	54,5	10,3	30,7	0,2	0,6	hypothetical protein
SCO4038	SLI4272	239,8	80,4	125,6	0,3	0,5	tRNA-specific adenosine-34 deaminase
SCO4039	SLI4273	430,3	121,6	245,9	0,3	0,6	hypothetical protein
SCO4040	SLI4274	31,4	5,5	21,6	0,2	0,7	hypothetical protein
SCO4053	SLI4288	10,7	3,3	8,1	0,3	0,8	Integral membrane protein, CopC & CopD domain
SCO4054	SLI4289	251,1	64,5	279,8	0,3	1,1	hypothetical protein
SCO4055	SLI4290	28,6	8,0	24,6	0,3	0,9	Threonine dehydrogenase and related Zn-dependent dehydrogenases
SCO4069	SLI4297	87,8	25,5	53,8	0,3	0,6	hypothetical protein
SCO4082	SLI4310	109,7	34,9	76,7	0,3	0,7	hypothetical protein
SCO4083	SLI4311	29,8	8,6	22,2	0,3	0,7	hypothetical protein
SCO4084	SLI4312	54,2	17,7	35,0	0,3	0,6	hypothetical protein
SCO4095	SLI4325	83,6	27,1	49,5	0,3	0,6	hypothetical protein
SCO4100	SLI4330	20,5	7,0	14,8	0,3	0,7	hypothetical protein
SCO4113	SLI4344	190,9	63,9	111,3	0,3	0,6	L-2-hydroxyglutarate oxidase
SCO4125	SLI4362	55,1	14,6	36,0	0,3	0,7	acetyltransferase
SCO4142	SLI4381	15,6	5,2	14,5	0,3	0,9	Phosphate ABC transporter, phosphate-binding protein PstS
SCO4167	SLI4408	65,1	21,4	58,6	0,3	0,9	Transcriptional regulator, TetR family
SCO4188	SLI4428	82,8	28,4	59,2	0,3	0,7	Transcriptional regulator, GntR family
SCO4190	SLI4430	298,3	80,4	172,7	0,3	0,6	Transcriptional regulator, GntR family, devA
SCO4234	SLI4472	86,4	29,8	67,4	0,3	0,8	2-C-methyl-D-erythritol 2,4-cyclodiphosphate synthase

SCO4262	SLI4497	36,1	12,6	37,2	0,3	1,0	hypothetical protein
SCO4268	SLI4503	83,6	24,3	64,7	0,3	0,8	hypothetical protein
SCO4287	SLI4524	138,9	46,9	95,6	0,3	0,7	hypothetical protein
SCO4289	SLI4526	477,5	58,8	299,0	0,1	0,6	secreted protein
SCO4290	SLI4527	190,0	31,6	99,6	0,2	0,5	Alpha,alpha-trehalose-phosphate synthase [UDP-forming] (EC 2.4.1.15)
SCO4291	SLI4528	26,5	8,7	18,6	0,3	0,7	hypothetical protein
SCO4292	SLI4529	69,9	24,2	51,8	0,3	0,7	putative glucosyl-3-phosphoglycerate synthase
SCO4302	SLI4539	15,7	3,2	10,7	0,2	0,7	secreted protein
SCO4322	SLI4559	86,3	28,7	55,6	0,3	0,6	hypothetical protein
SCO4343	SLI4582	30,4	10,4	21,0	0,3	0,7	Mobile element protein
SCO4386	SLI4620	91,0	30,5	66,7	0,3	0,7	hypothetical protein
SCO4409	SLI4645	101,2	32,4	64,0	0,3	0,6	hypothetical protein
SCO4410	SLI4646	45,3	11,2	44,9	0,2	1,0	putative anti anti sigma factor
SCO4412	SLI4650	31,3	10,2	20,5	0,3	0,7	putative regulatory protein
SCO4422	SLI4659	12,7	3,8	6,9	0,3	0,5	putative hydrolase
SCO4424	SLI4661	353,4	62,4	284,5	0,2	0,8	hypothetical protein
SCO4435	SLI4674	48,9	15,6	28,5	0,3	0,6	putative ADP-ribosylglycohydrolase
SCO4458	SLI4700	89,6	29,0	48,4	0,3	0,5	lipoprotein
SCO4467	SLI4746	283,0	83,6	163,1	0,3	0,6	hypothetical protein
SCO4477	SLI4756	16,4	5,1	14,0	0,3	0,9	Transcriptional regulator, MerR family
SCO4500	SLI4780	43,9	15,0	27,3	0,3	0,6	Acyl dehydratase
SCO4503	SLI4784	15,6	5,1	13,6	0,3	0,9	Long-chain-fatty-acid--CoA ligase
SCO4587	SLI4871	118,0	36,5	97,1	0,3	0,8	Multimeric flavodoxin WrbA
SCO4588	SLI4872	347,5	49,2	197,4	0,1	0,6	hypothetical protein
SCO4633	SLI4904	102,3	34,2	78,9	0,3	0,8	Cytosine deaminase
SCO4696	SLI4967	15,5	5,3	14,4	0,3	0,9	hypothetical protein
SCO4744	SLI5014	31,8	8,1	24,9	0,3	0,8	Holo-[acyl-carrier protein] synthase
SCO4779	SLI5050	158,2	44,9	92,6	0,3	0,6	putative serine/threonine protein kinase
SCO4804	SLI5076	15,4	4,8	8,0	0,3	0,5	hypothetical protein
SCO4818	SLI5089	12,5	3,9	6,5	0,3	0,5	hypothetical protein
SCO4895	SLI5167	192,8	50,5	118,1	0,3	0,6	RNA polymerase sigma-70 factor
SCO4908	SLI5180	2709,8	493,3	1387,1	0,2	0,5	putative RNA polymerase ECF-subfamily sigma factor
SCO4988	SLI5263	56,8	17,4	41,5	0,3	0,7	2-dehydro-3-deoxygluconate kinase
SCO5070	SLI5348	10,9	3,6	5,7	0,3	0,5	hypothetical protein
SCO5138	SLI5420	95,1	25,5	76,1	0,3	0,8	hypothetical protein
SCO5157	SLI5440	301,2	64,1	167,7	0,2	0,6	Magnesium and cobalt transport protein CorA
SCO5158	SLI5441	146,7	48,1	109,9	0,3	0,7	hypothetical protein
SCO5209	SLI5498	50,9	17,6	41,0	0,3	0,8	Transcriptional regulator, TetR family
SCO5254	SLI5545	4185,1	1183,8	3958,7	0,3	0,9	Nickel-dependent superoxide dismutase
SCO5401	SLI5672	83,9	20,3	59,8	0,2	0,7	probable integral membrane protein
SCO5403	SLI5674	116,5	35,7	134,9	0,3	1,2	Two-component response regulator
SCO5415	SLI5684	407,2	135,8	472,5	0,3	1,2	putative isobutyryl-CoA mutase, chain B
SCO5416	SLI5685	148,5	50,7	130,8	0,3	0,9	Transcriptional regulator, AraC family

Appendix

SCO5417	SLI5686	54,2	16,9	50,0	0,3	0,9	putative zinc-binding oxidoreductase
SCO5437	SLI5705	40,2	13,5	22,6	0,3	0,6	putative MerR-family transcriptional regulator
SCO5469	SLI5738	126,4	34,9	116,4	0,3	0,9	L-serine dehydratase
SCO5472	SLI5741	236,6	49,7	231,1	0,2	1,0	Aminomethyltransferase (glycine cleavage system T protein)
SCO5473	SLI5742	194,1	34,9	148,2	0,2	0,8	putative ATP/GTP binding protein
SCO5483	SLI5753	80,2	26,4	72,3	0,3	0,9	Transcriptional regulator, TetR family
SCO5528	SLI5803	90,1	30,7	74,1	0,3	0,8	Transcriptional regulator, TetR family
SCO5557	SLI5834	212,7	51,9	171,1	0,2	0,8	hypothetical protein
SCO5676	SLI5935	301,3	28,2	213,6	0,1	0,7	Gamma-aminobutyrate:alpha-ketoglutarate aminotransferase
SCO5679	SLI5939	192,8	20,7	132,7	0,1	0,7	aldehyde dehydrogenase family protein
SCO5681	SLI5941	26,7	1,6	16,4	0,1	0,6	Dolichol-phosphate mannosyltransferase
SCO5772	SLI6034	109,6	33,0	81,7	0,3	0,7	hypothetical protein
SCO5798	SLI6061	357,9	117,0	245,3	0,3	0,7	putative secreted protein
SCO5807	SLI6073	56,3	19,6	45,0	0,3	0,8	hypothetical protein
SCO5881	SLI6154	181,2	61,1	116,6	0,3	0,6	two-component system response regulator
SCO5915	SLI6190	12,3	3,5	8,3	0,3	0,7	hypothetical protein
SCO5919	SLI6197	27,1	5,8	22,9	0,2	0,8	hypothetical protein
SCO5920	SLI6198	52,6	7,6	63,1	0,1	1,2	ATP-dependent RNA helicase
SCO5985	SLI6267	13,5	2,6	9,7	0,2	0,7	Putative translation initiation inhibitor, yjgF family
SCO5986	SLI6268	116,8	22,5	78,5	0,2	0,7	putative oxidoreductase
SCO5987	SLI6269	144,2	27,5	118,4	0,2	0,8	hypothetical protein
SCO5991	SLI6274	122,1	29,8	71,6	0,2	0,6	secreted protein
SCO6045	SLI6439	198,7	53,9	144,9	0,3	0,7	hypothetical protein
SCO6084	SLI6477	127,2	43,2	87,9	0,3	0,7	putative DNA polymerase III epsilon subunit
SCO6526	SLI6874	13,7	4,0	13,7	0,3	1,0	hypothetical protein
SCO6540	SLI6888	83,3	27,8	43,4	0,3	0,5	Pterin-4-alpha-carbinolamine dehydratase
SCO6621	SLI6980	157,6	36,2	108,6	0,2	0,7	hypothetical protein
SCO6799	SLI7149	127,4	3,5	121,8	0,0	1,0	L-threonine 3-dehydrogenase
SCO6800	SLI7150	138,7	3,7	187,9	0,0	1,4	2-amino-3-ketobutyrate coenzyme A ligase
SCO6801	SLI7151	65,4	19,9	73,3	0,3	1,1	Transcriptional regulator, LysR-family
SCO7248	SLI7464	10,1	3,5	7,1	0,3	0,7	hypothetical protein
SCO7533	SLI7755	11,2	2,7	10,7	0,2	1,0	two-component system response regulator
SCO7597	SLI7819	26,4	9,0	19,2	0,3	0,7	putative N-acetylglucosamine kinase
	SLI5074	20,6	2,7	21,8	0,1	1,1	hypothetical protein
	SLI3439	526,9	107,8	356,3	0,2	0,7	hypothetical protein
	SLI7216	16,5	3,9	14,6	0,2	0,9	Transcriptional regulator, LacI-family
	SLI1383	17,0	4,0	17,4	0,2	1,0	hypothetical protein
	SLI3901	11,5	2,8	7,7	0,2	0,7	hypothetical protein
	SLI4663	69,4	17,7	60,9	0,3	0,9	hypothetical protein
	SLI3397	405,7	112,1	264,6	0,3	0,7	putative membrane protein
	SLI3436	14,1	4,0	11,4	0,3	0,8	hypothetical protein
	SLI0018	88,1	25,5	59,4	0,3	0,7	putative two-component system response regulator

SLI8089	12,1	3,6	8,6	0,3	0,7	hypothetical protein
SLI4844	15,6	4,7	9,7	0,3	0,6	hypothetical protein
SLI4699	25,8	8,0	14,5	0,3	0,6	hypothetical protein
SLI6125	35,3	10,9	27,3	0,3	0,8	hypothetical protein
SLI3499	18,4	5,7	11,7	0,3	0,6	two-component system response regulator
SLI3881	76,2	24,0	42,3	0,3	0,6	hypothetical protein
SLI3774	23,1	7,4	27,0	0,3	1,2	hypothetical protein
SLI7074	9,7	3,1	10,7	0,3	1,1	hypothetical protein
SLI5049	69,6	22,5	78,3	0,3	1,1	hypothetical protein
SLI1401	18,4	6,1	10,2	0,3	0,6	hypothetical protein
SLI5843	53,1	17,9	47,7	0,3	0,9	hypothetical protein
SLI1210	69,1	23,5	39,2	0,3	0,6	hypothetical protein
SLI5857	53,3	18,3	27,0	0,3	0,5	hypothetical protein
SLI2084	19,5	6,7	14,3	0,3	0,7	putative regulatory protein

CURRICULUM VITAE

Giulia Mangiameli was born on the 2nd of May 1984 in Torino, Italy. In 2003, she graduated from Liceo Classico Vincenzo Gioberti, Torino. Between 2003 and 2006, she studied Biotechnology at the University of Torino, obtaining her Bachelor of Science. In 2006, she started her Master's in Industrial Biotechnology at the same university. Between 2007 and 2008, she spent a year abroad at the University of Salamanca, Spain, following an Erasmus project and working on her Master's thesis. She graduated in 2009 with a MSc project on the degradation of textile dyes by the catalytic action of a peroxidase extracted from lentil plants. In the fall of 2009, she joined the group of Molecular Biotechnology at the University of Leiden under the supervision of Dr Erik Vijgenboom and Prof Gilles van Wezel. Her work was funded by the European Research Area for the Industrial Biotechnology (ERA-IB). In early 2014, she moved to London to work as an Executive Editor for the BMC-series at BioMed Central, Springer.

The work done during her PhD is presented in this thesis.

